MOLECULAR TOXICOLOGY STUDIES ON THE QUARTZ HAZARD

RODGER DUFFIN

A thesis submitted in partial fulfilment of the requirements of Napier University for the degree of Doctor of Philosophy

This research was carried out in collaboration with the ELEGI/Colt Research Laboratories at the University of Edinburgh

January 2003

This thesis is dedicated to the memory of

my Gran, Mrs. Agnes Duffin

and

my Aunt, Mrs. Anna Gooday.

January 2003.

"Quartz is like a box of chocolates.....

you never know what you're gonna get"

(based on a quote from the film Forest Gump, 1994.)

ABSTRACT

Silicon makes up almost 28% of the Earth's crust and within that crust, quartz (crystalline silica) is one of the most abundant minerals. Exposure to quartz can occur in a number of occupations, including the mining and construction industries in which respirable quartz particles are generated and become airborne. Inhalation of quartz can lead to the fibrosing lung disease silicosis and cancer. Silicosis has been recognised for many decades as one of the most prevalent occupational lung diseases. In 1997, an IARC working Group classified quartz as a class 1 lung carcinogen, but only in some industries, suggesting that the quartz hazard is a variable entity. The reactivity of the quartz surface may underlie its ability to cause inflammation and treatments that ameliorate this reactivity would then reduce the quartz hazard.

In the present study the effect of treating quartz with aluminium lactate, a procedure reported to decrease the quartz hazard, on the highly reactive quartz surface and on pro-inflammatory events in the rat lung were explored. Aluminium lactate-treated quartz showed a reduced surface reactivity as measured by electron spin resonance. Eighteen hours post-instillation of quartz into the rat lung, there was massive inflammation as indicated by the number of neutrophils in the bronchoalveolar lavage (BAL) and an increase in BAL macrophage inflammatory protein-2 (MIP-2). However, aluminium lactate-treated quartz had no significant effect when compared to control. Epithelial damage as indicated by BAL protein and gamma glutamyl transpeptidase also increased with quartz instillation but not with aluminium lactate-treated quartz and furthermore, quartz induced an increase in MIP-2 mRNA content of BAL cells while aluminium lactate-treated quartz had no effect compared to controls. There was an increase in nuclear binding of the transcription factor nuclear factor-kappa B (NF-κB) in the quartz

exposed BAL cells and again, no effect on nuclear NF-κB binding in BAL cells from aluminium lactate-treated quartz instilled rats.

In addition, the effect of aluminium lactate and PVNO quartz treatment on DNA damage, cell cytotoxicity and particle uptake by A549 cells was assessed. DNA strand breakage, as produced by quartz at non-toxic concentrations, could be completely prevented by both coating materials. Particle uptake by A549 cells appeared to be significantly inhibited by the PVNO coating, and to a lesser extent by the aluminium lactate coating, demonstrating that respirable quartz particles induce oxidative DNA damage in human lung epithelial cells and indicating that the surface properties of the quartz as well as particle uptake by these target cells are important in the cytotoxic and genotoxic effects of quartz *in vitro*.

Finally, the role played by surface area and specific reactivity in the acute inflammatory response to particles was investigated. Acute inflammatory response following instillation of particles has been used to evaluate hazard but has been criticised because of the non-physiological delivery and the problems of local overload. Here, a number of low toxicity dusts of various particle sizes were instilled and the neutrophil influx into the lung 18-24 hours post-instillation assessed. The extent of inflammation was shown to be a function of the surface area instilled and ultrafine particles, which present a case of high surface area per unit mass, were inflammogenic *pro rata* with their surface area. There is no evidence that ultrafine particles of carbon black, titanium dioxide or polystyrene have any special reactivity in addition to their large surface area. We further tested whether this approach could be used to model the reactivity of highly toxic dusts. Rats were instilled with either quartz or aluminium lactate-treated quartz

and , as anticipated, the high specific surface reactivity of quartz meant that it was much more inflammogenic than was predicted using the relationship described for 'low-toxicity' dusts. This approach represents the possibility of modelling potential toxicity for nuisance dusts based on the inflammatory response of a given instilled surface area dose.

ACKNOWLEDGEMENTS

The completion of this thesis would not have been possible without the help and support of my colleagues, friends and family. I would like to begin by thanking my supervisors Professor Ken Donaldson and Dr. Vicki Stone. Ken and Vicki, your advice, support, encouragement (which sometimes included a well deserved kick in the posterior!) and friendship have been invaluable over the course of my PhD, helping to make it a extremely worthwhile and enjoyable experience.....well most of the time! For that, I thank you both.

To my friends and colleagues at the ELEGI, thank-you all for making me laugh (usually at you, not with you – I think that's the right way round!!) and feel at home. Thanks for all your help, support and advice over the last 3 years – I couldn't think of a better place to do my PhD. Special thanks must go to Professor Bill MacNee, Dr. Ellen Drost and of course my guru and mentor, Dr. Peter Glimmer .....oops sorry Gilmour!.

I would like to extend my thanks to everyone within the Biomedicine Research Group at Napier who have helped and encouraged me throughout my PhD. I would especially like to thank Dr. David Brown for all his help and advice and for keeping us all entertained in the local hostelries, Dr. Anna Clouter for her encouragement and advice and Dr. Pamela Keir for her continued support and help with the preparation of this thesis. I would also like to thank Dr. Lang Tran at the I.O.M, for all his help and advice regarding the surface area experiments.

Further thanks must go to Professor Paul Borm, Dr. Roel Schins and Dr. Ad Knaapen - my Dutch friends and colleagues. *Bedankt voor jullie steun en advies gedurende mijn promotietijd. Jullie bijzondere bijdrage in 'getting to know Maastricht' werd en wordt door mij zeer gewaardeerd....en ik zal niet vergeten ' als je je gat verbrandt, moet je op de blaren zitten'!!.*

Special thanks must also go to the Colt Foundation for their generous funding and support over the last 3 years.

Finally and in my opinion most importantly, I would like to thank my family, especially my parents, for their unconditional support and encouragement over the past 27 years. Without it, I almost certainly would not be where I am today and for that, I truly thank you.

INDEX

CHAPTER 2 : MATERIALS AND METHODS

CHAPTER 5 : THE IMPORTANT ROLE OF SURFACE AREA AND SPECIFIC REACTIVITY IN THE ACUTE PULMONARY RESPONSE TO LOW AND HIGH TOXICITY PARTICLES BOTH *IN VIVO* AND *IN VITRO*.

ABBREVIATIONS

Al	Aluminium lactate
AM	Alveolar macrophage
ANOVA	Analysis of variance
AP-1	Activator protein-1
ATP	Adenosine triphosphate
BAL	Bronchoalveolar lavage
BALF	Bronchoalveolar lavage fluid
BCA	Bicinchoninic acid
BSA	Bovine serum albumin
CB	Carbon Black
cDNA	Complementary DNA
cNOS	Constitutive NOS
DEPC	Diethyl pyrocarbonate
DMEM	Dulbecco's modified eagle's medium
DMPO	5, 5-dimethyl-1-pyrroline-N-oxide
DMSO	Dimethylsulfoxide
DNA	Deoxyribonucleic acid
dNTP	Deoxynucleotide triphosphate
DQ12	Quartz
EDTA	Ethylenediamine tetraacetic acid
ELF	Epithelial lining fluid
ELISA	Enzyme-linked immunosorbent assay
EMSA	Electrophoretic mobility shift assay

ERK	Extracellular signal-regulating kinase
ESR	Electron spin resonance
FCS	Foetal calf serum
Fe^{2+}	Ferrous iron
Fe^{3+}	Ferric iron
GAPDH	Glyceraldehyde-3-phosphate dehydrogenase
GSH	Reduced glutathione
H_2O_2	Hydrogen peroxide
HCl	Hydrochloric acid
HEPES	N-[2-Hydroxyethyl]piperazine-N'-[2-ethanesulfonic acid]
HOCl	Hypochlorous acid
HPRT	Hypoxanthine-guanine phosphoribosyl transferase
HRP	Horseradish peroxidase
IARC	International Agency for Research on Cancer
IGF-1	Insulin-like growth factor-1
IgG	Immunoglobulin G
IL	Interleukin
iNOS	Inducible NOS
IκB	Inhibitory kappa B
JNK	c-Jun N-terminal kinase
LDH	Lactate dehydrogenase
LPS	Lipopolysaccharide
MAPK	Mitogen-activated protein kinase
MAPKK	MAPK kinase
MAPKKK	MAPK kinase kinase

MARCO	Macrophage receptor with collagenous structure
MIP-2	Macrophage inflammatory protein-2
MPO	Myeloperoxidase
mRNA	Messenger RNA
MTT	3-[4,4-dimethylthiazol-2-yl]-2,5-diphenyl-tetrazolium bromide
NADPH	Nicotinamide adenine dinucleotide phosphate
NaOH	Sodium hydroxide
NF-κB	Nuclear factor kappa B
NIBSC	National Institute for Biological Standards and Control
NIK	NF-kB inducing kinase
$NO^{\bullet}$	Nitric oxide radical
$NO_2^{\bullet}$	Nitrogen dioxide radical
NOS	Nitric oxide synthase
$^{\bullet}OH$	Hydroxyl radical
$^1O_2$	Singlet oxygen
8-OHdG	8-Hydroxydeoxyguanosine
$O_2^{\bullet-}$	Superoxide anion
O_3	Ozone
$ONOO^-$	Peroxynitrite
PBS	Phosphate buffered saline
PM_{10}	Particulate matter of 10 microns or less
PMF	Progressive massive fibrosis
PMN	Polymorphonuclear leukocyte
PVNO	Polyvinylpyridine-N-oxide

RBC	Red blood cell
RNA	Ribonucleic acid
RNS	Reactive nitrogen species
$RO^{\bullet}$	Alkoxyl radical
$RO_2^{\bullet}$	Peroxyl radical
ROS	Reactive oxygen species
RT-PCR	Reverse transcriptase-polymerase chain reaction
SiO_2	Silicon dioxide
SiOH	Silanol
Si-O-Si	Siloxane bridge
SOD	Superoxide dismutase
SR	Scavenger-type receptor
TEMED	N,N,N‘,N‘-tetramethylethylenediamine
TGF-β	Transforming growth factor beta
TiO_2	Titanium dioxide
TMB	3,3‘,5,5-tetramethylbenzidine
TNF-α	Tumour necrosis factor alpha
ufCB	Ultrafine CB
ufCo	Ultrafine cobalt
ufNi	Ultrafine nickle
$ufTiO_2$	Ultrafine TiO_2
γGT	gamma glutamyl transpeptidase

CHAPTER 1

INTRODUCTION

1.1 The lung as a target for the effect of quartz.

1.1.1 Gross Anatomy.

The respiratory tract is a complex and diverse system extending from the nose, down to the alveoli (Figures 1.1.1a and 1.1.1b). Its principle function is that of gas exchange, delivering oxygen to red blood cells passing through the pulmonary capillaries for transport to the tissues of the remaining body and in turn, removing released waste carbon dioxide from the body (McClellan, 2000).

1.1.1.1 The Airways.

The airways consist of a series of branching tubes which become narrower, shorter and more numerous as they penetrate deeper into the lung. The upper respiratory passages (nasal cavities and pharynx) serve to conduct the air and to warm and moisten it on the way to the lungs. The trachea, held open by incomplete c-shaped cartilaginous rings, bifurcates into the left and right main bronchi, which in turn divide into lobar, segmental and subsegmental bronchi (Gray, 1918). This process continues down to the terminal bronchioles, which are the smallest airways without alveoli. All of these bronchi make up the conducting airways, functioning to direct inspired air to the gas exchanging regions of the lung. In humans, the terminal bronchioles divide into respiratory bronchioles ending finally with the alveolar ducts, which are completely lined with alveoli (Figure 1.1.1a). Rats do not have respiratory bronchioles, their terminal airways being the terminal bronchioles. This alveolated region of the lung, where gas exchange takes place, is known as the respiratory zone (Figure 1.1.1b). The

portion of the lung distal to a terminal bronchiole, including its associated alveolar duct and alveoli, forms an anatomical unit called the acinus (West, 2000).

The respiratory system consists of more than 40 different individual cell types (Kovacikova and Tatrai, 1996), each cell type having a unique morphology and function. Ciliated epithelial cells and occasional goblet cells which provide a source of mucus, extend down the respiratory tract to the respiratory bronchioles. The cilia provide locomotion to the overlying mucous blanket that serves an important role in moving macrophages and particulate material upwards towards the oral cavity, where it can then be swallowed (McClellan, 2000). In the terminal airways there are fewer ciliated cells, and Clara cells which carry out a biotransformation function, increase in number. Alveolar macrophages also increase in number on the surface of the terminal airways.

1.1.1.2 Alveoli.

The terminal airways open out into an alveolar duct and the alveoli which are about 200-300 μm in diameter, are lined by very thin type I alveolar epithelial cells (McClellan, 2000) to facilitate gas exchange with the abundant surrounding capillaries. (Figure 1.1.1b). The alveolar type I cells which are thin, flat, membranous cells found overlying the airside of the alveolar septae covering approximately 95% of the alveolar surface (Castranova *et al.*, 1988). These cells plus their basement membrane, the capillary basement membrane and the capillary endothelial cells are the air-blood barrier over which gas exchange occurs. The thinness of this barrier minimise the

diffusion distance for air and carbon dioxide between the alveolar air space and blood in the pulmonary capillaries.

Type II cells are small, cuboidal cells usually found in the alveolar corners and also regions of respiratory bronchioles (Ten Have-Opbroek *et al.*, 1997). The type II cells are capable of division and are precursors for type I cells (McClellan, 2000). In response to type I cell damage, type II cells replicate to regenerate the air-blood barrier. It is proposed that proliferation is stimulated by the lack of contact inhibition as a consequence of type I cell destruction, the exposure of basement membrane component and release of mitogens by macrophages often associated with lung injury (Leslie *et al.*, 1985). The type II cells also produce surfactant, which contains a mixture of several phosholipids. The storehouses of surfactant are lamellar bodies situated in the cytoplasm (Dormans and van Bree, 1995). Secreted surfactant acts as a surface tension-lowering material that lines the alveoli and reduces the tendency of the extremely thin walled alveoli to collapse (McClellan, 2000).

1.1.1.3 Pleura.

The pleura is a serous layer of mesodermal origin that fulfils a lubricating function for the lung movements with the thoracic cavity. It functions to allow the thorax to shape the lungs and to move over them during breathing with the minimum loss of energy (Millard and Pepper, 1990). The pleural surface is covered with a single layer of mesothelial cells which have microvilli, providing an increased surface area for lubrication and secretion/absorption of pleural fluid. The visceral pleural mesothelial cells lie on a layer of compressed connective tissue which separates it from the most

peripheral alveoli. The visceral pleura is indented into the fissures of the lobes and is continuous at the hilum with the parietal pleura that lines and overlies the ribs and the chest wall (Seaton, 2000). Traditionally it was thought that the parietal and visceral layers were separated by a thin layer of fluid, but recent work suggests that boundary lubrication by a layer of surfactant absorbed onto the pleural surface is a more likely mechanism (Millard and Pepper, 1990).

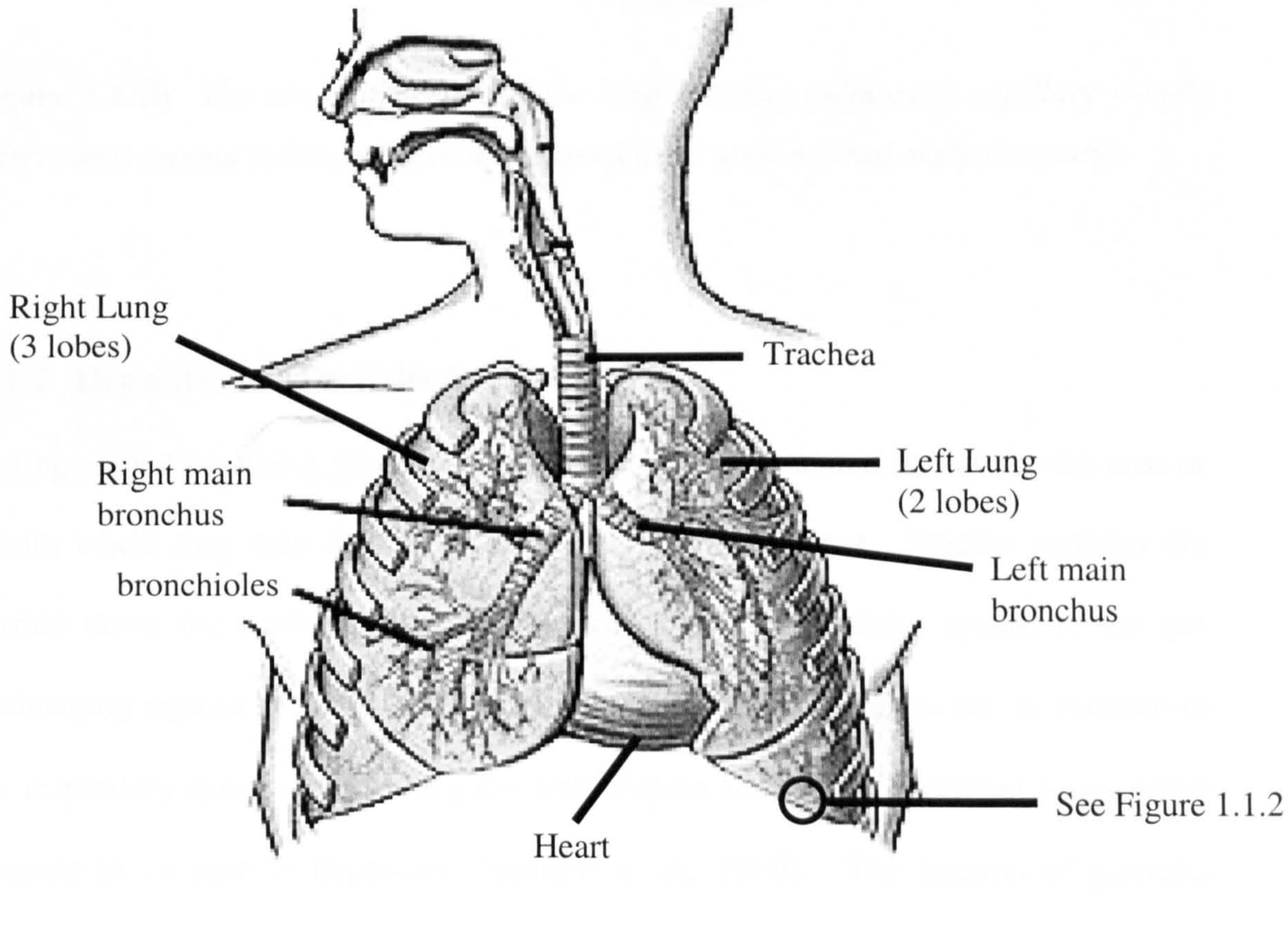

Figure 1.1.1a *Diagram of the Respiratory System (from* www.nhlbi.nih.gov/lung*).*

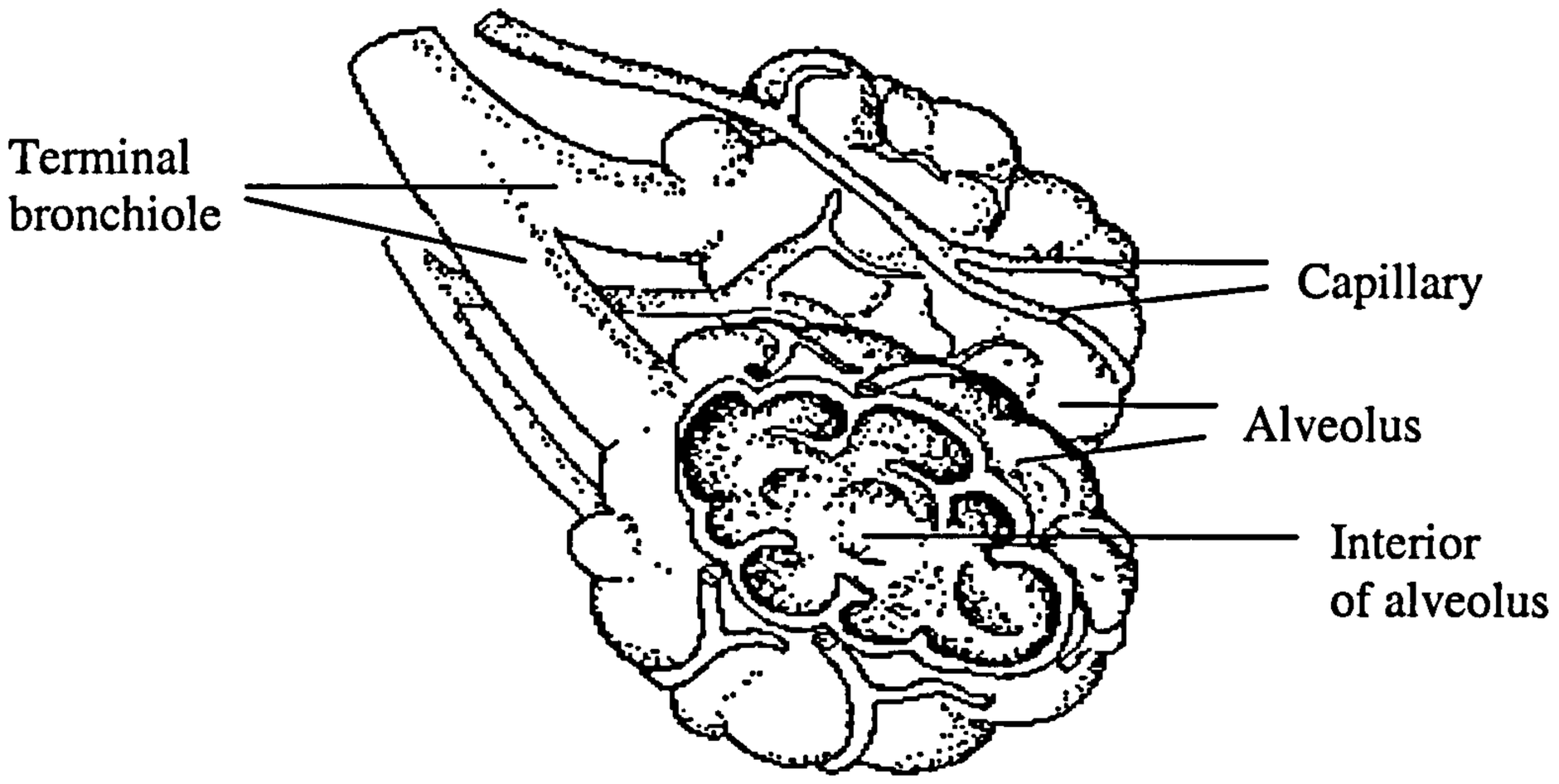

Figure 1.1.1b *The alveolar region of the lung showing pulmonary capillary vessels intertwined around individual alveoli (adapted from www.mtsinai.org/pulmonary).*

1.1.2 Deposition of Particles in the Lung.

During normal breathing, particles are transported in the inspired air through the nose or mouth where they may deposit in the upper respiratory tract. Smaller particles are carried down the trachea and the bifurcating tracheobronchiolar system to the gas exchanging regions of the lung. A certain number of these particles can be retained in the respiratory system by touching the wet airspace surfaces, a phenomenon generally referred to as particle deposition (Schultz *et al.*, 2000). The fraction of particles deposited in the respiratory system can be described as a function of particle aerodynamic diameter. Aerodynamic diameter is a notional diameter derived from the size, shape and density of the particle and can be described as the diameter of a notional particle of unit density with the same falling speed as the particle of interest (Donaldson

et al., 2002). Importantly, particle size not only determines whether a particle will deposit or not but also the region of the lungs in which the particles are deposited.

Deposition in the respiratory system of compact (non-fibrous) particles occurs by three main mechanisms, inertial impaction, sedimentation and diffusion (Figure 1.1.2). Inertia is the property by which matter continues in its state of rest or line of motion. Inertial impaction therefore is the phenomenon in which particles may continue to move in their original direction and fail to negotiate bends, such that they impact at bifurcations (Schulz *et al.*, 2000). Particle sedimentation occurs in response to gravitational settling, in which particles settle out by virtue of their mass. Finally, for particles with a diameter of less than 0.5 μm, particle deposition occurs mainly by diffusion (Schulz *et al.*, 2000).

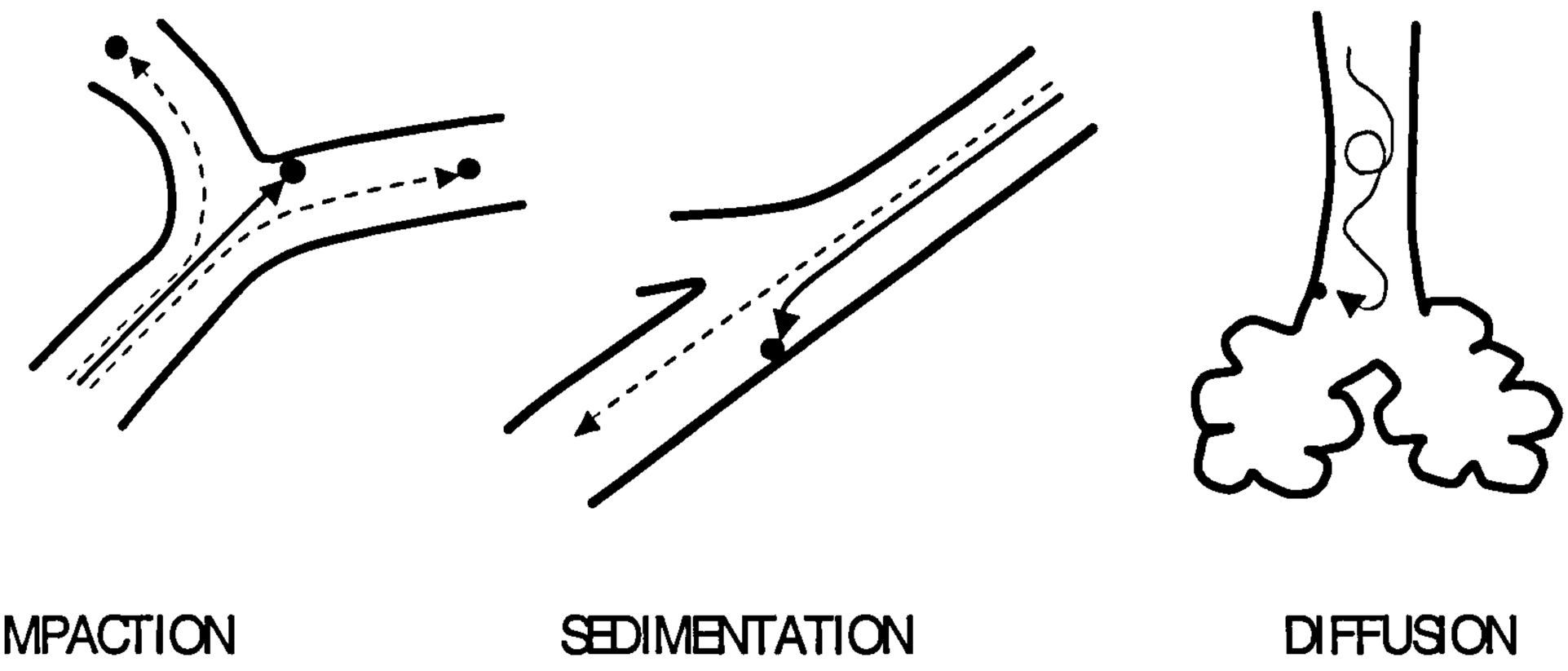

Figure 1.1.2 *Mechanisms of particle deposition in the lungs. Figure reproduced with permission from Prof. Ken Donaldson, Edinburgh.*

The previous mechanisms of particle deposition help to clarify why certain particle fractions deposit more readily than others and at certain sites. For example, deposition 'hotspots' are seen at bifurcations because of inertial impaction and at terminal bronchioles/proximal alveoli by sedimentation when the net movement of air is zero and there is ample time for the particles to settle by this mechanism (Donaldson *et al.*, 2002).

1.1.3 Inflammatory Responses in the Lung.

The inhalation of airborne particulates and microbes is an unavoidable consequence of breathing. Therefore, host defences have evolved to eliminate deposited micro-organisms and particles preferably before they have a detrimental effect on the host. Pulmonary host defences are found throughout the respiratory tract and co-ordinated interactions of cells and soluble factors are involved in most components of pulmonary host defences. One such host defence is the inflammatory response. This is the tissue's response to injury and is highly evolved, complex and although it is beneficial if it is small scale and resolving, it can be very harmful if it is large scale and chronic. Inflammation is characterised by the 'cardinal signs' i.e. pain, swelling, heat and redness at the site of injury, due to changes in local blood vessels. In the lung, inflammation is marked by the influx of white blood cells which may be separated into two main classes: polymorphonuclear or mononuclear leukocytes. The polymorphonuclear leukocytes (PMN) or granulocytes are characterised by a single, multi-lobed nucleus and prominent cytoplasmic granules. The staining of these granules allows for further classification into eosinophils, basophils and neutrophils. The mononuclear leukocytes contain non-segmented nuclei and comprise of the

monocyte/macrophage lineage and lymphocytes. Lung macrophages arise from monocytes which migrate out of the bloodstream into the tissues, where they mature into macrophages. PMNs and monocytes are active phagocytes, engulfing and digesting micro-organisms and other pathogens in the blood and tissues. However, there are considerable differences between their responses to phagocytosis. Following phagocytosis, PMNs either die by necrosis, forming pus if there are significant numbers or they undergo apoptosis and die 'silently' without inducing further inflammation. Macrophages respond to phagocytosis by releasing mediators that 'orchestrate' the behaviour of other cells.

1.1.3.1 Macrophages.

The term 'macrophage' was first proposed by Elie Metchnikoff in the late 19th century to describe the large mononuclear cells, present in inflamed tissues, which can phagocytose (Metchnikoff, 1905). Within the lung, it has been proposed that macrophages can be characterised into four different types; i) the alveolar macrophage, ii) the interstitial macrophage, iii) the intravascular macrophage and iv) the dendritic cell (Lohmann-Matthes *et al.*, 1994). Alveolar macrophages reside as free cells within the alveolar airspaces and terminal airways. They are located at the interphase between air and lung tissue, in the surfactant-rich alveolar lining fluid and serve as the first line of defence against inhaled pathogens and toxic particles (Fels and Cohn, 1986; Lohmann-Matthes *et al.*, 1994) in the region beyond the ciliated airways where mucocillary clearance does not occur. In healthy humans and most animals, more than 90% of the cells retrieved following bronchoalveolar lavage (BAL) are alveolar macrophages (Reynolds, 1987). The alveolar macrophages move around on top of, and

are in direct contact with, the type I and II epithelial cells where they interact with them by means of small pseudopodia (Fels and Cohn, 1986). Mediators released by alveolar macrophages following phagocytosis are likely to be in high concentrations at the epithelial cell surface and so could have profound effects on them.

The recruitment of alveolar macrophages occurs primarily from the migration of peripheral blood monocytes from the bloodspace into the alveoli via the interstitium, where they mature into macrophages (Bowden and Adamson, 1980; Blusse van Oud Alblas and van Furth, 1982). In addition macrophages are also replaced by proliferation of mononuclear phagocytes in the alveoli and interstitium (Bowden and Adamson, 1980). The macrophage is a functionally complex cell. One key macrophage function is the orchestration of the inflammatory response which is achieved by the huge secretory repertoire of the macrophage. Whilst the evolved function is defence, many of these mediators and indeed chronic inflammation itself has the potential to cause tissue injury (Adams and Hamilton, 1992).

1.1.3.2 Neutrophils.

Polymorphonuclear neutrophils (PMN) comprise 90% of the polymorphs circulating in the body and are produced in the bone marrow (Bernard *et al.*, 1984). PMNs play an important role in a variety of inflammatory lung diseases. The pulmonary vasculature represents the largest reservoir of PMNs in the human body, where the concentration of neutrophils within the pulmonary capillary blood is 35-100 fold greater than within the large vessels of the systemic circulation. Moreover, some of these neutrophils appear to adhere loosely to the endothelial wall of the pulmonary vasculature, even under normal conditions, thereby providing a pool of rapidly 'recruitable' neutrophils (Doerschuk *et*

al., 1987). Deformability of the neutrophils is a crucial factor in this sequestration process (Selby *et al.*, 1991). Recently it has been demonstrated that cytokines, including interleukin-8 (IL-8), play an important role in decreasing the deformability of the neutrophils and thus increasing their sequestration into the lung (Drost and MacNee, 2002). In the normal lung lumen alveolar macrophages are the resident cells, whereas PMNs are almost absent. The response to various inflammatory stimuli (including particles), can result in a very rapid and often massive influx of PMN into the lung (Albrecht *et al.*, 2002; Ghio *et al.*, 2001). PMN are therefore considered as a major effector cell in acute inflammatory processes. Within particle toxicology, the PMN has also been recognised as a crucial contributing factor in lung injury.

Once migrated into the lung lumen, the PMNs can become activated to release a myriad of products. Currently, more than 50 neutrophil-derived toxins have been identified including oxygen radicals, proteolytic enzymes and bactericidal proteins (Weiss, 1989; Sibille and Reynolds, 1990). The majority of these products are stored in lysosomal granules, which can be subdivided into azurophil (primary) and specific (secondary) granules. Some of the important products stored in azurophil granules are: elastase, lysozyme and myeloperoxidase, whereas collagenase and defensins can be found in the specific granules (Sibille and Marchandise, 1993). Upon activation, the granules migrate to the cell membrane and fusion with the membrane initiates exocytosis, which is followed by the release of the granule content into the extracellular environment, in a process called degranulation. Neutrophil degranulation can be elicited by several soluble mediators including the cytokines IL-8 and tumour necrosis factor-alpha (Mullen *et al.*, 1995). As well as soluble mediators, bacterial endotoxins, particles or other noxious stimuli present in the lung are also capable of activating neutrophil

degranulation following phagocytosis (Wilson, 1985; Sibille and Marchandise, 1993). In addition to the release of granule products, activated PMNs can undergo a respiratory burst, characterised by the production of large amounts of reactive oxygen species (see 1.4.1).

1.1.4 Macrophages and Particles.

Pulmonary macrophages play a key role in clearing inhaled particles from the lung (Warheit 1988, Donaldson *et al.*, 2001), thereby limiting any potentially damaging interaction between particles and the fragile epithelial cells. The phagocytic process involves the particles being engulfed and retained in vacuoles within the macrophage, before being removed from the lung via macrophage migration to the muco-cilliary escalator for clearance or migration to the pulmonary lymph nodes. The activation of the phagocytic process is a receptor mediated event. Complement activation may be involved (Warheit, 1988) where C5a attracts macrophages to the particle and opsonisation of the particles occurs by the surface binding of C3b. Immunoglobulins, e.g. IgG, may also opsonise particles which encourage the binding of macrophages to particles via the Fc receptor, again encouraging phagocytosis (Hill *et al.*, 1996; Reynolds *et al.*, 1975; Hoidal *et al.*, 1981; Palecanda *et al.*, 1999). Macrophages also have the ability to bind and ingest unopsonised environmental particles and bacteria through scavenger-type receptors (SRs). One such receptor is the macrophage receptor with collagenous structure (MARCO) belonging to the class A SRs, which bind to modified and acetylated low-density lipoprotein (LDL) (Kobzik, 1995; Palecanda *et al.*, 1999; Kraal *et al.*, 2000). MARCO has been suggested to play an important role in the lung's response to inhaled particles, via the binding of unopsonised dusts and pathogens (Palecanda *et al.*, 1999; Palecanda and Kobzik, 2001).

The phagocytic response to inhaled particles may range from an abundant production of pro-inflammatory cytokines (discussed in section 1.4.5) and reactive oxygen species, which can damage nearby macrophages and epithelial cells (Donaldson *et al.*, 1988), to the simple ingestion and clearance of inert dusts and particles, thereby avoiding an unnecessary inflammatory response (Palecanda *et al.*, 1999). The differential response of the macrophage to different particle types is considered to underlie the different kinds of effect that they have in the lung. For example, harmless (low toxicity) particles such as titanium dioxide at a moderate dose have little effect on the macrophage and therefore result in normal clearance. However, a harmful particle such as quartz can induce macrophage activation and/or damage. This in turn results in the release of products of cell death and mediators from cell activation thereby producing an inflammatory response and diminished clearance.

1.1.5 Epithelial Cells and Particles.

It is clear that macrophages play an important role in the defence of the peripheral lung against inhaled particles. The majority of particles which deposit in the alveoli and terminal airways are phagocytosed by macrophages and cleared either via the muco-cilliary escalator or in some circumstances, transported to the lymph nodes via the pulmonary lymphatics (Churg, 1996). However, to assume that these mechanisms remove all particles from the lung would be wrong. Particles which are not rapidly removed from the epithelial surface by macrophages are more than likely to interact with epithelial cells (Churg, 1996).

Although pulmonary epithelial cells are not normally considered phagocytic, uptake of particles by these cells appears to be a universal phenomenon. This hypothesis is supported by a number of studies showing numerous particle types, including asbestos, silica and diesel exhaust, entering epithelial cells (Suzuki *et al.*, 1972; Brody *et al.*, 1982; Adamson *et al.*, 1992; Churg, 1996). Particles may also interact with the epithelial cell membrane without phagocytosis. Interaction between epithelial cells and particles may lead to cytotoxicity, ranging from cellular dysfunction to cell death (Bowden and Adamson, 1984; Mossman *et al.*, 1978). The mechanisms of cellular cytotoxicity, as a result of particle uptake, are not fully understood. One common mechanism which may exist between mineral particles, especially in aqueous environments, is the generation of reactive oxygen species which may cause protein oxidation and lipid peroxidation, resulting in further radical formation and additional injury (Mossman and Marsh, 1989; Farber *et al.*, 1990).

Mineral particle ingestion by epithelial cells may play a key role in the carcinogenic or potentially carcinogenic events within a cell (Churg, 1996). Mineral particles with sufficient surface reactivity, that enter or interact with pulmonary epithelial cells, may cause oxidative DNA damage. This can be due to the production of highly reactive free radicals such as hydroxyl radicals in the cell cytoplasm or as a result of a direct DNA-particle interaction within the nucleus. Particles with surface complexed iron, which come into physical proximity to DNA can cause oxidation of individual bases as well as DNA strand breaks, because the iron catalyses the formation of hydroxyl radicals, via Fenton chemistry (Hardy and Aust, 1995; Moyer *et al.*, 1994).

1.2 Quartz.

1.2.1 Structure, Morphs and Exposure.

Silicon dioxide or silica is one of the most abundant materials in the earth's crust. It is formed, under conditions of increased heat and pressure, from silicon and oxygen and has the general formula SiO_2. Silica exists in the crystalline and amorphous forms. The crystalline forms are based on a tetrahedral structure, in which the central atom is silicon and the corners are occupied by oxygen. These interlink at their apices in a variety of ways to produce the silica polymorphs – quartz, cristobalite, coesite, tridymite and stishovite (Wycoff, 1963) and, when combined with a number of other elements, the silicate minerals, such as clays (Seaton, 1995). In a crystalline substance, the atoms and molecules make up a three dimensional repeating pattern. The pattern is then repeated indefinitely in three directions, forming the crystalline structure. Silica refers to the family of SiO_2 crystal structures, the most common of which is quartz, which is present in all rocks and minerals to some extent. For example, granite contains 30% free silica (i.e. quartz which has not been combined with other minerals, as in the case of the silicate minerals), slate approximately 40% and sandstone is almost pure quartz (Lapp, 1981).

Quartz itself may be split up into two dimorphs which have closely related structures – α-quartz and β-quartz. If α-quartz, the most common form found, is heated above 575°C, it transforms into β-quartz (Mandel and Mandel, 1995).

The vast majority of human exposures to respirable crystalline silica are in fact exposures to α-quartz, as a result of its sheer ubiquity. These exposures can occur in a vast array of industries, including construction, sand and gravel, tunnelling and mining, the clay/pottery industry, agriculture, foundries and sandblasting (Donaldson and Borm, 1998). Quartz is also present in many mineral dusts, including coal mine dust and coal fly-ashes. Sandstone and granite are extensively used in building where these materials may also be ground or crushed and used as fillers and abrasives and in road building. Exposure to quartz depends mainly on the degree of dust suppression by water and the adequacy of ventilation, especially in areas where stones are shaped or crushed (Seaton, 1995).

Foundries, for the castings of iron, steel and non-ferrous materials, such as bronze generate molten metal which is cast into a preformed mould. The solidified casting is removed from the mould and quartz, as well as other contaminants that have burnt onto the surface of the casting then need to be cleaned off. Here, exposure to silica can occur both in the production of the moulds, which are made of quartz-sand bonded by clays and resins, and in the knocking out of castings (Seaton, 1995). Furthermore, the high temperatures generated can convert the quartz to cristobalite – generally considered to be more harmful than α-quartz (IARC Monograph, 1997).

In the United States, the worst incidence of quartz exposure occurred during the construction of the Gauley Bridge tunnel in West Virginia between 1930 and 1932. In this unfortunate, yet preventable disaster, 4887 men were employed, of which approximately 3000 worked underground. Between 500 and 700 men died of respiratory causes and 1500 contracted silicosis, the fibrosing lung disease attributed to

silica exposure (see section 1.3). Gauley Mountain was almost pure silica sandstone, and a quote taken from an eye witness stated that, "the dust was so thick that one could not identify anyone he met, even when the man was only a few feet in front of him" (Cherniack, 1986).

Amorphous silica is non-crystalline and is non-toxic to the lungs. It occurs as a diatomite (skeletons of prehistoric marine organisms) or as vitreous silica - the result of carefully melting and then quickly cooling crystalline silica (Green and Vallyathan, 1995).

1.2.2 The Quartz Surface.

The 'clean' or freshly fractured quartz surface is highly reactive and it is this surface reactivity which is of prime importance in determining the adverse effects on the lung, since it is the surface which makes contact with biological molecules and cell surfaces (Donaldson and Borm, 1998). The quartz surface has been shown to include reactive siloxane bridges (Si-O-Si) and silanols (SiOH). Reaction of water with the silica surface results in the hydrolysis of surface silicon-oxygen bonds, producing the surface silanol groups. It is these reactive silanol groups that can form hydrogen bonds with cell membranes, leading to damage and toxicity (Fubini, 1998a; Nash *et al.*, 1966). As mentioned previously, crystalline silica dusts of respirable size are usually generated by processes which involve the grinding of large crystals of quartz, or other polymorphs (Fubini, 1998a). Mechanical fracture does not commonly follow crystal planes so that the shape of the particles generated is extremely irregular, constituting sharp edges and points. Small particles (less than 50 nm in diameter) stick to bigger particles, firmly

held by the surface charges generated from grinding (Fubini, 1998b). Continued or prolonged milling progressively converts the outer parts of the particles from a crystalline state to an amorphous state, which is thought to lower the dust toxicity (Fubini, 1998). Removal of this amorphous outer layer (Beilby layer) from the quartz by chemical etching with hydrofluoric acid, produces an increase in the fibrogenicity of the dust (Engelbrecht *et al.*, 1958).

1.2.3 International Agency for Research on Cancer.

In 1987, the Carcinogen Identification Unit of the International Agency for Research on Cancer (IARC) considered quartz as part of its monograph series. IARC classified crystalline silica (quartz) as a Group 2 carcinogen i.e. a probable carcinogen, based on an evaluation stating that there was 'sufficient evidence' for carcinogenicity in experimental animals and 'limited evidence' for carcinogenicity in humans (IARC Monograph, 1987). In 1997, a follow-up meeting reclassified silica as a Group 1 carcinogen, concluding that there was 'sufficient evidence' for carcinogenicity in experimental animals and 'sufficient evidence' for carcinogenicity in humans (IARC Monograph, 1997). However, in light of the many studies showing no clear link between silica exposure and cancer, and abundant experimental evidence from cell and animal studies, part of the final evaluation stated that:

'In making the overall evaluation, the Working Group noted that carcinogenicity to humans was not detected in all industrial circumstances studied. Carcinogenicity may be dependent on inherent characteristics of the crystalline silica or on external factors affecting its biological activity or distribution of its polymorphs.'

This unique statement in an IARC monograph has engendered much debate about the validity and usefulness of the IARC quartz classification.

1.2.4 Variability In The Quartz Hazard.

The variability of the quartz hazard, reviewed by Donaldson and Borm (1998), helps to shed some light on the inconsistent association between lung cancer and quartz exposure. The key findings, from many studies, is that the reactivity of quartz can be reduced or modified by a range of substances that act upon its surface (Brown *et al.*, 1989; Fubini, 1998). There are several experimental studies that show the damaging effect of quartz can be modified (Donaldson and Borm, 1998). For instance, the haemolytic activity of quartz can be inhibited following coating with polyvinylpyridine-N-oxide (PVNO) (Stalder and Stober, 1965; Nash *et al.*, 1966). Coating with aluminium lactate has been reported to reduce cytotoxicity of quartz (Fenoglio *et al.*, 2000), and has been demonstrated to result in a reduction in the ability of quartz to cause pulmonary inflammation when instilled into the lungs of rats or sheep (Begin *et al.*, 1987; Brown *et al.*, 1989; Dufresne *et al.*, 1994). A reduction in the toxicity of quartz has also been demonstrated after iron treatment. Iron salts have been shown to protect against haemolysis *in vitro* and to limit the extent of inflammation *in vivo* (Nolan *et al.*, 1981; Cullen *et al.*, 1997). However, the oxidation state of the iron is likely to be a controlling factor in determining the surface reactivity. Although metallic iron can have the above inhibitory effects, ferrous or ferric iron contamination could result in Fenton chemistry-mediated generation of hydroxyl radicals, as has been suggested for some quartz samples (Castranova *et al.*, 1997). Various agents containing

lipid and protein can also decrease the harmful effects of the quartz surface (Antonini and Reasor, 1994; Wallace *et al.*, 1985), raising questions about how quartz acts in the lung when it is inevitably coated with these materials. Vallyathan *et al.* (1991) further demonstrated that the cell stimulatory and injurious effects of freshly fractured quartz could be lowered by coating the quartz with organosilane.

Further evidence towards the variability of the quartz hazard can be taken from several epidemiological studies. Scoring of small opacities on chest x-rays against cumulative quartz exposure in mg/m^3/year in a variety of industries, including Scottish coal miners, South African gold miners, granite workers and Ontario hard rock miners show a large variability in the silicosis risk across these different epidemiological studies, again highlighting a variation or difference in the ability of these quartz-containing dusts to induce adverse effects throughout the range of differing exposure groups (Hnizdo and Sluis-Cremer, 1993; Miller *et al.*, 1998; Muir *et al.*, 1989; Ng and Chan, 1992).

1.3 Diseases Caused By Quartz Exposure.

1.3.1 Silicosis.

Silicosis is the name given to the fibrotic lung disease caused by the inhalation of crystalline silica (quartz). Due to the ubiquity of this mineral the possibilities of exposure to the dust are numerous and almost any occupation involving the mining into or the cutting, shaping or polishing of rock can be associated with a risk of silicosis (Seaton, 1995). Silicosis is by no means a recent problem. A man-made disease, it is probably as old as human history and was known to the ancient Egyptians and Greeks

(Corn, 1980). It was later further described by Agricola , in his work on mining and metals in *De re metallica* published in 1556 and also by Ramazzini in the 18th century, describing the diseases afflicting miners (Seaton, 1995).

The pathology of the disease is such that the silicotic lung is firm and blacker in colour than normal (Rom, 1992). The surface of the lung is coarse and nodular, with the visceral pleura having areas of fibrosis and may even be covered by plaque-like lesions (Seaton, 1995). In individuals with silicosis, the peribronchial and hilar lymph nodes are typically enlarged (Balaan and Banks, 1992). The silicotic nodule is the pathologic hallmark of silicosis. Microscopically, these early lesions are characterised by nodular aggregates of dust-laden macrophages arranged around a collagenous central region, which is often acellular. With time, the central collagen becomes distinctly whorled and the relative number of inflammatory cells around the periphery decreases (figure 1.3.1a). Several of these nodules may appear to become confluent to produce the very large lesions of progressive massive fibrosis (PMF) (Seaton, 1995; Mossman and Churg, 1998) (figure 1.3.1b). Under polarised light microscopy, birefringent particles may be seen in the centre of the nodule, likely the result of trapped crystalline silica mixed with other dusts.

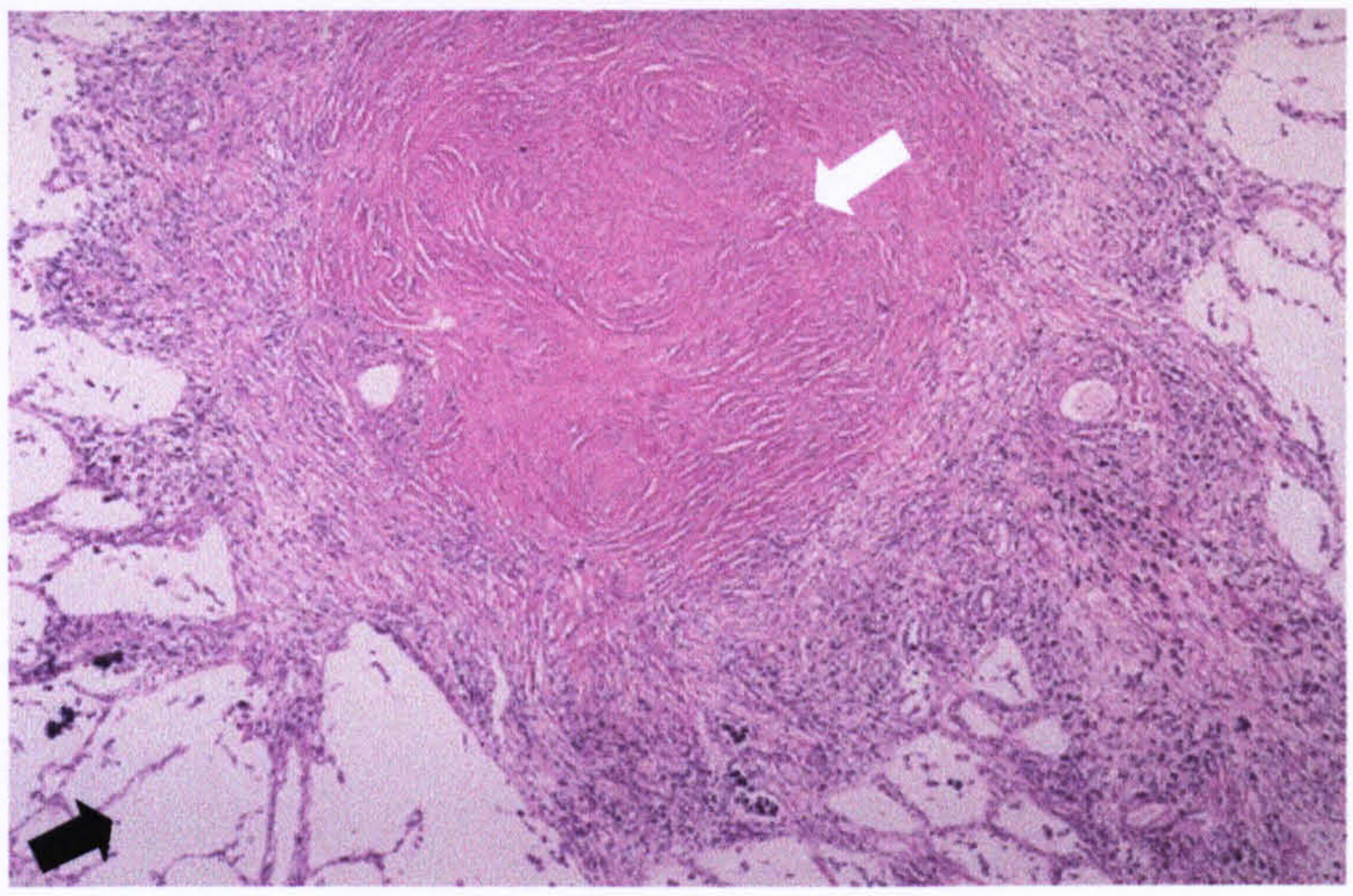

Figure 1.3.1a *Histological section of a silicotic nodule stained with hematoxylin and eosin. White arrow shows the characteristic whorls of acellular hyalinized collagen, surrounded by a rim of fibroblasts and inflammatory cells, resulting in a net loss of lung function. Black arrows shows normal lung tissue. (adapted from www-medlib.med.utah.edu)*

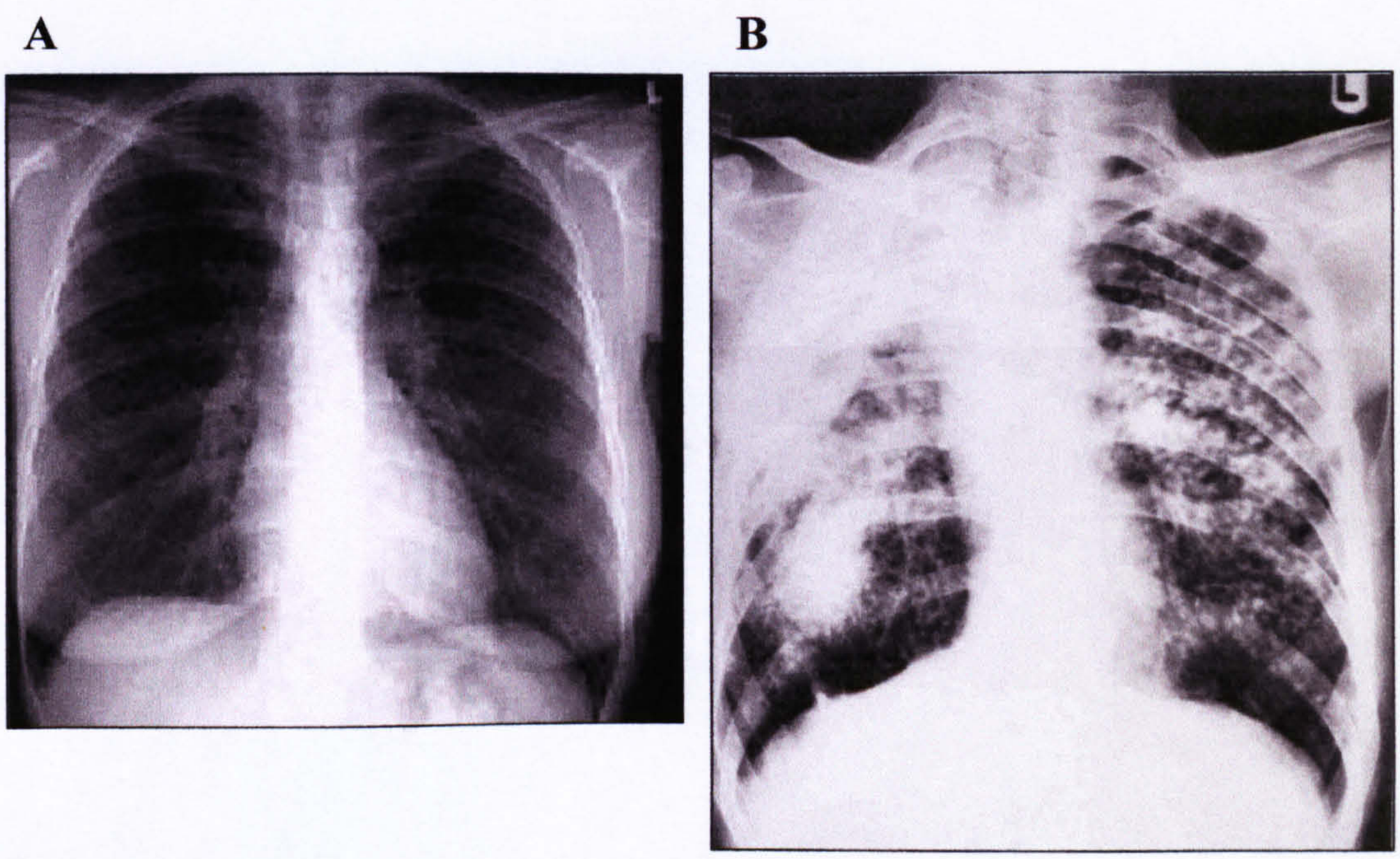

Figure 1.3.1b ***A****. Normal Chest X-ray.* ***B****. Chest X-ray of complicated silicosis, taken from a Welsh lead miner with heavy exposure to silica dust. (From Morgan and Seaton, Occupational lung diseases.) On the X-ray, radio-opaque nodules are apparent as white areas, some confluent.*

There are three types of silicosis, depending on the extent of the exposure to quartz. These are chronic (or classic) silicosis, accelerated silicosis and acute silicosis.

1.3.1.1 Chronic Silicosis.

Chronic or classical silicosis is the most frequently recognised clinical presentation of silicosis. It results from low to moderate exposure levels of silica dust for 20 years or more. Patients may complain of cough, sputum or breathlessness, however these symptoms are more likely to be related to accompanying disease of the airways (Seaton, 1995). The primary health concerns associated with chronic silicosis are mycobacterium infections and progressive massive fibrosis (PMF), which causes respiratory impairment. Large opacities develop in the upper lung zones, resulting in restriction of lung volumes and a decrease in gas transfer (Rom, 1992; Seaton, 1995).

1.3.1.2 Accelerated Silicosis.

Accelerated silicosis results from exposure to higher concentrations of silica over a period of 5 – 10 years. Progression of the disease is almost certain, even if the worker is removed from the workplace. Furthermore, antinuclear antibodies and clinical autoimmune connective tissue diseases are frequently associated with accelerated silicosis (see 1.3.3) (Balaan and Banks, 1992). Several rapidly progressive and fatal cases have been described in sandblasting (Bailey *et al.*, 1974) and stonemasonry with high-quartz sandstone (Seaton *et al.*, 1991). There is no effective treatment for this condition, other than lung transplantation.

1.3.1.3 Acute Silicosis.

Acute silicosis is the most frequent yet the most devastating form of this disease. Occurring in subjects exposed to very high concentrations of silica over periods of as little as a few weeks (Seaton, 1992), it was first described by Middleton in 1929 as an occupational hazard for those involved in the production of abrasive soap powders (Middleton, 1929). The disease may present as a result of occupations such as sandblasting and drilling through silica-containing rock e.g. Hawk's Nest tunnelling disaster (see 1.2.1). The history of the disease is typically one of progressive dyspnoea (shortness of breath), fever, cough and weight loss after a heavy but relatively short exposure to silica. The exposure may vary from a few weeks to 4 or 5 years, with death occurring from respiratory failure (Seaton, 1995). Again, the lack of any effective treatment renders such patients suitable candidates for lung transplantation.

1.3.2 Cancer.

Many animal studies and human epidemiological studies have addressed the issue of whether crystalline silica plays an important role in the development of lung cancer. Respirable crystalline silica, in the form of quartz or cristobalite, in occupational settings has been classsified as a human carcinogen (IARC, 1997) but debate continues concerning the mechanism of action (Donaldson and Borm, 1998; Hessel *et al.*, 2000). It is not yet known whether crystalline silica can react directly with cellular DNA or to cause endogenous oxidative stress in exposed cells which in turn can cause oxidative adducts leading to mutations i.e. acting as a primary or direct genotoxin, or whether the resultant chronic inflammation following silica exposure is a prerequisite to tumour formation, i.e. acting as a secondary or indirect genotoxin. Support for this secondary

pathway comes from chronic inhalation studies in rats which have demonstrated the occurrence of lung tumours by quartz particles, but also at high 'overload' exposure for low toxicity dusts such as carbon black and titanium dioxide (Lee *et al.*, 1985; Muhle *et al.*, 1989a; Gallagher *et al.*, 1994). In these exposure conditions in rats a situation of persistent inflammation and epithelial cell proliferation occurs and as such, inflammatory cell-derived reactive oxygen species (ROS) and growth factors have been implicated respectively for secondary (indirect) genotoxic and proliferating events that lead to the tumour formation by these poorly soluble dusts (Oberdorster, 1995,1997; Borm and Driscoll, 1996).

Animal studies, in particular studies in rats, provide compelling evidence that the carcinogenicity of quartz occurs in a dose-dependent manner. These tumours are usually found in close proximity to silicosis lesions (Saffiotti *et al.*, 1998; Muhle *et al.*, 1989b). In other species such as mice and hamsters, quartz has not been found to be carcinogenic. It is generally recognised that the rat is more sensitive than other rodents to the effects of inhaled particles (Saffiotti *et al.*, 1993). The rat response to long term quartz exposure results in fibrosis, epithelial cell hyperplasia and lung tumours, including malignant neoplasms. In contrast, mice develop fibrosis but no epithelial cell hyperplasia or lung tumours. Hamsters develop granulatomous, 'silica storing' lesions but no fibrosis or tumours (Saffiotti *et al.*, 1993; Williams and Saffiotti, 1995). Interestingly however, the rat neoplastic response resembles a human fibrosis-associated lung cancer known as scar cancer (Williams and Saffiotti, 1995) and the rat is the only rodent species that exhibits lung cancer as observed in some human studies (Kuempel *et al.*, 2001).

Epidemiological studies have reported an increased risk of lung cancer in humans with occupational exposure to respirable quartz. Exposure-response relationships have been demonstrated in several studies, ranging from diatomaceous earth workers (Rice *et al.*, 2001) to industrial sand workers (McDonald *et al.*, 2001). As in most cases, there are however exceptions. Just as there are studies supporting the relationship between silica exposure and lung cancer (Hessel *et al.*, 1990; Checkoway *et al.*, 1993) there are also studies which fail to demonstrate this relationship (Hessel *et al.*, 1986; Kusiak *et al.*, 1991). In studies of occupational exposure to respirable coal mine dust, which contained quartz, no increased lung cancer has been observed (Kuempel *et al.*, 1995; Miller and Jacobsen, 1985). In such a situation, it is highly possible that the quartz particles are coated with other substances within the dust thus inactivating the reactive surfaces considered important in quartz pathogenicity (see 1.2.2 and 1.2.4). With regard to some of the conflicting epidemiological evidence, a reasonable explanation could be that, in some circumstances, exposure to respirable crystalline silica is carcinogenic, but not in others and so adding further weight to the idea that quartz is indeed a variable entity.

1.3.3 Other Diseases.

Exposure to silica can result in, or contribute to, many other diseases including pulmonary tuberculosis, interstitial fibrosis, small airway disease, industrial bronchitis, emphysema, rheumatoid complications, glomerulonephritis and immunological reactions (Ding *et al.*, 2002).

Workers with silicosis are at an increased risk for developing tuberculosis despite the reduced prevalence of tuberculosis in the general population. This was shown in a

study by Cowie (1994), where a cohort of 1,153 South African gold miners with and without silicosis, were followed for 7 years by a routine mine surveillance program for the detection of tuberculosis. The incidence of tuberculosis during this 7 year study suggested that one quarter of the men with silicosis would have developed tuberculosis by the time they were 60 years old (Cowie, 1994).

Autoimmune diseases have been linked to silica or silicosis including rheumatoid arthritis, systemic sclerosis (scleroderma) and systemic lupus erythematosis (Craighead *et al.*, 1988). Increases in serum polyclonal immunoglobulins associated with increased levels of circulating rheumatoid factor, anti-nuclear antibodies and immune complexes are often associated with these conditions (Ding *et al.*, 2002), however little is known of the actual mechanisms involved.

1.4 Mechanisms Of Lung Diseases Caused By Quartz.

1.4.1 The Generic Role of Reactive Oxygen Species.

Reactive oxygen species (ROS) is a collective term often used to describe oxygen radicals, such as the hydroxyl radical ($^{\bullet}OH$), peroxyl radicals ($RO_2^{\bullet}$), alkoxyl radicals ($RO^{\bullet}$) and superoxide ($O_2^{\bullet-}$). The term also applies to certain non-radicals that are either oxidising species or that can be easily converted into radicals. These include hypochlorous acid (HOCl), hydrogen peroxide (H_2O_2), ozone (O_3) and singlet oxygen ($^1O_2$). Reactive nitrogen species (RNS), is a similar collective term that includes nitric oxide radical ($NO^{\bullet}$), peroxynitrite ($ONOO^-$) and the nitrogen dioxide radical ($NO_2^{\bullet}$).

The potential for generation of free radicals in tissue was discovered less than 50 years ago (Commoner *et al.*, 1954). In 1956, Denham Harman hypothesised that oxygen radicals may be formed as by-products of enzymatic reactions *in vivo* and described free radicals as a 'Pandora's box of evils' that may account for gross cellular damage, mutagenesis, cancer and, last but not least, the degenerative process of biological ageing (Harman, 1956). In cellular systems, unintended or accidental generation of the most common of the ROS (i.e. $O_2^{\bullet-}$, $^{\bullet}OH$, H_2O_2) may occur via leakage from mitochondrial respiration and can account for approximately 1-2% of the total oxygen consumption under reducing conditions (Freeman and Crapo, 1982). This also includes auto-oxidation of small molecules such as dopamine, flavins and hydroquinones which can be an important source of intracellular ROS. In most cases, the direct product of such auto-oxidation reactions is $O_2^{\bullet-}$ (Freeman and Crapo, 1982). Interestingly, there is a suggestion that the direct effects of dopamine auto-oxidation may be involved in the dopamine-induced apoptosis (programmed cell death) that is implicated in the pathogenesis of neurodegenerative diseases such as Parkinson's disease (Yoshikawa *et al.*, 1994; Offen *et al.*, 1996, 1997).

In contrast, ROS can also be endogenously generated by deliberate synthesis in a variety of cell types, including fibroblasts, endothelial cells and lung epithelial cells (Meier *et al.*, 1990; van Klaveren *et al.*, 1997; Arroyo *et al.*, 1990). Peroxisomes (organelles which function to rid the body of toxic substances) are an important source of total cellular H_2O_2 production as they contain a number of H_2O_2-generating enzymes including glycolate oxidase, D-amino acid oxidase, urate oxidase and catalase (Boveris *et al.*, 1972). Peroxisomal catalase utilises H_2O_2 produced by these oxidases to oxidise a variety of other substrates in 'peroxidative' reactions (Tolbert and Essner, 1981).

These types of oxidative reactions are particularly important in liver and kidney cells, where peroxisomes detoxify a number of toxic molecules e.g. ethanol, that enter the circulation (Thannickal and Fanburg, 2000).

The most significant and important cellular ROS/RNS generating system in the lung, is brought about by the pool of inflammatory phagocytes. Vast amounts of oxidants are produced during their role in host defence and these not only kill invading micro-organisms but can also prove to be detrimental to neighbouring host tissues. The first observation that oxygen species may be involved in the defence function of phagocytes was the discovery of the 'respiratory burst' by Baldridge and Gerard (1933), who found that neutrophils displayed an immediate increase in oxygen uptake upon exposure to bacteria. This increase in oxygen consumption was though to arise from a need for oxygen to supply energy for the ingestion of the microorganisms. However, this was later thought not to be the case following the discovery that activated neutrophils produced hydrogen peroxide (Iyer *et al.*, 1961). Klebanoff (1967) contributed further to the understanding of the mechanism of ROS production by phagocytes with the discovery of the enzyme myeloperoxidase (MPO). Klebanoff showed that MPO catalysed the reaction between H_2O_2 and chloride to generate the highly potent PMN microbicidal compound HOCl (Klebanoff, 1967) .

The spectrum of oxidants initially generated by phagocytes, can be thought of as occurring via the action of four different enzymes, catalysing different reactions. NADPH-oxidase is the enzyme by which oxidant generation is initiated. It is a membrane-bound enzyme that is usually dormant in resting cells but which, when activated, carries out a one electron reduction of molecular oxygen. When a cell is

activated via phagocytosis of either microorganisms or particles, the enzyme is assembled to the active form. NADPH-oxidase is composed of a number of subunits which are distributed in the cytoplasm and the membranes of intracellular vesicles and organelles. Following activation, the cytoplasmic subunits migrate to the membranes where they bind to membrane-associated subunits, assembling the active oxidase. The intracellular organelles then fuse with the plasma membrane resulting in the release of $O_2^{\bullet-}$ into the extracellular environment and into the phagocytic vesicle (Babior, 1999; 2000). Soluble activators, including the pro-inflammatory cytokines interleukin-8 (IL-8) and tumour necrosis factor-alpha (TNF-α) are also recognised as specific and potent activators of the oxidative burst of neutrophils in the lung (Nathan, 1987; Djeu *et al.*, 1990).

The enzyme superoxide dismutase (SOD) was first discovered in 1969 by McCord and Fridovich. It catalyses the formation of hydrogen peroxide from superoxide in a reaction known as dismutation, due to the fact that $O_2^{\bullet-}$ reacts with itself to generate an oxidised and a reduced product (O_2 and H_2O_2). Hydrogen peroxide is relatively stable and is known for its capacity to diffuse across cellular membranes. In doing so, this provides the phagocyte with the capacity to act at a distance. In neutrophils, much of the H_2O_2 is consumed by the enzyme MPO. The main product of the reaction of MPO with H_2O_2 is HOCl, due to the relatively high concentrations of chloride ions (Cl^-) in body fluids. MPO is a haem enzyme and is present in very high concentrations in neutrophils (5% of dry weight). MPO also has a strong green colour, causing the green colour often observed with 'pus' in inflamed tissue (Klebanoff, 1967; 1999). Finally, the fourth enzyme, nitric oxide synthase (NOS) catalyses the production of $NO^{\bullet}$ from L-arginine, O_2 and NADPH. Typically, there are two forms of the enzyme. The

constitutive form (cNOS) produces small amounts of $NO^{\bullet}$ for signalling purposes and is mainly found in the vascular endothelial cells and in the nervous system. In contrast, the inducible form (iNOS) is produced by phagocytes following specific stimulation and is able to generate large amounts of $NO^{\bullet}$ (Hevel *et al.*, 1991; Weinberg *et al.*, 1995). It is well documented that macrophages generate nitric oxide in response to cytokines, LPS or particles in an iNOS-mediated reaction (Gross *et al.*, 1998; Huffman *et al.*, 1998).

1.4.1.1 Oxidative Stress and Antioxidant Defences in the Lung.

To combat ROS, the lung has a number of antioxidant defences which detoxify harmful oxidants and are crucial in maintaining the oxidant/antioxidant balance (Rahman and MacNee, 1996). When this balance is upset, either by the accumulation of oxidants and/or the depletion of antioxidants, a state of intracellular or extracellular oxidative stress is induced, resulting in the detrimental changes to biological molecules. Antioxidant defences can generally be divided into enzymatic and non-enzymatic forms and into extracellular and intracellular defence systems. The first line of defence against inhaled oxidants are the extracellular antioxidant defence systems present in the epithelial lining fluid (ELF). ELF contains enzymatic antioxidants such as SOD, catalase and glutathione peroxidase, as well as low molecular weight antioxidants such as ascorbate (vitamin C), uric acid, glutathione and alpha tocopherol (vitamin E) (van der Vliet *et al.*, 1999; Rahman and Macnee, 2000). A second line of antioxidant defence is found within the lung target cells themselves, again consisting of both enzymatic and non-enzymatic antioxidant mechanisms. The resistance to oxidants may differ greatly between various lung target cells, mainly due to differences in the

antioxidant capacity of particular target cell. For example, rat alveolar type II cells and Clara cells are known to be specific target cells for particle-induced carcinogencity (Johnson *et al.*, 1987; Driscoll *et al.*, 1997), despite containing higher amounts of catalase compared to endothelial cells and pleural mesothelial cells. However when compared with alveolar macrophages, these levels are relatively low (Kinnula *et al.*, 1992; Kinnula *et al.*, 1995). As such, it is likely that the vulnerability of a particular site in the lung to oxidative stress is determined not only by the local level and characteristics of oxidant exposure, but also by the level and specificity of the antioxidant capacity of the target cells.

1.4.2 Generation of Reactive Oxygen Species by Quartz.

Freshly fractured quartz surfaces have been found to be more fibrogenic than aged surfaces (Vallyathan *et al.*, 1995). Mechanical cleavage of chemical bonds usually produces a very reactive surface, in terms of surface radicals ($Si^{\bullet}$ and $Si\text{-}O^{\bullet}$) and ROS (Figure 1.4.2), and the state of the surface depends on the environment in which the cleavage takes place (Fubini *et al.*, 1989; Costa *et al.*, 1991). In aqueous media, the $Si^{\bullet}$ and $Si\text{-}O^{\bullet}$ radicals on the fracture planes of the quartz particles can generate highly reactive hydroxyl radicals ($^{\bullet}OH$) via the Fenton reaction (see Figure 1.4.2) due to trace amounts of ferrous iron as an impurity on the quartz particle (Castranova *et al.*, 1995). Reaction of water with the silica surface results in the hydrolysis of surface silicon-oxygen bonds, producing the surface silanol groups. It is these reactive silanol groups that can form hydrogen bonds with cell membranes, leading to damage, toxicity and oxidative stress (Fubini, 1998; Nash *et al.*, 1966).

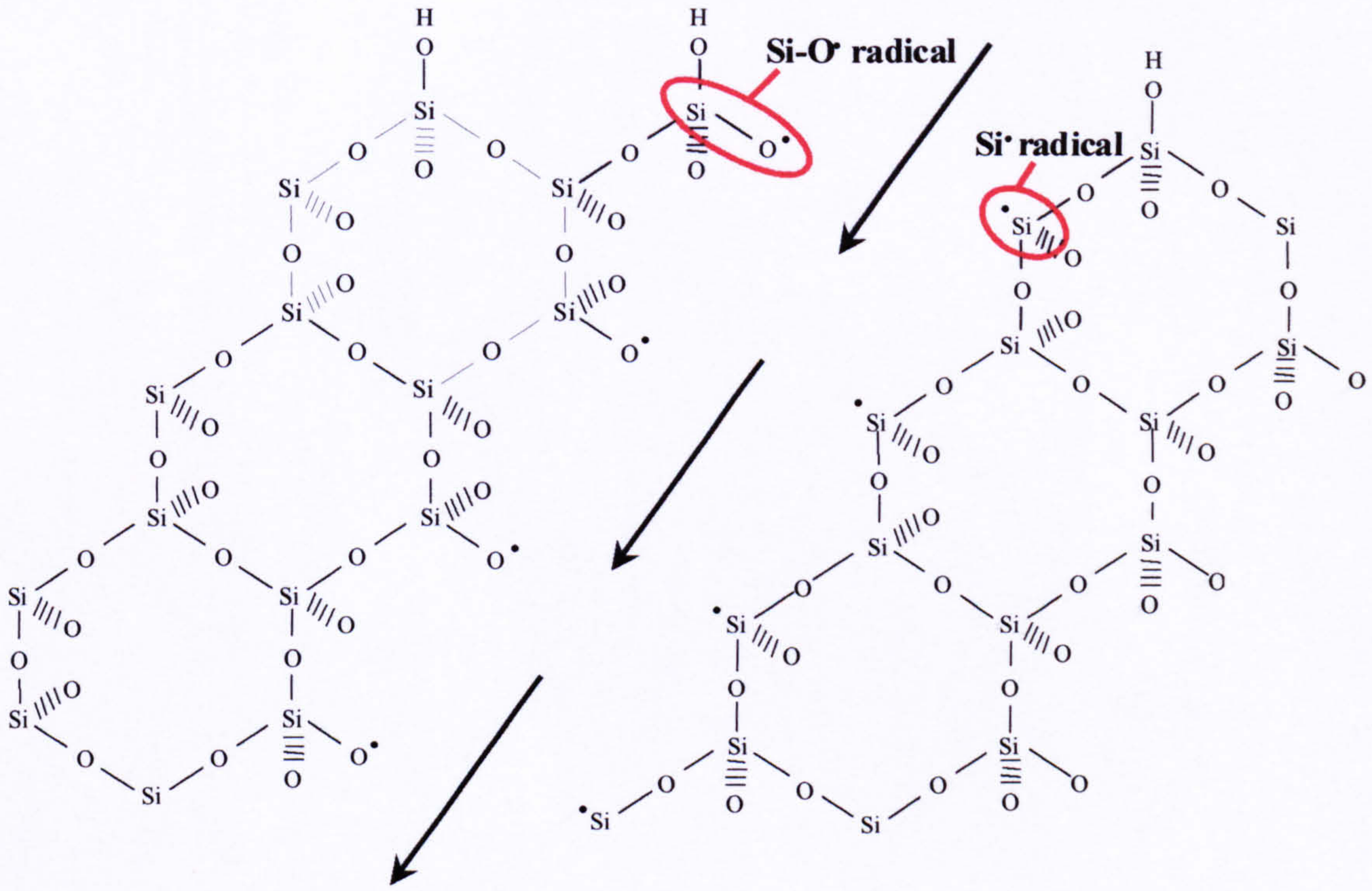

In solution

$$Si\text{-}O^{\bullet} + H_2O \longrightarrow SiOH + {}^{\bullet}OH$$

$$Si\text{-}O^{\bullet} + {}^{\bullet}OH \longrightarrow SiOOH$$

$$SiOOH + H_2O \longrightarrow SiOH + H_2O_2$$

$$Fe^{2+} + H_2O_2 \longrightarrow Fe^{3+} + {}^{\bullet}OH + OH^{-}$$

Figure 1.4.2. *Schematic diagram of the crystalline lattice structure of quartz. Fracture of the crystalline lattice generates $Si^{\bullet}$ and $Si\text{-}O^{\bullet}$ radicals on the quartz surface and as shown in the chemical equations can lead to the production of hydroxyl radicals via Fenton chemistry. (Diagram based on an original by Prof. Bice Fubini, Italy).*

1.4.3 Cytotoxicity.

Cytotoxicity is generally used as a term to describe the potential for a compound to induce cell-killing. In principle, there are two mechanisms involved in cytotoxicity, necrosis and apoptosis.

1.4.3.1 Necrosis.

Necrosis is the pathological process which occurs when cells are exposed to physical or chemical insult. Cell death via necrosis is a passive event, where there is loss of cell membrane integrity and release of the cellular contents which may result in an inflammatory response (Majno and Joris, 1995).

1.4.3.2 Apoptosis.

Apoptosis or programmed cell death, is a biological process by which cells die via a coordinated series of events and during which the integrity of the cell membrane is maintained. It is a non-inflammatory form of cell death where there is no release of pro-inflammatory cell contents, as is the case with necrosis and the membrane bound cell products are taken up 'silently' by adjacent cells and macrophages. Apoptosis is a distinct form of cell death characterised by cell shrinkage, plasma membrane blebbing, nuclear chromatin condensation and DNA fragmentation. Different from necrosis, apoptosis is a genetically controlled, active cell death process which has been implicated as a critical physiological or pathological mechanism in development and tissue homeostasis as well as in many diseases including cancer (Wyllie *et al.*, 1999). Although the mechanisms of apoptosis have not been fully established, activation of cysteine proteases called caspases play a critical role in the execution of apoptosis (Budihardjo *et al.*, 1999; Thornberry, 1998). Among the various caspases, caspase-9

and caspase-3 seem to be particularly important. Procaspase-9 forms an important part of the apoptosome, the functional unit of apoptosis, resulting in caspase-9 activation. The then activated caspase-9 cleaves downstream caspases such as caspase-3, initiating the biochemical execution of apoptosis. Caspase-3 is one of the major effector caspases and plays an important role in the characteristic apoptotic changes mentioned earlier, i.e. chromatin condensation, DNA fragmentation and formation of apoptotic bodies (Green and Reed, 1998; Kuida, 2000; Porter and Janicke, 1999). It has been shown, in several studies, that quartz is able to induce apoptosis in alveolar macrophages (considered as the principle target cells in quartz exposure) (Iyer *et al.*, 1996, 1997; Leigh *et al.*, 1997). More recently, in a study by Shen *et al* (2001), quartz-induced apoptosis in alveolar macrophages was associated with ROS production and activation of caspase-9 and caspase-3. The authors suggested that elevated ROS levels resulting from silica exposure may act as an initiator, leading to caspase-9 and caspase-3 cleavage and hence the execution of the apoptotic process.

1.4.4 Cell Signalling.

Much emphasis is now placed on understanding how harmful agents cause inflammation, especially the signalling pathways. These are the molecular pathways that lead from the initial contact between the particle (in this case) and expression of genes which play an important role in inflammation. Considerable progress has been made in understanding the pathways for a number of pathogenic particles and those of likely or proven importance to quartz effects are described.

1.4.4.1 Mitogen Activated Protein Kinases.

The mitogen-activated protein kinases (MAPK) are a super-family of protein kinases that are ubiquitously expressed in mammalian cells and are strongly involved in signal transduction from the cell membrane to the nucleus via activation in response to extracellular stimuli (Karin, 1995). MAPK signalling is linked to transcriptional activation of several genes associated with important cellular events such as apoptosis, cell proliferation and development (Karin, 1995). Signalling occurs via the phosphorylation of a sequence of protein kinases by the transfer of a phosphate group from a molecule of ATP from one kinase to another (Chang and Karin, 2001). The first is the mitogen activated protein kinase kinase kinase (MAPKKK), which dually phosphorylates and activates the second member, mitogen activated protein kinase kinase (MAPKK) and this in turn then activates MAPK via dual phosphorylation (Cobb and Schafer, 1996). Important scaffold proteins bind these proteins in close proximity thereby allowing for the efficient transduction of the signal through these cascades (Catling *et al.*, 2001). The MAPK family is divided into three signalling pathways: extracellular-signal-regulated kinases (ERK), the c-Jun N-terminal kinases (JNK) and p38 (Kyriakis and Auvruch, 2001).

1.4.4.2 NF-κB.

Nuclear factor-kappa B (NF-κB) is a collective term referring to ubiquitously expressed redox-sensitive transcription factors, belonging to the Rel family of proteins. These proteins are characterised by the presence of a Rel homology domain i.e. a conserved region of approximately 300 amino acids responsible for sequence specific DNA-binding, dimerisation, nuclear localisation and interaction with inhibitory proteins

(Chytil and Verdine, 1996). NF-κB classically exists as a p65/p50 heterodimer, although it may also be found as a p50/p50 homodimer or a p50/105 heterodimer. NF-κB is found in the cytoplasm of resting cells in an inactive state bound to the inhibitory protein I kappa B (IκB), a member of a family of inhibitory proteins which function to prevent the nuclear translocation of NF-κB by masking the nuclear localisation sequence (Rahman and MacNee, 1998) (Figure 1.4.4.2). NF-κB may be activated in response to various forms of oxidative stress, such as ozone and hydrogen peroxide. Pro-inflammatory cytokines such as tumour necrosis factor-alpha (TNF-α) and interleukin-1 beta (IL-1β) are also capable of activating NF-κB via receptor-mediated mechanisms (Karin and Delhase, 2000). Intracellular signalling proteins such as NF-κB-inducing kinase (NIK) lead to the activation of the inhibitory kappa B kinase (IKK). IKK is among a family of closely related proteins which is comprised of IKK-α, IKK-β, IKK-γ. When activated, IKK causes the phosphorylation of IκB on serine residues 32 and 36, resulting in its ubiquitination and degradation by the 26S proteosome (Karin and Ben-Neriah, 2000). The unveiling of the nuclear localisation sequence of NF-κB opens the way for its translocation to the nucleus where it is free to activate transcription via binding to specific κB-concensus motifs within gene promoter loci (Baldwin, 1996). Genes which have κB-concensus motifs include pro-inflammatory cytokines such as TNF-α, IL-1β, IL-8 and IL-6. Also included are iNOS, growth factors, chemokines and adhesion molecules (Rahman and MacNee, 1998; Janssen *et al.*, 1998).

Importantly, NF-κB has the ability to auto-regulate its own activity via the transcription of IκB. IκB is synthesised in the cytoplasm after which it then migrates to the nucleus

and binds to NF-κB and in doing so, switches off NF-κB-mediated transcription. NF-κB is an oxidative stress-responsive transcription factor (Rahman and MacNee, 1998) that is involved in the pro-inflammatory effects of many pathogenic particle types including quartz (Schins and Donaldson, 2000). Activation of NF-κB has been previously reported following quartz exposure in rats (Sachs *et al.,* 1998) and *in vitro* as shown by IκB depletion (Schins *et al.,* 2000). In addition, NF-κB-dependent genes are up-regulated after quartz exposure of cells (Rojanasakul *et al.,* 1997; Schins *et al.,* 2000; Driscoll *et al.,* 1996).

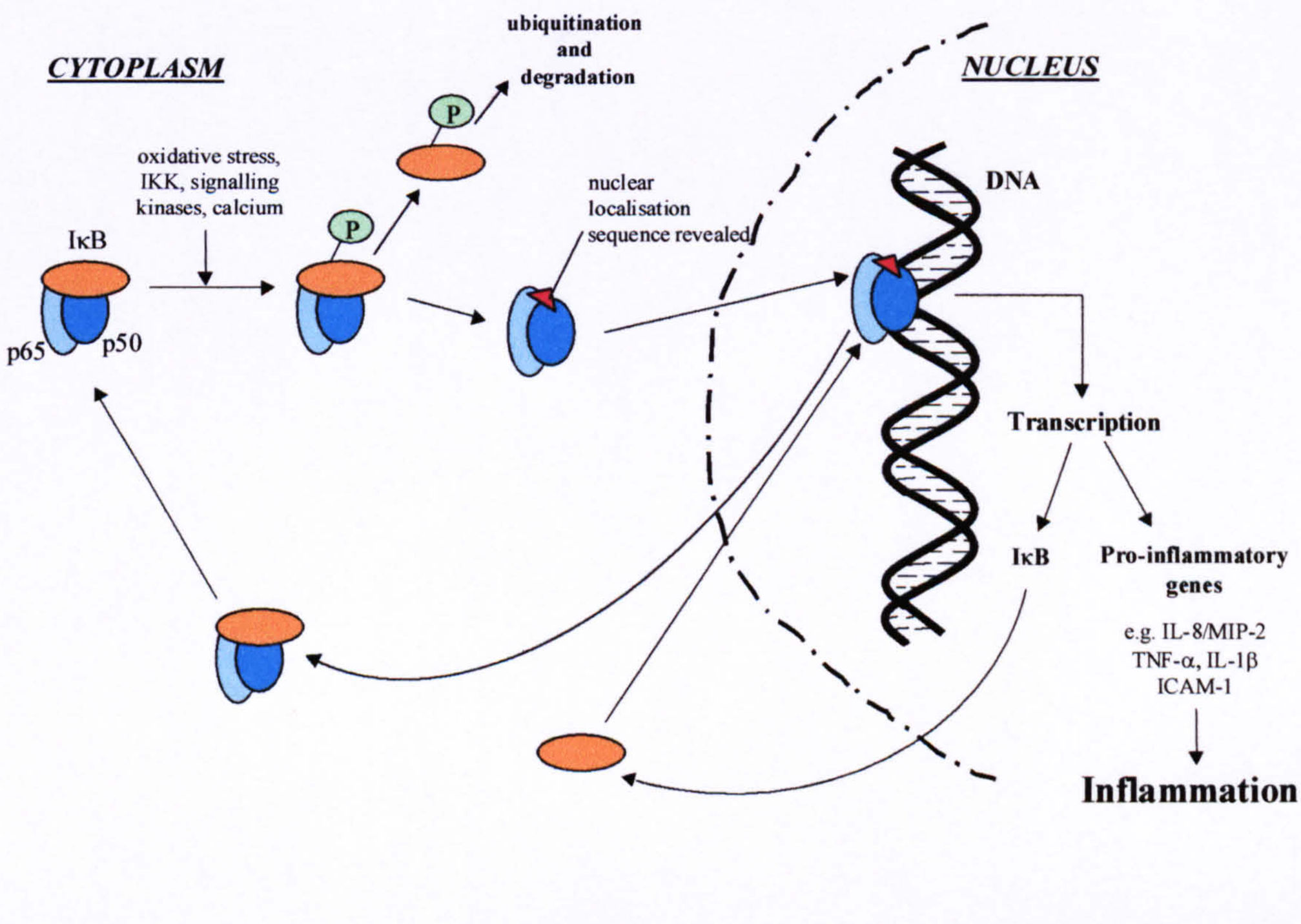

Figure 1.4.4.2 *Diagram showing the regulation of NF-κB-stimulated gene transcription.*

1.4.5 Inflammation.

Chronic inflammation is considered the hallmark of quartz-induced lung injury (Castranova and Vallyathan, 2000). It can be hypothesised that this inflammation plays a key role in the pathological sequence which leads to cancer in quartz exposed lungs (Figure 1.4.5). Chronic inhalation of many harmful mineral dusts is known to result in an inflammatory state in the lung, characterised by leukocyte recruitment and enhanced expression of proinflammatory cytokines and chemokines which are commonly regulated by the oxidative stress-responsive transcription factor NF-κB (Driscoll *et al.*, 1990; Schins *et al.*, 2000).

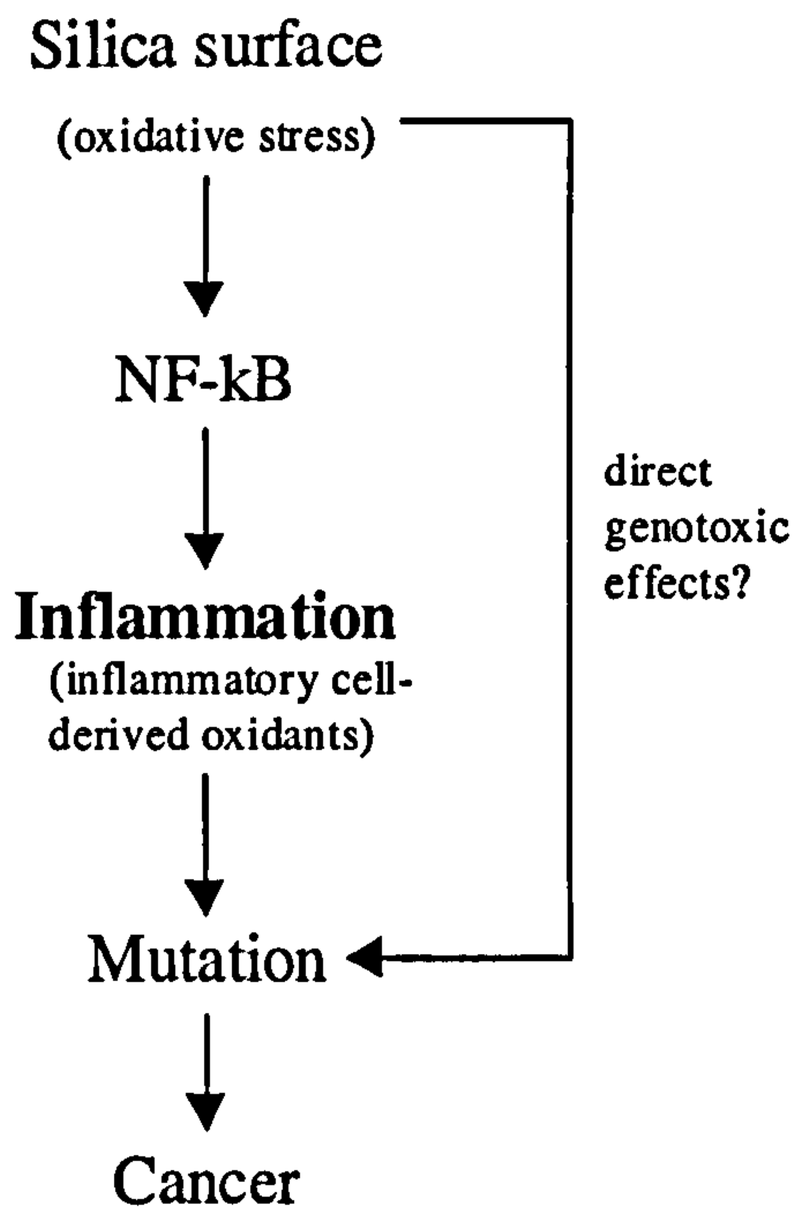

Figure 1.4.5 *Likely role of inflammation in the gentotoxic and carcinogenic effects of quartz*

1.4.5.1 Chemokines.

The chemokines (chemotactic cytokines) are a group of small proteins that play an important role in attracting leukocytes and regulating their recruitment to tissues during inflammation (Luster, 1998). The chemokines can be divided into three subfamilies based on structural and functional considerations. The C-X-C chemokine structure consists of the first two NH_2-terminal cysteines being separated by one non-conserved amino acid. In contrast, the C-C chemokine structure is such that the first two NH_2-terminal cysteines are adjacent to one another and finally, the C chemokines contain one lone NH_2-terminal cysteine (Driscoll, 2000).

Interleukin-8 (IL-8) is a 10 kD, C-X-C chemokine which has the potent ability to elicit attraction and activation of neutrophils and as such is a crucial factor in lung inflammation (Kelley, 1990). A wide variety of cells have the ability to secrete IL-8 (Mukaida *et al.*, 1998). Monocytes and macrophages are potent sources of IL-8, particularly in response to proinflammatory mediators such as TNF-α and IL-1 (Metinko *et al.*, 1992). A study by Schins *et al* (2000), demonstrated that treatment of human pulmonary epithelial cells (A549) with quartz enhanced both IL-8 expression and production which were in line with other investigators who have reported dose-dependant increases in IL-8 production from epithelial lung cells exposed to quartz particles (Steerenberg *et al.*, 1998; Stringer and Kobzik, 1998).

Macrophage inflammatory protein-2 (MIP-2), the rat IL-8 homologue, is a 6 kDa C-X-C chemokine. It plays a major role in mediating the recruitment of neutrophils following exposure to harmful particles. This was effectively illustrated in studies by Driscoll *et al.*, who showed that pre-treatment of rats with an antibody to MIP-2 prior to

exposure to quartz particles, resulted in a 60% reduction in neutrophil recruitment (Driscoll *et al.*, 1993, 1995). MIP-2 can be produced by non-immune cells such as epithelial cells and fibroblasts. In rats exposed to quartz, the predominant cell type expressing MIP-2 mRNA 2 hrs post exposure, was the epithelial cells in the terminal bronchioles. At later time points, alveolar macrophages as well as recruited neutrophils were observed to be expressing MIP-2 (Driscoll *et al.*, 1996).

1.4.5.2 TNF-α.

The cytokine tumour necrosis factor-alpha (TNF-α), belongs to a family of structurally related molecules known as the TNFα-ligand family (Bazzoni and Beutler, 1996). TNF-α has been recognised as a key early or initiating cytokine, as it is considered to be the initiator of pulmonary inflammation. It is produced rapidly by many different cell types in response to proinflammatory agents. Mononuclear phagocytes and in particular alveolar macrophages are potent sources of this cytokine (Rich *et al.*, 1989; Djeu *et al.*, 1990a). Recruitment of inflammatory cells is aided by TNF-α activation of endothelial cells to express adhesion molecules which facilitate cell attachment and emigration (Bevilacqua *et al.*, 1989; Driscoll, 2000). Phagocytic cells also are stimulated by TNF-α to produce potentially damaging reactive oxygen species and proteolytic enzymes (Klebanoff *et al.*, 1986; Warren *et al.*, 1988). TNF-α plays an important role as a mediator of the pulmonary response to particles. Studies showing the production of TNF-α by alveolar macrophages, *in vitro*, demonstrated that a variety of particles which induce marked lung inflammation can activate macrophages to release TNF-α (Dubois *et al.*, 1989; Driscoll *et al.*, 1990; Gosset *et al.*, 1991). In particle-exposed animal and human studies, TNF-α levels are increased, contributing further to the central role of this cytokine in the particle-induced inflammatory reaction (Zhang *et al.*, 1993;

Driscoll, 1994; Ghio *et al.*, 2001). Interestingly, a study by Piguet *et al.* (1990), showed that treatment of quartz-instilled mice, with an anti-TNF-α antibody was able to inhibit lung fibrosis (as measured by hydroxyproline levels) suggesting an important role for TNF-α in the mechanisms of silicosis. Importantly, TNF-α itself is not directly chemotactic for neutrophils or monocytes and so, its role in the recruitment of these cells is mediated indirectly through the induction of adhesion proteins on endothelial cells and stimulation of other cells, such as epithelial cells, to produce chemokines such as IL-8 (Driscoll, 2000).

1.4.6 Genotoxicity.

Initiation of the multistep carcinogenic process is mainly characterised by genotoxic processes, which may lead to irreversible changes in the structure of a cells genetic material. These changes (mutations) may involve a single gene, a block of genes or even whole chromosomes. The chemistry of DNA damage by several ROS has been well characterised. Generally, the reactions leading to ROS-induced DNA damage are oxidation, nitration, depurination, methylation and deamination (Wiseman and Halliwell, 1996). The most potent ROS that reacts with DNA is the hydroxyl radical (Spencer *et al.*, 1995), which can form the hydroxyl radical specific DNA lesion, 8-hydroxydeoxyguanosine (8-OHdG) (Schins *et al.*, 2002b). Numerous studies investigating the genotoxic properties of various particle types have been performed (reviewed by Schins, 2002). Particles, when compared with chemicals, form a rather specific group of possible genotoxins since their behaviour and characteristics (both physical and chemical) are very different and often complex. The genotoxic effects of poorly soluble particles in rats are closely associated with their ability to elicit an

inflammatory response (Driscoll *et al.*, 1996a; Greim *et al.*, 2001) and so necessitates the discrimination between primary (direct particle-induced) and secondary (inflammation-induced) particle genotoxicity. However, in both these mechanisms of particle-induced genotoxicity, ROS are known to play an important role (Schins, 2002). In terms of secondary (inflammatory cell-induced) gentoxicity, an *in vitro/in vivo* study by Driscoll *et al.*, (1995) took PMN-rich bronchoalveolar lavage (BAL) cells removed from rats instilled with 2 mg of quartz. When they were incubated overnight with a rat epithelial cell line they induced mutations in the hypoxanthine-guanine phosphoribosyl transferase (hprt) gene. These mutations could be significantly inhibited upon co-treatment of the BAL cells with superoxide dismutase, suggesting the a role for superoxide radicals. A further study by Knaapen *et al.* (2002), showed a significant increase in DNA strand breakage (as measured by the comet assay) in lung epithelial cells isolated from quartz-instilled rats, whereas no enhanced DNA strand breakage was observed when quartz was coated with either PVNO or aluminium lactate, treatments reported to reduce the surface reactivity of quartz (see 1.1.4). Inhibition of DNA damage by both coatings was paralleled by a reduction in neutrophil influx, suggesting an involvement of the neutrophil in the observed strand breakage, however, further investigations are warranted to elucidate the exact mechanism of this DNA damage.

In the case of quartz exposure, several *in vitro* studies have shown that the induction of 8-OHdG or DNA strand breaks could be directly linked to its capacity to generate ROS in aqueous suspension (Shi *et al.*, 1994; Van Maanen *et al.*, 1999; Schins *et al.*, 2002b), thus lending support to primary (direct particle-induced) gentoxic effects.

1.4.7 Cell Proliferation.

Alveolar type II epithelial cells respond by proliferating and differentiating into type I cells, following alveolar injury and during repair. Due to their ability to proliferate, type II cells are the main precursor cells which are transformed into adeno-carcinomas following inhalation of poorly soluble particles. The mechanism leading to initial proliferative events in these cells remains unclear (Albrecht *et al.*, 2002) but are likely to involve loss of contact inhibition and release of mitogens from activated cells. Studies in rats have shown an increase in epithelial cell proliferation and lung cancer after exposures to coal dusts (Nikula *et al.*, 1997; Friemann *et al.*, 1999). Albrecht *et al.* (2001) also showed that both alveolar type II epithelial cells and bronchiolar nonciliated Clara cells (stem cells of the bronchiolar epithelium) exhibited increased proliferation 130 weeks post intra-tracheal instillation with various quartz containing coal mine dusts. However, animals exposed to fine titanium dioxide (TiO_2), a non-pathogenic low toxicity particle, did not show this response. Alveolar macrophages are also thought to play a role in orchestrating proliferative responses in a variety of lung cells. Human macrophages activated via incubation with quartz, respond by secreting the cytokines insulin-like growth factor-1 (IGF-1) and transforming growth factor-beta (TGF-β), which stimulate lung fibroblasts and epithelial cells to proliferate (Olbruck *et al.*, 1998).

Despite decades of research, it is still unclear what properties of particles or related biological mechanisms play a role in quartz and/or coal mine dust induced fibrosis, epithelial injury or carcinogenesis (Schins and Borm, 1999). Evidence, however, exists for the involvement of ROS in the stimulation of cell signalling cascades that may trigger transcriptional events important in cell proliferation and repair from particle-induced injury (Mossman *et al.*, 2000; Schins and Donaldson, 2000). For example,

recent work has shown that quartz stimulates JNK (a member of the MAPK family – see 1.4.4.1), via the formation of hydroxyl radicals (Shukla *et al.*, 2001). The phosphorylation of MAPK signalling cascades is thought to result in the activation of a number of transcription factors linked to cellular responses such as differentiation and proliferation, including activator protein-1 (AP-1). AP-1 is comprised of homodimers of the Jun family or heterodimers of members of the Jun and Fos families and has been shown to be a key transcription factor causally associated with the development of epidermal cell proliferation and tumour promotion in a mouse skin model of carcinogenesis (Young *et al.*, 1999).

1.5 The Role Of Surface Reactivity.

1.5.1 The Surface Reactivity of Low and High Toxicity Dusts.

Chronic rat inhalation studies have shown that a number of different poorly soluble, low toxicity particle types have the ability to induce significant adverse health effects such as impaired lung clearance, chronic pulmonary inflammation, fibrosis and lung tumours (Oberdorster, 1996). These adverse effects are believed to arise due to the high lung burden of particles leading to a particle 'overload' situation in the lung. This overload-induced inflammation has been found to be related to particle dose, expressed as surface area rather than mass dose (Tran *et al.*, 2000). For a high toxicity particle, such as quartz, the inflammatory effects observed occur at a much lower lung burden and hence surface area, emphasising the involvement of the highly reactive quartz surface. Therefore a high lung burden of low toxicity particle surface or a low burden of high toxicity particle surface is likely to be inflammogenic.

1.5.2 Overload and its Associated Mechanisms.

As mentioned earlier in section 1.1.4, when particles reach the terminal bronchioles and proximal alveolar regions, they are rapidly detected by the 'patrolling' alveolar macrophages (AM). This particle-macrophage encounter normally results in the macrophage phagocytosing the particles and then transporting them to the mucociliary escalator for clearance. However, several experimental studies have shown that exposure to relatively high concentrations of inert dusts results in an impairment of particle clearance (Jones *et al.*, 1988; Muhle *et al.*, 1988). Tran *et al.* (1997) demonstrated that at low exposure concentrations, the dust clearance rate eventually approaches the daily rate of dust deposition. However, at higher exposure concentrations the clearance mechanism fails and as clearance becomes more and more impaired, the lung particle burden accumulates almost at a linear rate. In 1988, Morrow proposed the idea of volumetric overload. Here he hypothesised that dust overloading, which is typified by a progressive reduction of particle clearance from the deep lung, reflected a breakdown in AM-mediated clearance due to the loss of AM mobility. Overload was hypothesised to be initiated, based on the assumption of an even distribution of the whole particle burden over the AM population, when the particle volume exceeded 60 μm^3/AM. When the distributed particle volume exceeded approximately 600 μm^3/cell, the AM mobility would virtually cease and particle-laden macrophages would remain in the alveolar region (Morrow, 1988). However, studies by Tran and co-workers emphasised the role of surface area where an accumulated surface area lung burden of 300-600 cm^2 in a rats lung is the onset of impaired clearance and inflammation i.e. overload (Tran *et al*, 2000). This was also confirmed by onset of overload in rats inhaling ultrafine particles at a relatively low volumetric burden but a

high surface area burden (Oberdorster, 2001). Studies carried out by Renwick and co-workers may also be of importance. These *in vitro* studies showed that ultrafine particles were more likely to impair phagocytosis of AM's to a greater extent when compared to fine particles, at equal mass dose (Renwick *et al.*, 2001).

1.5.3 Ultrafine Particles.

Particles that are less than 100 nm in diameter are commonly described as ultrafine and several reviews have highlighted the toxicity associated with exposure to ultrafines in rats (Donaldson *et al.*, 2001; Oberdorster, 2001). Ultrafine particles occur as components of environmental particulate air pollution, which is measured by a global sampling convention called PM_{10}. This measures the mass of particles collected with a 50% efficiency for particles with an aerodynamic diameter of 10 μm. Exposure to ultrafine particles also occurs in the pigment industry i.e. exposure to ultrafine carbon black and titanium dioxide. Ultrafine particles may exist as either singlet or aggregate particles. Aggregation of the particles can effect their deposition potential, as they will have a larger aerodynamic diameter when compared with singlet particles. There are a number of factors which could suggest that ultrafine particles may be more toxic than larger particles. One such factor relates to the large surface area of ultrafine particles since they have a larger surface area per unit mass than fine particles, which may be able to act as a catalyst for specific reactions with cells. The increased surface area may also act as a carrier for co-pollutants such as gases and chemicals (Oberdorster, 2001).

A considerable body of research now suggests that the high surface area of ultrafine particles causes oxidative stress in exposed cells (Brown *et al.*, 2001), alterations in

intracellular calcium (Brown *et al.*, 2000) and is proinflammatory (Wilson *et al.*, 2002). The exact mechanism of these effects are unknown but the ability to cause oxidative stress seems to be a powerful contributor. The relationship between surface area dose and overload means that ultrafine particles, with the high surface area per unit mass, are likely to cause overload at lower mass doses compared to fine particles. The role of oxidative stress in driving such an effect is as yet unknown but it could be hypothesised that oxidative stress would drive ultrafine particle-mediated overload.

CHAPTER 2

MATERIALS AND METHODS

2.1 Particles.

2.1.1 DQ12 Quartz.

DQ12 quartz is a standard experimental quartz sample which originated from a tertiary quartz sand extracted from the Dörentrup deposit in Westphalia, under the name "Ground Product No. 12". A size fraction of less than 5 μm was prepared via centrifugal separation in air (Robock, 1973).

2.1.2 Aluminium Lactate and PVNO Treatment of Quartz.

Quartz was treated with aluminium based on the method of Begin *et al* (1986). The quartz was suspended at a concentration of 5 mg/ml in a 1% solution of either aluminium lactate or polyvinylpyridine-N-oxide (PVNO) in phosphate buffered saline (PBS). The quartz particles were sonicated for 5 minutes and then agitated for at least 3 hours at room temperature. Quartz suspended in PBS alone and treated in the same manner was used as a control to determine the effect of the coating procedure. After treatment with either aluminium lactate, PVNO or PBS, the quartz was washed twice with saline before being resuspended in fresh saline for intratracheal instillation (for Electron Spin Resonance, particles were resuspended in distilled, deionised water).

2.1.3 Preparation of the Clay Extracts.

The differing clay samples (listed in Table 2.1.3) were suspended at a concentration of 200 mg/ml in 1M hydrochloric acid in PBS (HCl-PBS). The clay samples were agitated for 24 hours at room temperature, centrifuged at 1000g for 10 minutes and the supernatants retained. The retained supernatants were then neutralised to between pH 7.0 and 7.2 using 1M sodium hydroxide in PBS (NaOH-PBS).

Table 2.1.3 Clay panel used to obtain extracts for the treatment of quartz. All clay samples were kindly donated by Dr. Laurie Davies, Institute of Occupational Medicine, Edinburgh.

Name	**Chemical Formula**
Kaolin (well crystallized)	Si_2O_5 **Al_2** $(OH)_4$
Kaolin (poorly crystallized)	Si_2O_5 **Al_2** $(OH)_4$
Hectorite	$Na_{0.4}Mg_{2.7}Li_{0.3}Si_4O_{10}(OH)_2$
Attapulgite	Si_4O_{10} **Al_2** $(OH).4H_2O$
Calcium-montmorillonite	$CaAl_6(Si_4O_{10})_3(OH)_6.nH_20$
Sodium-montmorillonite	$NaAl_6(Si_4O_{10})_3(OH)_6.nH_20$
Feruginous smectite	$(K,H_20)Al_2Fe_2Si_4O_{10}(OH)_2H_2O$

2.1.4 Clay Extract Treatment of Quartz.

Quartz was treated with clay extracts using the same protocol as for aluminium lactate coating of quartz (section 2.1.2). Quartz suspended in 1M HCl-PBS, neutralised with 1M NaOH-PBS alone and treated in the same manner was used as a control to determine the effect of the coating procedure.

2.2 Assays.

2.2.1 Haemolysis.

The haemolytic potential of the treated and untreated quartz was measured based on the method of Harington *et al.*, 1971, with modifications. Erythrocytes were obtained from fresh human venous blood, from healthy donors. Ten millilitres of blood was added to 1 ml of 3.8% sodium citrate solution (Phoenix Pharmaceuticals Ltd., Poole, UK) in a 15 ml falcon tube to prevent coagulation of the blood. The blood was mixed by gentle inversion of the tube and centrifuged at 1200g for 10 minutes. The plasma supernatant was discarded and the red blood cells (RBC) were washed 4 times by suspending in saline (0.9 %) before centrifugation at 1200g for 10 minutes. The final suspension consisted of 4% by volume RBC in saline. Quartz and aluminium lactate/clay-treated quartz were prepared as described previously, and diluted to give a final concentration of between 0.625 and 5 mg/ml, in saline. One hundred and fifty microlitres of quartz suspension, in triplicate, was added to a flat-bottomed 96-well plate. Negative control wells consisted of 150 µl of saline and positive control wells consisted of 150 µl of 0.1% triton X-100 (Sigma, UK). To each well, 75 μl of erythrocyte suspension was added and mixed gently by pipetting. The plates were incubated for 15 minutes at room temperature, shaking gently on an orbital plate shaker. Following incubation, plates were centrifuged at 717g for 5 minutes and 100 µl carefully removed from each well, so as not to disturb the pelleted RBC's and transferred to the corresponding wells of a new 96-well plate. The amount of haemoglobin released into the supernatant was determined spectrophotometrically at a wavelength of 540 nm. The percentage haemolysis was calculated using the equation of a straight line, $y = mx + c$, as follows:

$$\% \text{ haemolysis } (x) = \frac{[\text{optical density } (y) - \text{ negative control optical density } (c)]}{[(\text{positive control optical density} - \text{negative control optical density})/100] \ (m)}$$

2.2.2 Enzyme-Linked Immunosorbent Assay (ELISA).

2.2.2.1 Macrophage Inflammatory Protein-2.

Bronchoalveolar lavage fluid (BALF) MIP-2 concentration was assessed using an ELISA kit, which uses peroxidase and tetramethylbenzidine as a detection method (BioSource International, Camarillo, California). Flat bottomed 96-well microtitre plates (E.I.A/R.I.A plate, Costar, Cambridge, MA) were coated overnight at room temperature with 100 µl of coating antibody (1.25 µg/ml in coating buffer (50 mM $NaHCO_3$, 50 mM Na_2CO_3 in distilled water)). Plates were washed 3 times with wash buffer (0.1% Tween 20 in saline) and incubated for 2 hours with blocking buffer (0.5% BSA in PBS) to block non-specific binding sites. After blocking, plates were washed 3 times with wash buffer followed by the addition of 100 µl of either sample or standard per well in triplicate. The plates were incubated for 1.5 hours at room temperature on a plate shaker. After incubation, the plates were again washed 3 times with wash buffer and 100 µl of biotinylated detection antibody (125 ng/ml of diluent) was added per well and incubated for 1 hour at room temperature. Following rinsing 3 times with wash buffer, 100 µl of streptavidin–horse radish peroxisdase, diluted 1 in 2500 in diluent was added to each well and incubated for 45 minutes at room temperature on a plate shaker. A substrate stock of 3,3', 5,5-tetramethylbenzidine (TMB) was prepared by dissolving 10 mg/ml in dimethlsulfoxide (DMSO). To prepare the substrate buffer, 100 µl of TMB was added per 10 ml of a 100 mM solution of sodium acetate/citrate, pH 4.9 with 5 µl

of H_2O_2 (30%). After washing, 100 µl of substrate buffer was added to each well and allowed to incubate for 30 minutes in the dark, as TMB is light sensitive. The reaction was stopped by the addition of 100 µl of 1 M sulphuric acid. The absorbance was quantified at an emission of 450 nm with reference wavelength at 650 nm (Dynex MRX plate reader) and BALF samples were compared with a standard curve of rat MIP-2 protein.

2.2.2.2 IL-8.

Monoclonal and biotinylated anti-human IL-8 antibodies were obtained from the National Institute for Biological Standards and Control – NIBSC (Pottersbar, Hertfordshire, UK). Flat-bottomed 96-well plates (E.I.A/R.I.A plate, Costar, Cambridge, MA) were coated overnight at 4°C with 100 µl of coating antibody (2µg/ml in 1 times PBS). Plates were washed 3 times with wash/dilution buffer (0.1% Tween 20, 0.5 M NaCl, 2.5 mM NaH_2PO_4, 7.5 mM Na_2HPO_4, pH 7.2) and incubated for 1 hour with 100 µl/well of blocking buffer (1% ovalbumin in 1X PBS) to block non-specific binding sites. After blocking, plates were washed 3 times with wash buffer and 100 µl of either sample or standard was added per well in triplicate. Plates were incubated for 4 hours at room temperature on a plate shaker. After incubation, plates were again washed 3 times with wash buffer and 100 µl of biotinylated detection antibody (1 in 2000 dilution of stock antibody, in diluent) was added per well and incubated for 1 hour at room temperature. Following rinsing 3 times with wash buffer, 100 µl of streptavidin–horse radish peroxisdase (Dako, Denmark), diluted 1 in 20000 in diluent was added to each well and incubated for 20 minutes at room temperature on a plate shaker. A substrate stock of 3,3', 5,5-tetramethylbenzidine (TMB) was prepared by dissolving 10 mg/ml in DMSO. To prepare the substrate buffer, 100 µl of TMB was

added per 10 ml of a 100 mM solution of sodium acetate/citrate, pH 4.9 with 5 µl of H_2O_2 (30%). After washing, 100 µl of substrate buffer was added to each well and allowed to incubate for 30 minutes. This was carried out in the dark as TMB is light sensitive. The reaction was stopped by the addition of 50 µl of 1 M sulphuric acid. The absorbance was quantified at an emission of 450 nm with reference wavelength at 590 nm (Dynex MRX plate reader) and samples were compared with a standard curve of IL-8.

2.2.3 Single Cell Gel Electrophoresis (Comet Assay).

DNA strand break formation was determined by the comet-assay (Singh *et al.*, 1988; Olive et al. 1990), the methodological principle of which, is shown by the cartoon in Figure 2.2.3. A549 cells were seeded into 60 mm diameter culture dishes (5 x 10^5 cells/dish) in 10% FCS and grown for a further 48 hours. On the day before the experiments, fully frosted slides were covered with a layer of 0.65% agarose using a coverslip and stored overnight at 4°C. Following treatment of the cells with treated and untreated quartz for 4 hours, the monolayers were rinsed twice with PBS. Cells were detached with trypsin-EDTA (500μl, 2 minutes), and immediately suspended in complete culture medium. Cells were centrifuged for 5 minutes at 800g, and resuspended in PBS. Cell yield and viability of each incubation was assessed by haemocytometer using trypan blue dye exclusion. Slides (covered the day before with agarose), were then covered with a second layer containing a mixture of 25μl cell suspension and 75μl 0.65% low melting point agarose. The slides were stored for 1 hour at 4°C to allow solidification, and then covered with another layer of the low melting point agarose. Following solidification for at least 1 hour at 4°C, slides were immersed in lysis buffer (2.5 M NaCl, 100mM EDTA, 10mM Tris-base, 1% Sodium Lauryl sarcosinate, pH=10;

10% DMSO and 1% Triton X-100 - added just before use) and stored overnight at 4°C. The following day, slides were rinsed with distilled water and then placed in an electrophoresis tank filled with ice-cold electrophoresis buffer (300 mM NaOH, 1mM EDTA, pH=13) for 20 minutes. The electrophoresis tank was kept in an ice bath. Electrophoresis was conducted at 300mA and 25V for 15 minutes. Slides were then neutralised 3 times for 5 min using neutralisation buffer (0.4M Tris, pH=7.5). All steps described were performed in the dark or under dimmed red light to prevent additional DNA damage. Slides were stained with ethidium bromide (2µg/ml in H_2O) and comet appearance were analysed on an Olympus BX60 fluorescence microscope at 1000x magnification. For each individual experiment, per treatment at least 2 x 25 cells were analysed randomly, and classified into one out of five categories according to tail length (I, II, III, IV, and V, in which I = undamaged cells without comet tail) (Collins *et al.*, 1995).

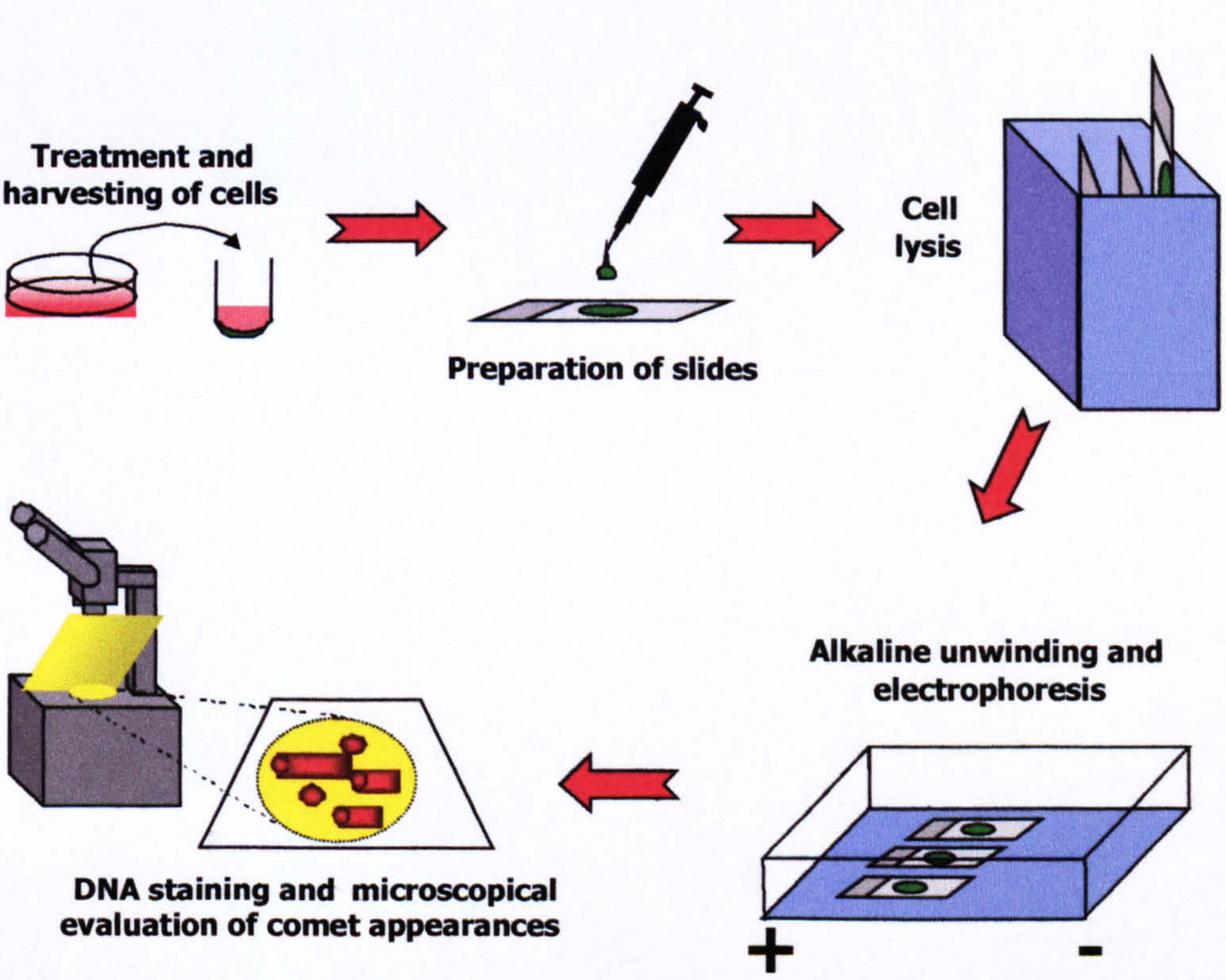

Figure 2.2.3 *The methodological principle of Single Cell Gel Electrophoresis (Comet Assay). Figure modified from Dr. Roel Schins (IUF, Germany).*

2.2.4 Bicinchoninic acid (BCA) Protein Assay.

Protein concentrations were determined using bicinchoninic acid (BCA), a sensitive and stable reagent specific for the cuprous ion (Cu^{1+}). This assay utilises the principle of the Biuret reaction: the reduction of Cu^{2+} by protein to Cu^{1+} in an alkaline medium (Smith et al., 1985). Two molecules of BCA react with Cu^{1+} forming a purple-coloured, water-soluble complex, exhibiting a strong absorbance at 560 nm, that is linear with increasing protein concentrations over a range of 20 to 2000 µg/ml (Pierce).

To prepare the working reagent, 50 parts of the Pierce Reagent A was mixed with 1 part of Reagent B, the copper sulphate solution. Protein standards were prepared by serial dilution of a stock of 2 mg/ml bovine serum albumin (BSA). Ten microlitres of standard or BALF sample were pipetted into a flat-bottomed, 96-well plate followed by the addition of 200 µl of working reagent. Two hundred microlitres of working reagent was used as a blank. Standards and blanks were incubated for 30 minutes with reagents at 37°C and the absorbance measured at 560 nm in a spectrophotometric plate reader. Protein concentrations of the unknown samples were calculated from the BSA standard curve.

2.2.5 Electron Spin Resonance.

The ability of aluminium lactate treated and untreated quartz to induce hydroxyl radical formation in the presence of hydrogen peroxide was measured by Electron Spin Resonance (ESR) as described elsewhere (Fubini *et al.*, 1995). The spin trapping agent 5, 5-dimethyl-1-pyrroline-N-oxide (DMPO) is used to detect the formation of radical species in aqueous suspensions of materials. In aqueous medium, DMPO forms stable radical adducts, allowing evaluation of free radical release. The target molecule,

hydrogen peroxide, allows detection of hydroxyl radicals. This can be summarised by the following schematic diagram:

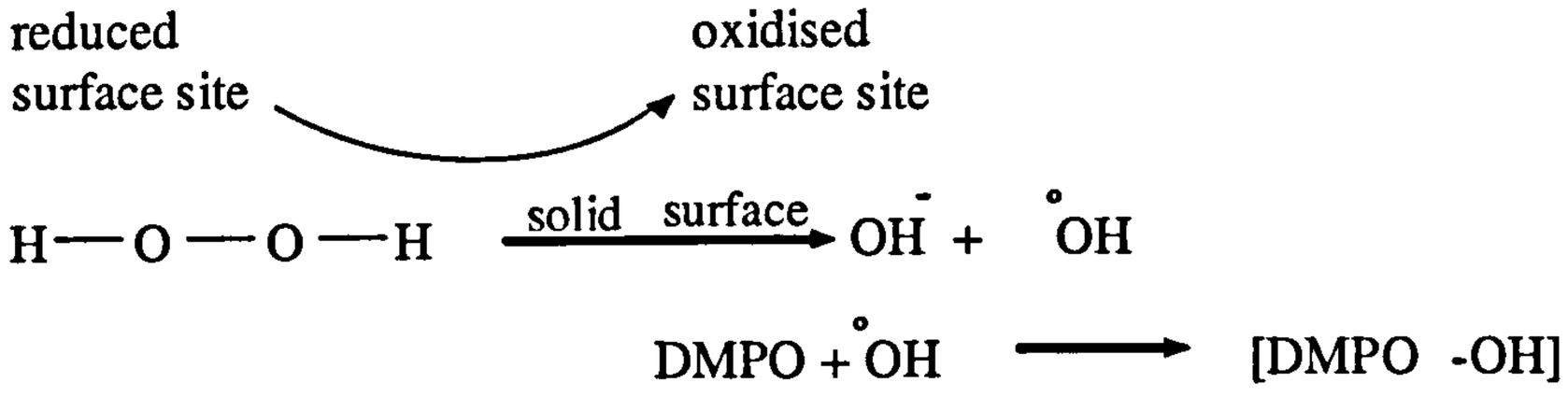

Two hundred and fifty microlitres of distilled, deionised water, 250 µl of 0.5M H_2O_2 in PBS and 500 µl DMPO, 0.05M in distilled, deionised water were added to 20 mg of DQ12 or aluminium lactate coated DQ12. The suspensions were incubated in a shaking water bath for 15 minutes at 37°C and filtered through a 0.22 µm pore filter. The clear filtrate was then transferred to a capillary tube and DMPO-OH adduct formation was measured with a Miniscope ESR spectrometer (Magnettech, Berlin, Germany). The ESR-spectra were recorded at room temperature using the following instrumental conditions: Magnetic field: 3360 G, sweep width: 100G, scan time: 30 seconds, number of scans: 3, modulation amplitude: 1880G

2.2.6 Gamma Glutamyl Transpeptidase Activity.

BALF gamma glutamyl transpeptidase (γGT) activity determination was assessed using a diagnostic kit adapted for 96-well plate use (Sigma-Aldrich Company Ltd, Dorset, UK). The principle of the assay is based on the transfer of the glutamyl group from L-glutamyl-p-nitroanilide to glyclglycine catalysed by the enzyme γGT. The absorbance of the pink azo-dye measured at 530 - 550 nm is proportional to the γGT activity.

γGT substrate solution prepared in Sigma Trizma buffer solution (25 µl) was added to 25 µl of BALF. γGT substrate solution (25 µl) was also added to a BALF-free well as a blank and the samples incubated at 37°C for 20 minutes. The reaction was stopped by the addition of 10% acetic acid (100 µl) and then sodium nitrite solution (50 µl of a 1 mg/ml solution) was added to each well and left at room temperature for 3 minutes. Ammonium sulphamate solution (50 µl) was then added to each well and left for a further 3 minutes. Following incubation with ammonium sulphamate, napthylethylenediamine solution (50 µl) was added to each well and the plate left at room temperature for 5 minutes before reading the absorbance at 550 nm on a Dynatech MRX microplate reader. A standard curve was obtained using Sigma γGTP calibration solution to give activity corresponding to 0-100 Units/ml (where 1 unit of γGT is defined as that amount of activity that will liberate 1 nanomole of p-nitroaniline per minute at 25°C, under the conditions specified in Sigma Diagnostics Procedure No. 415.) Acetic acid (10%, 100 µl) was added to these standard wells which were then treated as for samples, beginning with the addition of 50 µl of ammonium sulphamate solution. The γGT activity of the test wells was calculated from the standard curve obtained.

2.2.7 MTT Cell Viability.

The MTT cell viability assay was utilised to determine sub-lethal doses of particulate over a maximum of 24 hours. The assay, based on the original method of Mosmann (1983), determined the viability of pre-treated cells by incubating the treated and washed cells with the MTT tetrazolium salt dissolved in PBS. Tetrazolium salts, such as MTT (3-[4,4-dimethylthiazol-2-yl]-2,5-diphenyl-tetrazolium bromide), measure the activity of various dehydrogenase enzymes that require reduced pyridine nucleotides

(Berridge et al., 1996). The tetrazolium ring is cleaved in active mitochondria, converting the MTT into an insoluble purple formazan and therefore the reaction only occurs in living cells – dead cells are almost completely negative (Mosmann, 1983). The amount of formazan produced is proportional to the number of living cells and their energy metabolism.

A549 cells were seeded in 96-well tissue culture plates at a density of 1 X 10^5 cells/well. The cells were maintained at 37°C in 5% CO_2 overnight prior to particle treatment. The following day, the culture medium was removed before washing the cells with PBS and the addition of fresh medium containing the particle suspensions. Cells were incubated with particles for 24 hours, then MTT (20 µl of a filtered 5 mg/ml solution in PBS) was added to the medium in each test well and the plates incubated for 1 hour at 37°C. After incubation, the medium was removed from the wells and replaced with 100 µl of dimethyl sulphoxide (DMSO) to solubilise the purple formazan product. The plate was left at room temperature for 10 minutes before shaking for 5 seconds and the absorbance in each well was measured at 550 nm using a Dynex MRX microplate reader. Control wells contained cells and medium alone. Any additional absorbance caused by the particles themselves was controlled for by measuring the absorbance of wells containing particles and medium but no cells. The mean absorbance of these cells was subtracted from the corresponding test wells.

2.2.8 Lactate Dehydrogenase Release.

Lactate dehydrogenase (LDH) measurement was carried out using a Roche Cytotoxicity Kit (Cat No 1 644 793). Cell death is classically evaluated by the quantification of plasma membrane damage. LDH is a stable cytoplasmic enzyme present in all cells. It

is rapidly released into the culture supernatant upon damage to the cell membrane. The culture supernatant is collected and incubated with the reaction mixture from the kit. The LDH activity is determined in an enzymatic test. In the first step, released LDH reduces NAD^+ to NADH plus H^+ by oxidation of lactate to pyruvate. In the second step, the catalyst (diaphorase) transfers 2 H atoms from NADH plus H^+ to the yellow tetrazolium salt which is reduced to the red formazan salt.

A549 cells were seeded in 96-well tissue culture plates at a density of 9×10^4 cells/ml (100 µl/well). The cells were maintained at 37°C in 5% CO_2 overnight before being serum-starved for a further 24 hours. After treatments, including a low control (untreated cells) and a high control (total cell lysis with 1% Triton-X 100), plates were centrifuged at 250g for 10 minutes. One hundred microlitres of supernatant from each well was carefully transferred into a new 96-well plate and diluted 1 in 3 with culture medium. LDH reagent was made by adding 1 part Solution I to 45 parts Solution II and then 100 µl of LDH reagent added to 100 µl of the diluted cell supernatant. The samples were then incubated for 30 minutes in the dark and read at 490 nm on a Dynex MRX microplate reader. The mean absorbance for treatments was determined using the following equation:

$$\textbf{\% Cytotoxicity} = \frac{\text{experimental value} - \text{low control}}{\text{high control} - \text{low control}} \times 100$$

2.3 Molecular Biology Techniques.

2.3.1 Preparation of Diethyl Pyrocarbonate (DEPC) Water.

DEPC water was prepared by adding 50 µl of diethyl pyrocarbonate in 500 µl of ethanol to 500 ml MilliQ water and warming to 37°C with gentle stirring overnight in a fume hood. The DEPC-treated water was then autoclaved (15 minutes at 121°C at 200 Kpa). Pipette-tips and glass-ware were also rendered Rnase-free by autoclaving.

2.3.2 Isolation of RNA.

Total RNA was isolated from bronchoalveolar lavage (BAL) and A549 cells using TRIzol reagent (Life Technologies, Inc., Paisley, UK). Following lavage, BAL cells were resuspended in a final volume of 1 ml of cold TRIzol (4°C). In the case of A549 cell treatments, the culture media was removed and the cells washed twice with PBS. Cold TRIzol was added to each well and triplicates pooled to give a final volume of 1 ml. Samples were transferred into sterile 1.5 ml eppendorfs and placed on ice. One hundred microlitres of chloroform was added to each tube and vortexed at full speed for 15 seconds. Samples were allowed to incubate on ice for 5 minutes before being centrifuged at 12000g for 15 minutes at 4°C. The top layer (aqueous layer) from each tube was transferred to a new, sterile eppendorf tube and 0.5 ml of ice-cold isopropanol was added. Samples were again incubated for 15 minutes at 4°C, vortexed briefly and centrifuged at 12000g for 15 minutes at 4°C. The supernatants were removed and the RNA pellets washed with 1 ml of ice-cold 75 % ethanol, vortexed and centrifuged at 7500g for 10 minutes at 4°C. Supernatants were discarded and the eppendorf tubes allowed to air dry for 15 minutes. The resultant pellets were dissolved in 40 µl of DEPC-treated, deionised water. Samples were stored at -70°C until ready to use. RNA

concentration was determined spectrophotometrically. Two microlitres of RNA solution was added to 998 µl of DEPC-treated, deionised water, placed into a quartz cuvette and read at the optical densities of 260 and 280 nm. RNA samples having an absorbance$_{260/280}$ ratio of less than 1.6 were used. The RNA concentration was calculated by multiplying the absorbance$_{260}$ value by a factor of 10.

2.3.3 Assessment of Rat MIP-2 mRNA and Human IL-8 mRNA by Reverse Transcriptase Polymerase Chain Reaction.

Two micrograms of RNA were added to a solution containing 5 times reverse transcription buffer (Promega), 100 µg/ml oligodeoxythymidine (dT), 100 mM dithiothreitol (DTT), 10 mM deoxynucleotide triphosphates (dNTPs) and RNAse inhibitor; reverse-transcribed into complementary DNA (cDNA) at 37°C for 1 hour and 30 minutes using Moloney-Murine Leukaemia Virus Reverse Transcriptase (200 U/µl) and incubated at 94°C for 10 minutes. Using a thermal cycler (Hybaid, Ashford, UK), 5 µl of cDNA was PCR-amplified in 40 µl reaction volumes containing Polymerase Chain Reaction mix (1X TAQ polymerase buffer, 2.5 mM $MgCl_2$, 0.2 mM dNTPs)(Promega) and TAQ polymerase (1 Unit/µl). Conditions for PCR were as follows: for MIP-2, 35 cycles of denaturation (94°C for 1 minute), annealing (55°C for 1 minute), extension (72°C for 2 minutes) and final extension of 72°C for 7 minutes; for ß-actin, 22 cycles of denaturation (94°C for 1 minute), annealing (60°C for 1 minute), extension (72°C for 1 minute) and final extension of 72°C for 5 minutes; IL-8, 27 cycles of denaturation (92°C for 1 minute), annealing (60°C for 1 minute), extension (72°C for 1 minute) and final extension of 72°C for 5 minutes; GAPDH, 23 cycles of denaturation (72°C for 1 minute 30 seconds), annealing (94°C for 45 seconds), extension (60°C for 45 seconds) and a final extension of 72°C for 10 minutes.

Oligonucleotide primers were chosen using the published sequences of rat MIP-2 and β-actin cDNA (Driscoll *et al.*, 1993), human IL-8 cDNA (Lindley *et al.*, 1988) and GAPDH (Gilmour *et al.*, 2001). All primers were synthesised by MWG-Biotech (Milton Keynes, UK). The sequence of the primers used in the PCR reaction were as follows: MIP-2 (sense 5'-GGC ACA TCA GGT ACG ATC CAG-3') and (anti-sense 5'-ACC CTG CCA AGG GTT GAC TTC-3'); β-actin (sense 5'-CTC ATA GAT GGG CAC AGT GTG-3') and (anti-sense 5'-AAC CGG TCC GCC ATG TGC AAG-3'); IL-8 (sense 5'-ATG ACT TCC AAG CTG GCC GTG GCT-3') and (anti-sense 5'-TCT CAG CCC TCT TCA AAA ACT TCT C-3'). PCR products were electrophoresed in 1.5% agarose containing ethidium bromide. Bands were visualised and scanned using a white/UV transilluminator (Ultra Violet Products, Cambridge, UK) and quantified by densitometry. β-actin and GAPDH were used as the housekeeping genes.

2.3.4 Preparation of Nuclear Extracts.

Nuclear extracts of BAL and cells were prepared based on the method of Staal *et al.*, (1990). Pelleted BAL cells were lysed by incubation on ice for 15 minutes in 400 µl of buffer A (10 mM Hepes, 10 mM KCl, 2 mM $MgCl_2$, 1 mM DTT, 0.1 mM EDTA, 0.4 mM PMSF, 0.2 mM NaF, 0.2 mM $NaVO_3$, 1 µg/ml leupeptin) and 25 µl of buffer B (10% NP-40). After incubation, the lysed cells were centrifuged for 1 minute at 1200g at 4°C. The supernatant was decanted off and the pellet containing the nuclei was re-suspended in 50 µl of buffer C (50 mM Hepes, 50 mM KCl, 300 mM NaCl, 0.1 mM EDTA, 1 mM DTT, 0.4 mM PMSF, 10% glycerol, 0.2 mM NaF and 0.2 mM $NaVO_3$). Samples were agitated for 20 minutes at 4°C and centrifuged at 1200g for 5 minutes at 4°C. The supernatant was removed and stored at -20°C until further analysis.

2.3.5 Radiolabelling of Concenus Oligonucleotides.

The cold (unlabelled) oligonucleotide containing the binding sequence for the transcription factor of interest was radiolabelled with γ-^{32}phosphate-ATP, by incubating 2 µl of concensus oligonucleotide (1.75 pmol/µl) with 1 µl of 10 times T4 polynucleotide kinase buffer (700 mM Tris-HCl pH 7.6, 100mM $MgCl_2$, 50 mM DTT), 1 µl of γ-^{32}P-ATP (3000 Ci/mmol at 10 mCi/ml), 5 µl of deionised water and 1 µl of T4 polynucleotide kinase (5 units/ µl) at 37°C for 30 minutes. The reaction was terminated by the addition of 1 µl of 0.5M EDTA. A further 89 µl of TE buffer (10mM Tris-HCl, pH 8.0; 1 mM EDTA) was added to give a 1 times stock solution of labelled oligonucleotide in a final volume of 100 µl.

2.3.6 Electrophorectic Mobility Shift Assay (EMSA).

Ten micrograms of nuclear protein was incubated for 20 minutes at room temperature with 5 times binding buffer (20% glycerol, 5 mM $MgCl_2$, 2.5 mM EDTA, 2.5 mM DTT, 250 mM NaCl, 50 mM Tris-HCl, pH 7.5, 0.25 mg/ml poly (dI-dC) · poly (dI-dC) (Promega, Southampton, UK) and γ-^{32}P-labelled NF-κB consensus oligonucleotide according to the manufacturer's protocol, before electrophoresis at 100 volts on a 6% non-denaturing polyacrylamide gel. A non-denaturing (i.e. in the absence of sodium dodecyl sulphate) 6% polyacrylamide gel was prepared by adding 10 ml of 30% acrylamide/bis-acrylamide solution, 10 ml of 5X Tris-buffered EDTA (0.45 M Tris base, 0.45 M boric acid, 10 mM EDTA), 20.46 ml of double-distilled water, 500 µl of freshly prepared 10% ammonium persulphate and 40 µl of TEMED. Gels were poured immediately and allowed to polymerise for at least 30 minutes. The gel was dried for between 45 and 60 minutes onto Whatman paper using a vacuum heat dryer. The NF-κB oligonucleotides used (5'-AGT TGA GGG GAC TTT CCC AGG C-3', 3'-TCA

ACT CCC CTG AAA GGG TCC G-5') were obtained from Promega. DNA-binding was assessed by phosphorimaging using a Storm 860 (Molecular Dynamics, UK) and quantitative analysis was performed using ImageQuant software.

2.4 *In Vitro* Techniques.

2.4.1 Cell Culture of A549 Cells.

The human type II alveolar epithelial cells, A549, were cultured in Dulbecco's Modified Eagle's Medium (Sigma) containing 10% foetal calf serum (FCS), glutamate (2 mM) and penicillin (100 IU/ml)/streptomycin (100 μg/ml) at 37°C in the presence of 5% CO_2.

2.4.2 Particle Treatment of Cells.

The differing particles used for all the relevant experiments and the doses at which the A549 cells were treated are shown in Table 2.4.2.

Table 2.4.2 Particle treatment of A549 cells, showing the different particle types and doses used.

Experiment	Particles Used	Dose
MTT and LDH assays	Quartz	8, 10, 16, 20, 40, 80, 200 μg/cm^2
	Quartz/Al	
	Quartz/PVNO	
	TiO2	32, 64, 125, 250 μg/ml
	ufTiO2	
	CB	
	ufCB	
	ufCo	
	uNi	
Comet assay	Quartz	40 μg/cm^2
	Quartz/Al	
	Quartz/PVNO	
Particle Uptake	Quartz	40 μg/cm^2
	Quartz/Al	
	Quartz/PVNO	
IL-8/surface area	Quartz	10, 20, 40 μg/cm2
	Quartz/Al	10, 20, 40 μg/cm2
	TiO2	15, 32, 64, 125, 250 μg/ml
	ufTiO2	
	CB	
	ufCB	
	ufCo	
	uNi	

2.4.3 Measurement of Particle Uptake.

Particle uptake in A549 cells was determined as follows. Cells cultured in 60-mm diameter tissue culture dishes, were treated with (coated) particles for 2, 4 and 24 hours. At the end of each incubation, the monolayers were fixed with 2% glutaraldehyde in 0.1M cacodylate buffer for 1 h at 4°C. After postfixation in 2% OsO4, samples were stained with 1.5% uranyl acetate dihydrate and tungstphosphoric acidhydrate, dehydrated in ethanol series and embedded in Epon (Serva, Heidelberg, Germany). Sections of 800 nm, two blocks per sample, were then stained with azurII-methyleneblue (Richardson), and analysed by light microscopy at 1000x magnification. This method allows analysis of the intracellular localisation of particles with preservation of the native organisation and polarity of the monolayer cultures. For each section, at least 200 cells were counted interactively, using digital imaging (SIS, Münster) at 1500 times magnification. For each individual cell the number of visibly ingested particles was determined. Separate sections were also prepared for transmission electron microscopy analysis (Philips CM12).

2.5 *In Vivo* Techniques.

2.5.1 Instillations.

Male Wistar rats, approximately 4 months old, were used in all experiments. The animals were anaesthetised with halothane, cannulated with a laryngoscope to expose the trachea and 0.5 ml of a particle suspension in saline was instilled into the lungs. The dose and surface area of particles instilled are shown in Table 2.5.1. Animals instilled with 0.5 ml of saline were used as controls. Animals were either sacrificed 6, 18 or 72 hours post instillation and immediately subjected to bronchoalveolar lavage.

Table 2.5.1 Instilled mass and equivalent surface area for each particle type.

Particle	Mass instilled (μg)	Surface Area instilled (cm^2)
TiO2	125	8.3
ufTiO2	125	62.3
CB	125	9.9
ufCB	125	317.4
Latex 64	125	111.6
Latex 202	125	35.4
Latex 535	125	13.4
Latex 64	1000	893
Latex 202	1000	283
Latex 535	1000	107
DQ12	126	12.7
DQ12	189	19.2
DQ12	250	25.3
AL/DQ12	250	25.3
AL/DQ12	1240	125
AL/DQ12	2470	250
AL/DQ12	4940	500
RH1	250	13
OM	250	19.9
RH1	1000	52.2
OM	1000	79.9
ufNi	125	45.3
ufCo	125	46.1

2.5.2 Bronchoalveolar Lavage.

Rats were killed with a single intraperitoneal injection of 2 ml sodium pentobarbitone (200 mg/ml). The diaphragm was opened via the peritoneal cavity and the rib cage removed. The trachea was cannulated using a luer port cannula (Portex, Kent) which was then tied in place. The trachea and lungs were removed by dissection and the lungs lavaged with a single 8 ml volume of sterile saline. The lungs were gently massaged to ensure the saline reached all areas. This first lavage was retained in a separate tube for analysis of a bronchoalveolar lavage fluid (BALF) profile (protein, gamma glutamyl transpeptidase (γGT) and macrophage inflammatory protein-2 (MIP-2)). Subsequently the lungs were lavaged with a further 3, 8 ml volumes of sterile saline, again employing gentle massage. All samples were centrifuged at 180g for 5 minutes at 4°C, the supernatant was removed and the cell pellet from the first lavage was combined with the cells from the subsequent lavage before resuspension in 1 ml of PBS. Total cell numbers were counted using a haemocytometer (Weber Scientific, Middlesex) and cytocentrifuge smears prepared and stained with Diff-Quik (Raymond A Lamb, London) for differential cell counts to be assessed. Three hundred cells per slide were counted and the results expressed as total number of neutrophils in the lung lavage.

2.6 Statistical Analysis.

Data are expressed as means ± SEM and were analysed using one-way ANOVA. Multiple comparisons were analysed using Tukey-HSD method, unless otherwise stated. In all cases, $p<0.05$ was considered as significant.

Chapter 3

THE *IN VIVO* EFFECTS OF ALUMINIUM LACTATE TREATMENT OF DQ12 QUARTZ ON INFLAMMATION, CHEMOKINE EXPRESSION AND NUCLEAR FACTOR kappa B ACTIVATION.

3.1 Aims and Hypothesis.

The capacity of the quartz surface to have its harmfulness changed might explain why the quartz hazard, and hence the incidence of lung cancer, is variable between different industries. The geological processes affecting quartz provide the potential for contact with several minerals in the earth's crust, e.g. aluminium silicate clays, coal mine dust components and metal salts. It is therefore feasible that, through contact with such compounds, the surface of industrial or workplace respirable quartz samples could be modified, thereby reducing their inflammogenicity and potential carcinogenicity.

In this study the effects of modifying the surface of a standard experimental, respirable quartz with aluminium lactate, a procedure predicted to modify its inflammogenicity and to abolish quartz-induced proinflammatory molecular events was investigated. Furthermore, it is hypothesised that it is possible to detect a difference in the surface reactivity of the quartz, which would help in explaining the protective effect of the treatment.

3.2 Size Distribution of Quartz and Aluminium Lactate Treated Quartz.

Images of the DQ12 quartz and aluminium lactate coated quartz were obtained by scanning electron microscopy in order to determine whether coating of the DQ12 with aluminium lactate resulted in a different particle-size distribution as a result of aggregation. Treating the quartz particles with a soluble aluminium lactate salt did not have any significant effect on the size or aggregation of the quartz particles compared with the untreated quartz, as shown in Figure 3.2. One hundred and twenty randomly selected particles of aluminium lactate treated and untreated quartz were sized by scanning electron microscopy. The complete size distribution is shown in Figure 3.2 and the summary statistics in Table 3.2. A *t* test on the two size distributions yielded no significant difference ($t = 1.65$; $p = 0.21$).

Table 3.2 Summary statistics of the full size distribution of quartz and aluminium lactate-treated quartz.

	Size Distribution (μm)			
Particle	**Mean**	**Minimum**	**Maximum**	**SEM**
Quartz	0.91	0.08	2.67	0.05
Quartz/aluminium lactate	1.04	0.17	4.5	0.08

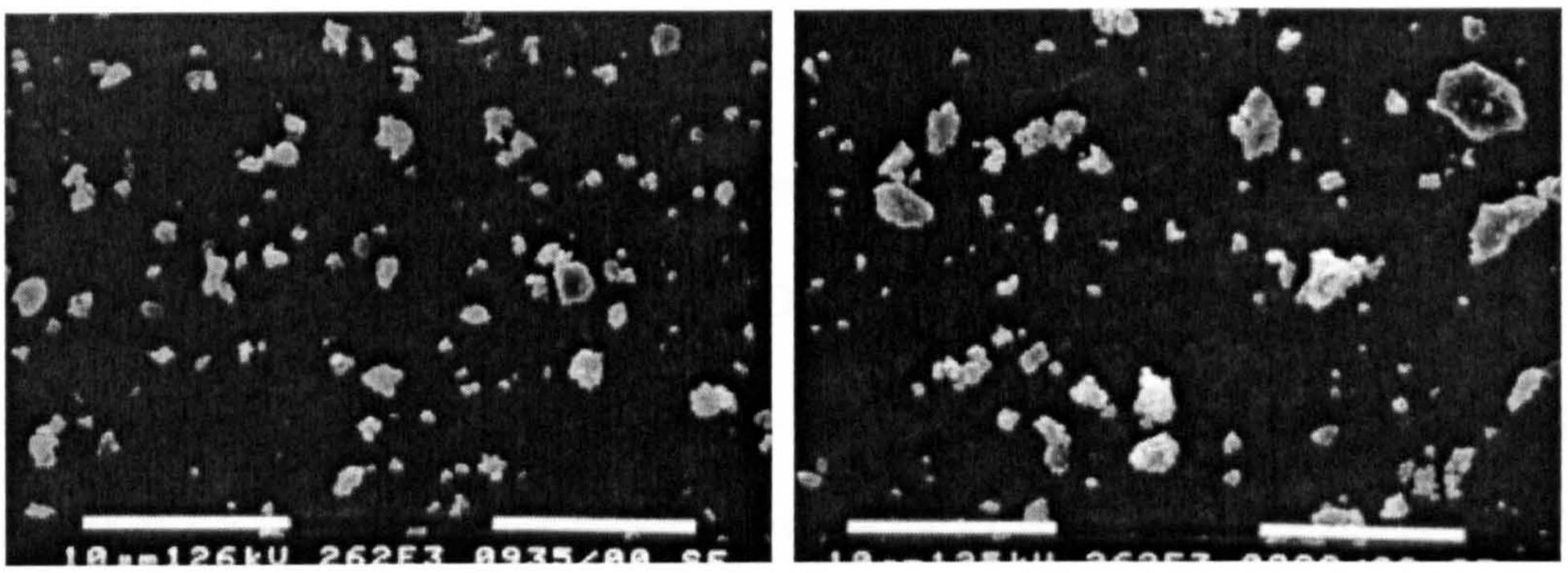

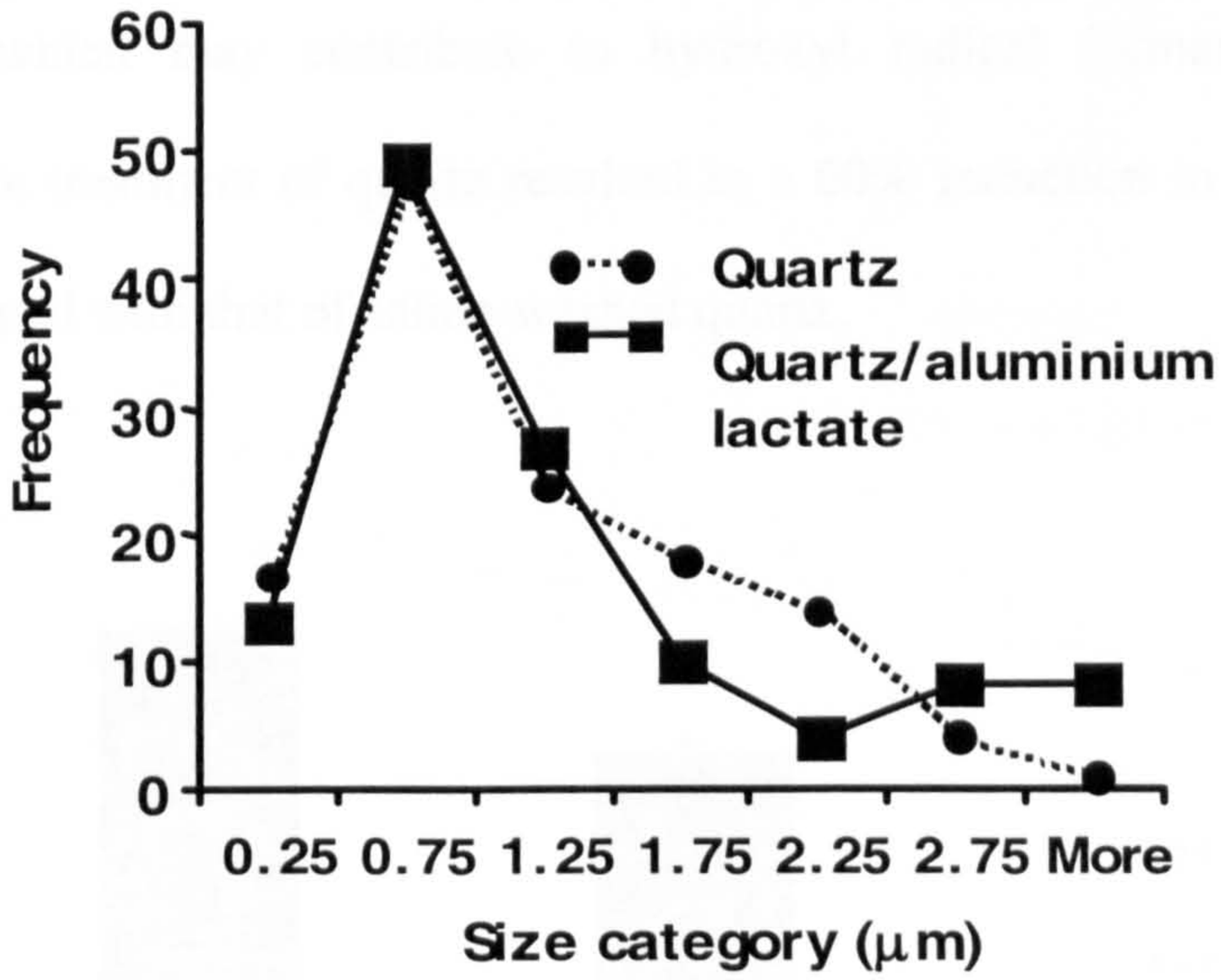

Figure 3.2 *Morphology of quartz and quartz/aluminium lactate. Top: Scanning electron micrograph of (A) quartz and (B) aluminium lactate treated quartz. Bars represent 10 μm. Bottom: Size distribution of particles.*

3.3 Hydroxyl Radical Generation by Quartz and Aluminium Lactate Treated Quartz.

ESR was used to determine the hydroxyl radical production by untreated (dry) quartz or quartz that had been incubated in either saline or aluminium lactate solution for 3 hours. Untreated quartz induced the formation of hydroxyl radicals in the presence of hydrogen peroxide and the spin-trapping agent DMPO (Figure 3.3). Saline-washed quartz (treatment control) exhibited an 18% reduction in hydroxyl radical formation compared with that of the untreated (dry) quartz, showing the effect of washing alone. The effect observed with washing alone, is most likely due to transition metal impurities on the quartz surface which may contribute to hydroxyl radical formation. However, aluminium lactate treatment of quartz resulted in a 60% reduction in hydroxyl radical formation compared with that of saline-washed quartz.

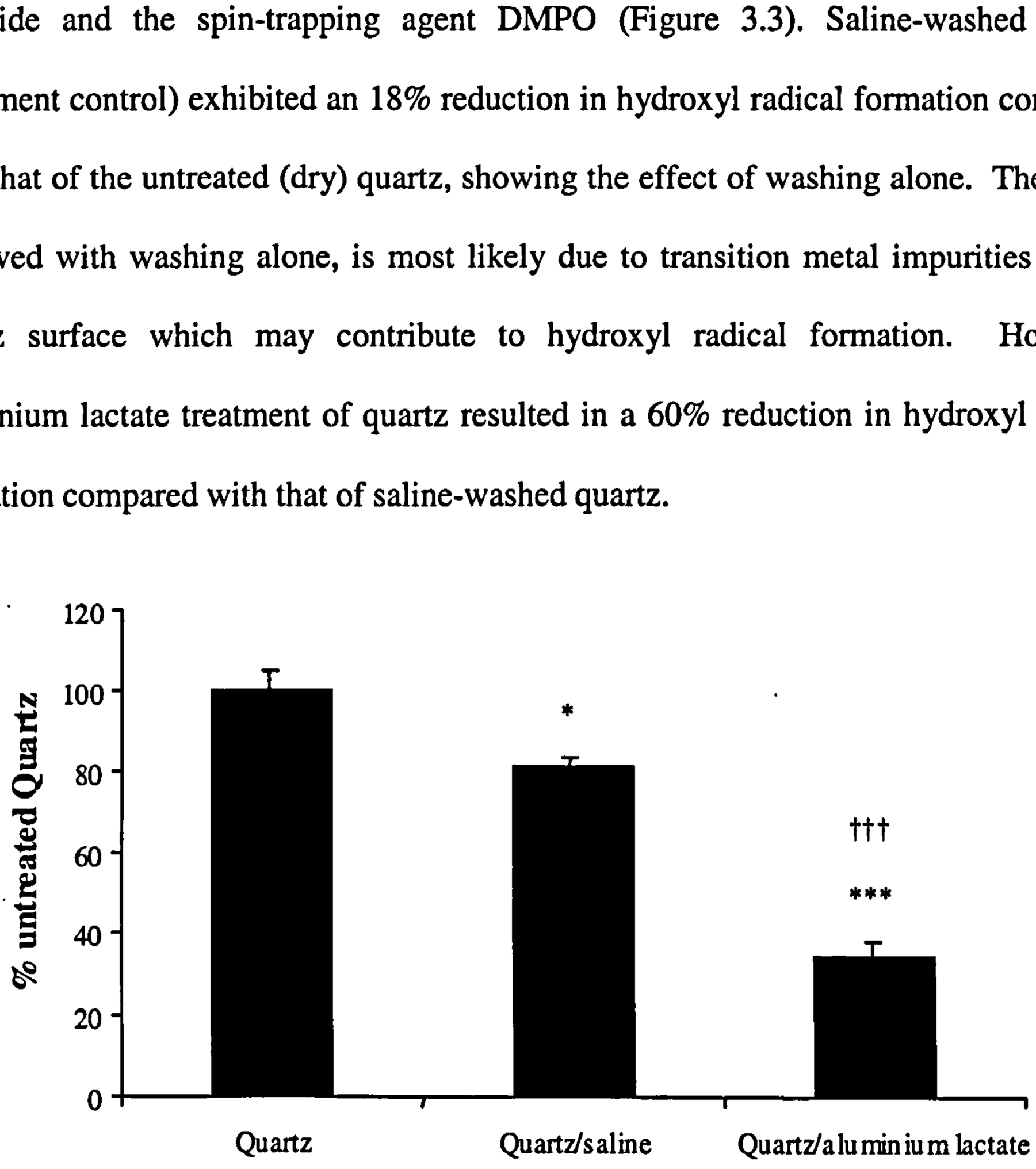

*Figure 3.3 Hydroxyl radical generation of quartz and aluminium lactate treated quartz as measured by ESR. Data are means and SEM of three replicates in three experiments. * p< 0.05, quartz/saline compared to untreated (dry) quartz. *** p< 0.01, untreated quartz compared to quartz/aluminium lactate. ††† p< 0.001, quartz/saline compared to quartz/aluminium lactate.*

3.4 Inflammation

The inflammatory potential of quartz and quartz treated with aluminium lactate can be demonstrated by the total number of inflammatory cells, i.e. neutrophils and macrophages in the bronchoalveolar lavage of rats instilled with quartz intratracheally. The data are expressed as both total cell number (Figure 3.4.1) and total neutrophil number (Figure 3.4.2) at 6, 18 and 72 hours post-instillation. Quartz-instilled animals exhibited a significant increase in BAL total cell number at 18 and 72 hours and neutrophil number at 6, 18 and 72 hours compared to both that of saline and aluminium lactate treated quartz-instilled animals. In addition, there was no significant increase in the inflammation observed with saline instilled and aluminium lactate-treated quartz instilled animals.

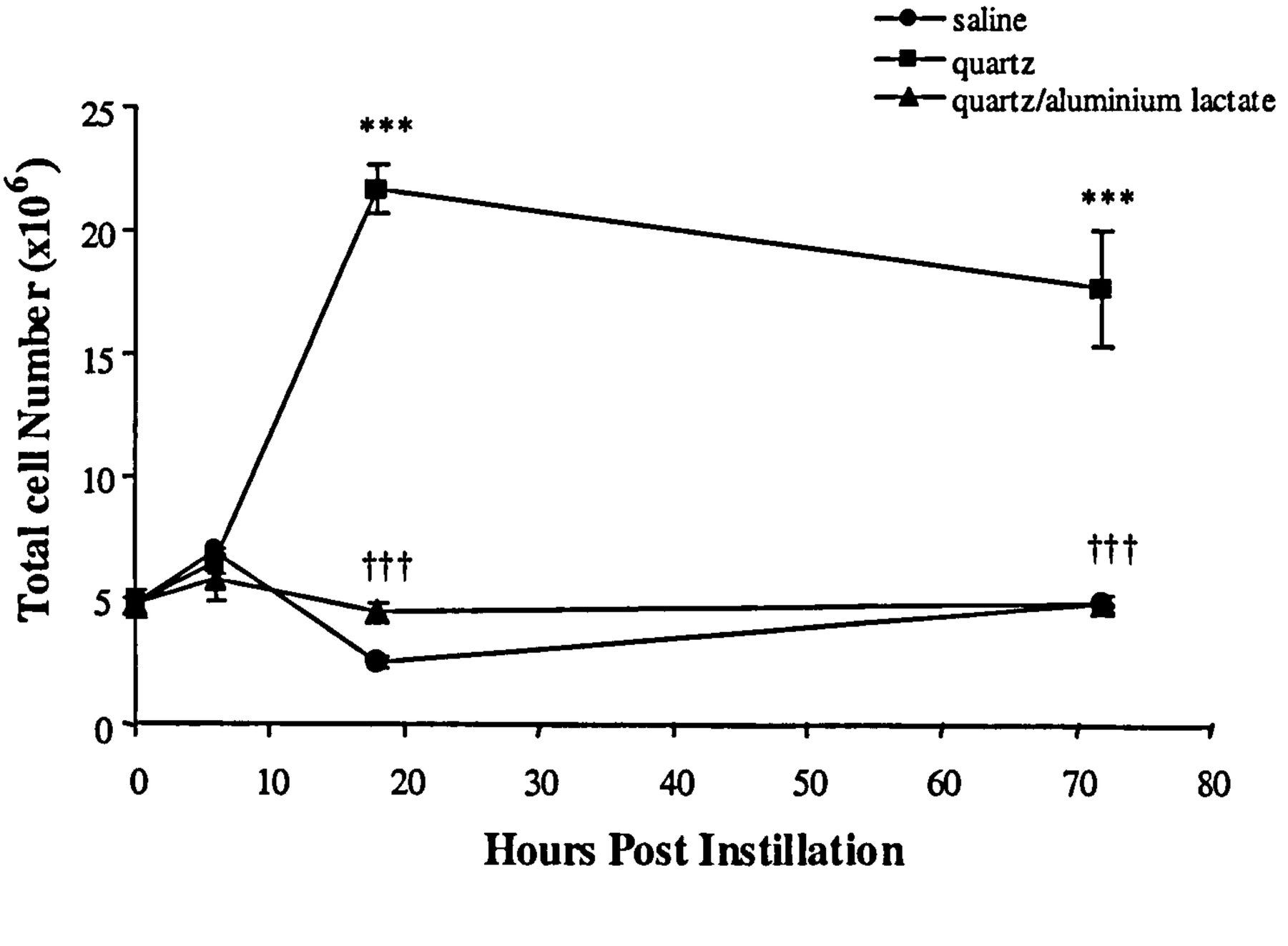

*Figure 3.4.1 Total cell numbers obtained from BAL 6, 18, and 72 hours post intratracheal instillation of either saline, quartz or aluminium lactate-treated quartz (250 μg). Each point is the mean and SEM of three rats in each group. *** p< 0.001, quartz/saline compared to saline. ††† p< 0.001, quartz /saline compared to quartz/aluminium lactate.*

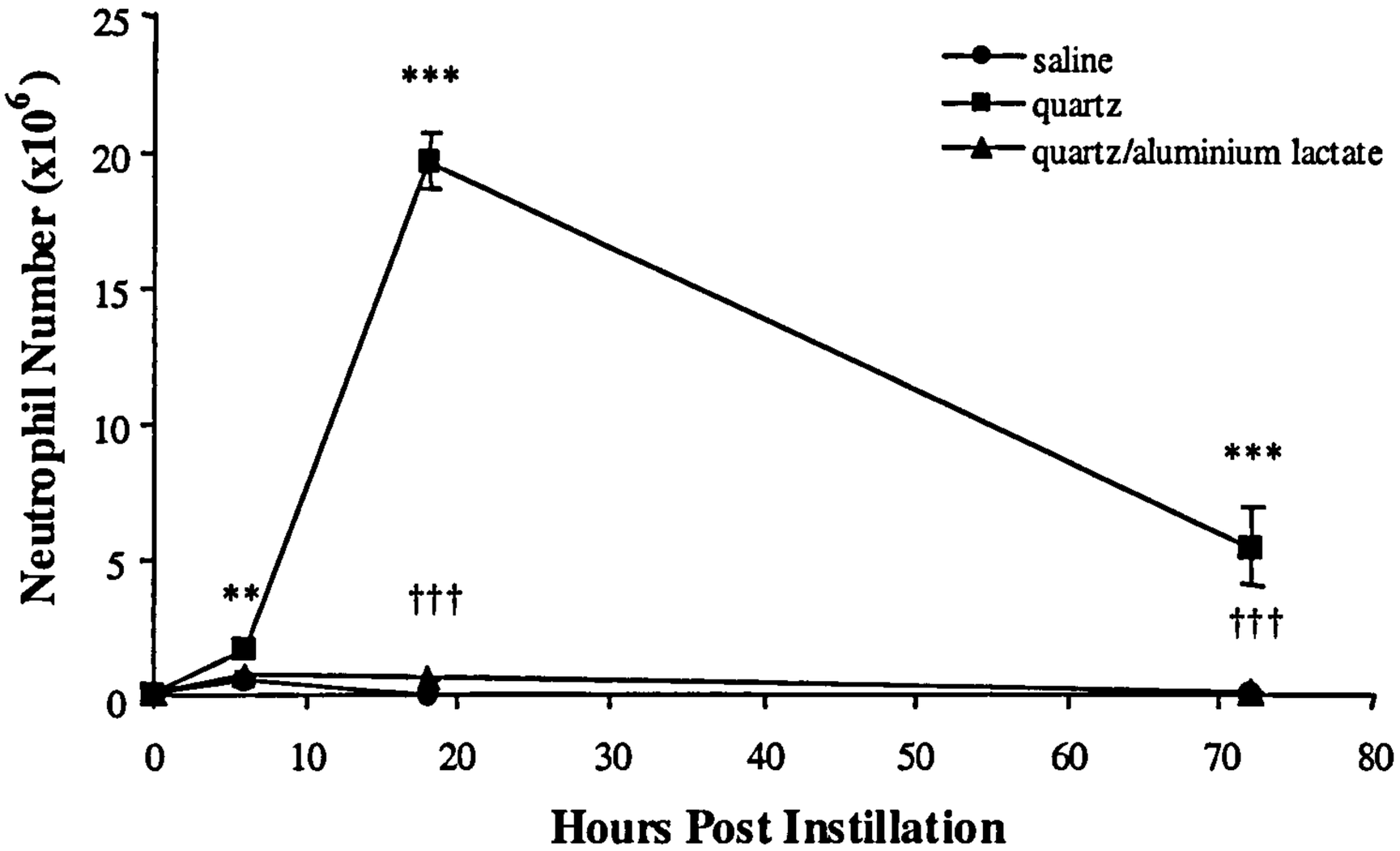

*Figure 3.4.2 Numbers of neutrophils identified in BAL 6, 18, and 72 hours post intratracheal instillation of either saline, quartz or aluminium lactate-treated quartz (250 μg). Each point is the mean and SEM of three rats in each group. ** p< 0.01, *** p< 0.001, quartz/saline compared to saline. ††† p< 0.001, quartz/saline compared to quartz/aluminium lactate.*

As well as measuring the inflammatory potential of quartz and surface-treated quartz, via the total number of inflammatory cells, the BALF profiles of protein (Figure 3.4.3), γGT activity (Figure 3.4.4) and MIP-2 protein (Figure 3.4.5) were also used as indicators of inflammation and damage. In each instance, quartz induced a significant increase in the quantity of each of these markers in BALF compared to saline instilled and the aluminium lactate-treated quartz instilled animals. This indicates that quartz surface treatment with aluminium lactate prevents quartz-induced lung damage. There was also no significant difference with respect to BALF content of total protein, γGT activity or MIP-2 protein concentration between saline instilled and aluminium lactate-treated quartz instilled animals.

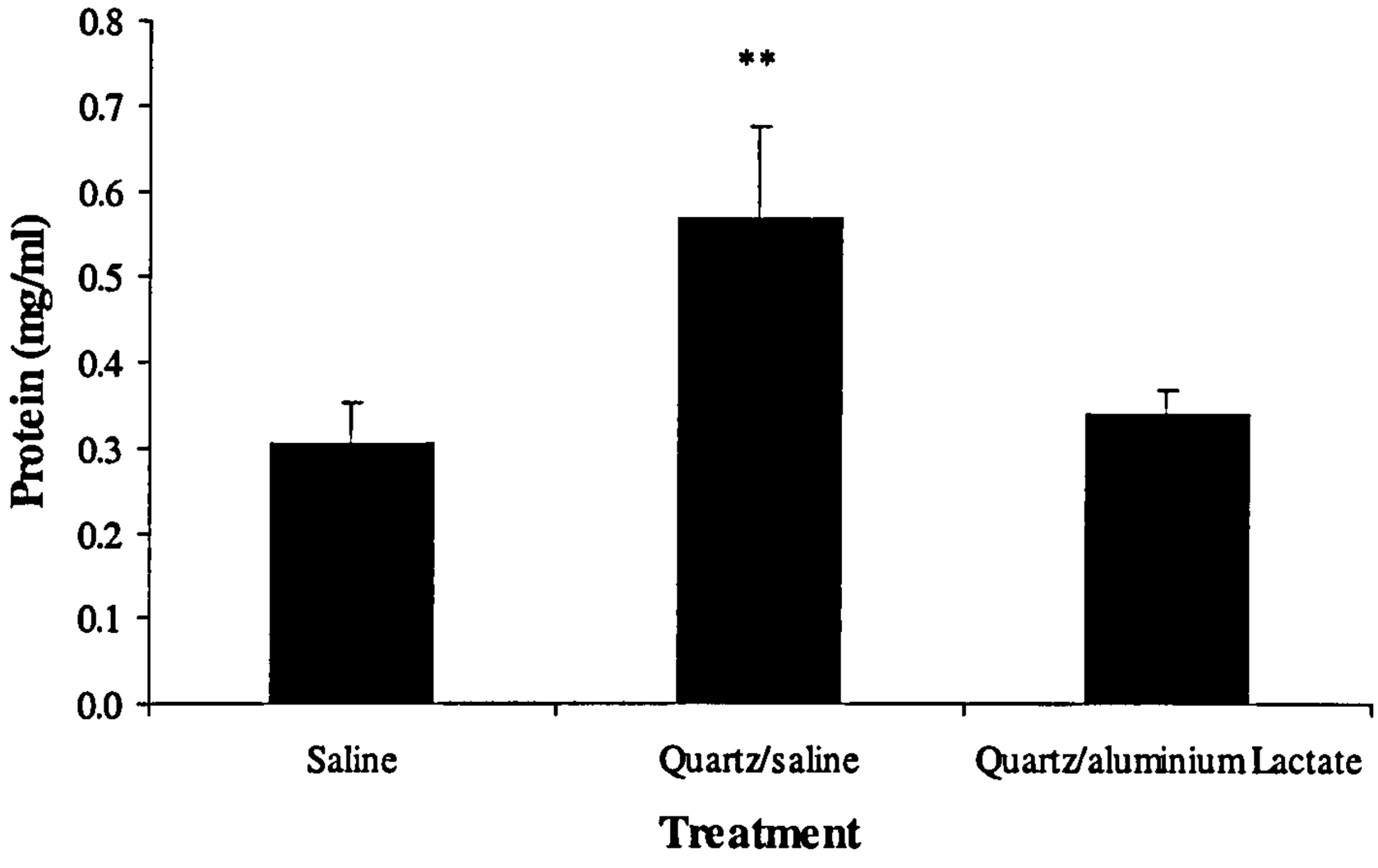

*Figure 3.4.3 Total protein concentration in BALF 18 hours post intratracheal instillation with saline, quartz/saline and quartz/aluminium lactate (250 μg). Values are expressed as mean and SEM of three rats in each group. ** p< 0.01, quartz/saline compared to saline.*

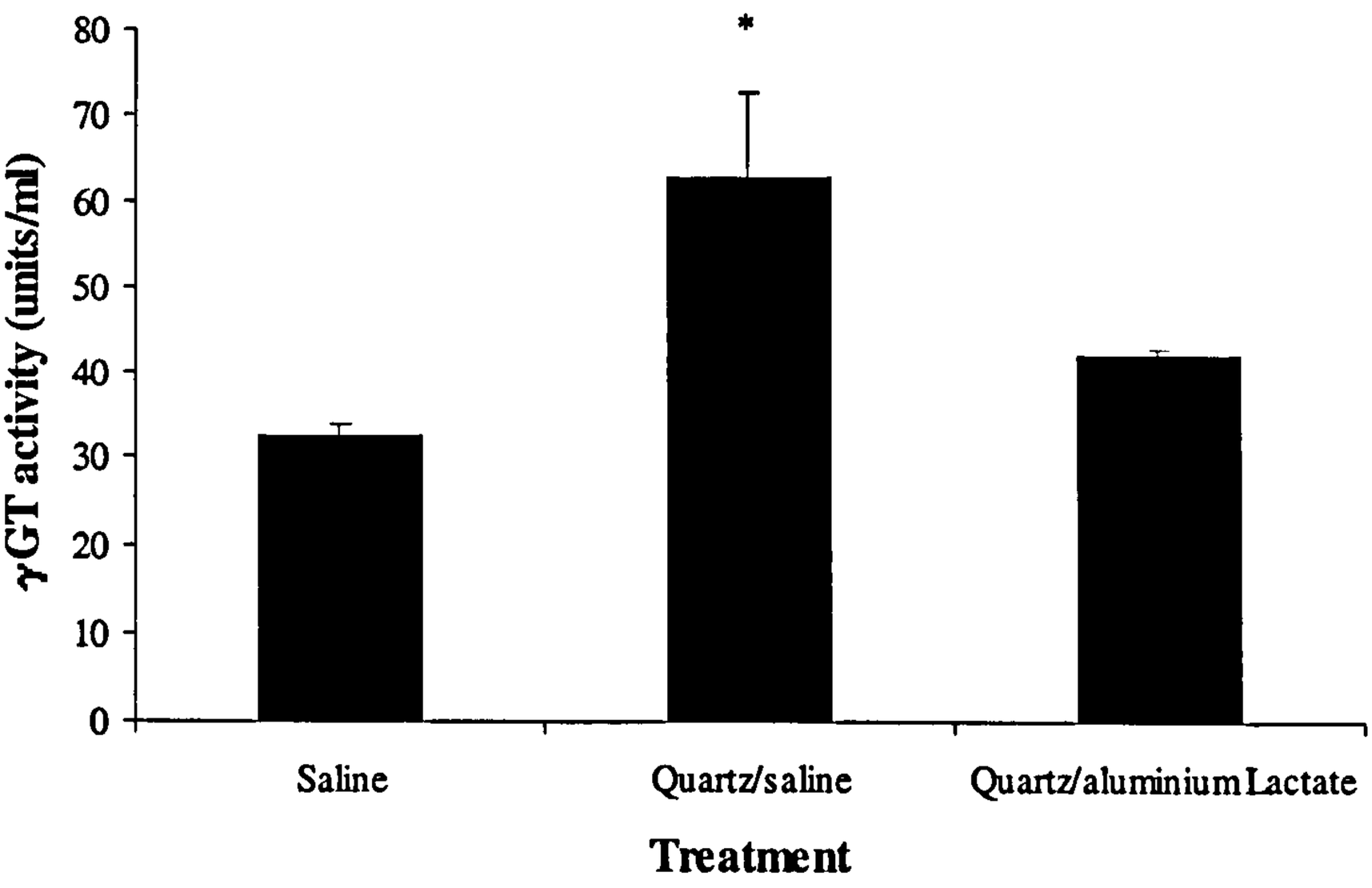

*Figure 3.4.4 γGT activity in BALF 18 hours post intratracheal instillation of saline, quartz/saline and quartz/aluminium lactate (250 μg). Values are expressed as mean and SEM of three rats in each group. * p< 0.05, quartz/saline compared to saline.*

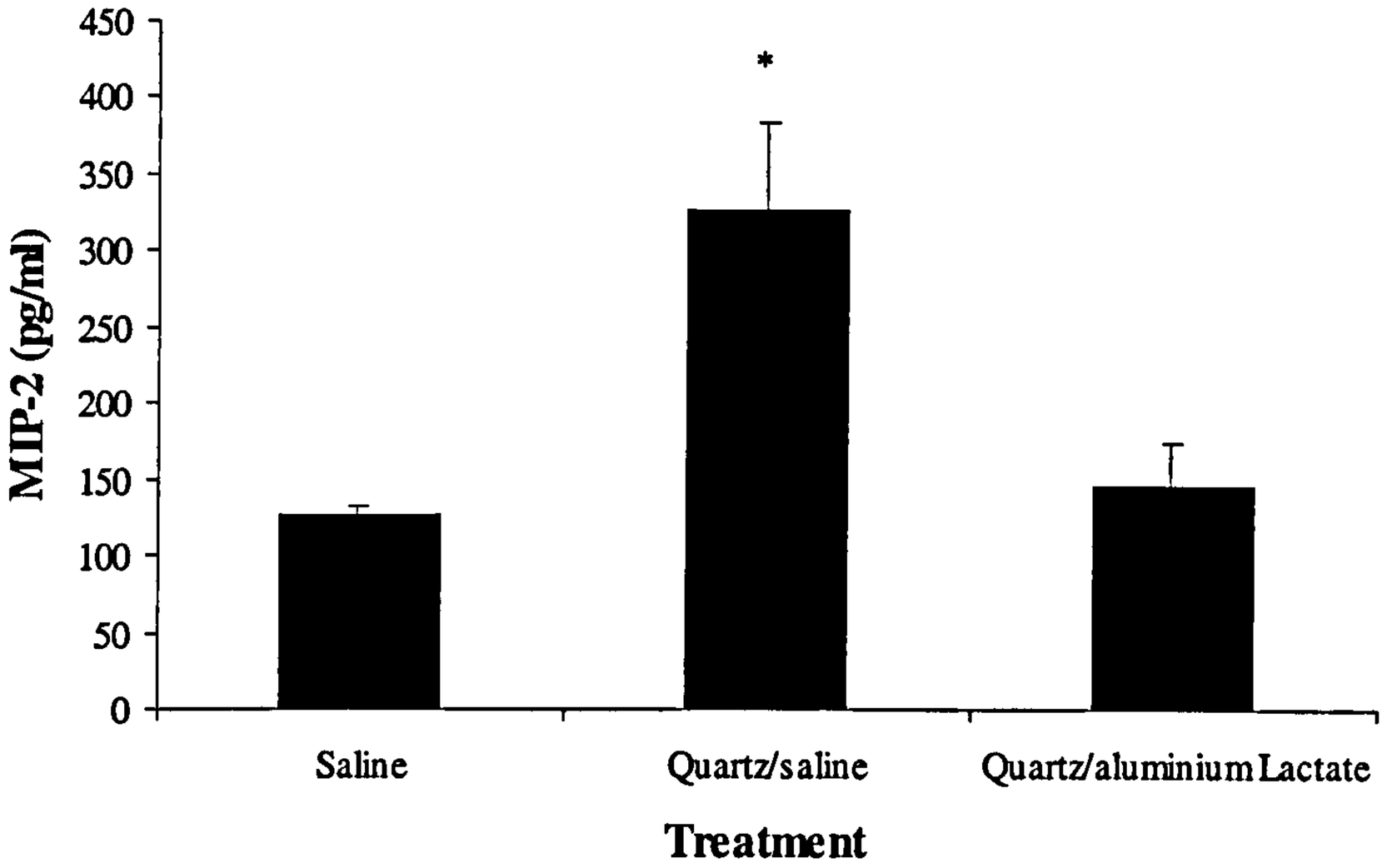

*Figure 3.4.5 MIP-2 protein in BALF 18 hours post intratracheal instillation with saline, quartz/saline and quartz/aluminium lactate (250 μg). Values are expressed as means and SEM of three rats in each group. * p< 0.05, quartz/saline compared to saline.*

3.5 NFκB Activation

In order to further investigate the inflammatory potential of quartz and surface-treated quartz, an electrophoretic mobility shift assay was carried out to demonstrate the effect of quartz and aluminium lactate-treated quartz on NFκB activation in BAL cells. The nuclear protein extract of BAL cells from quartz instilled animals exhibited a significant 3.5-fold greater NFκB DNA binding compared to nuclear protein of BAL cells from saline instilled animals alone. In contrast, BAL cells from aluminium lactate-treated quartz instilled animals induced a small (1.7-fold) but insignificant ($p > 0.05$) increase in NFκB DNA binding, 6 hours post intratracheal instillation (Figure 3.5)

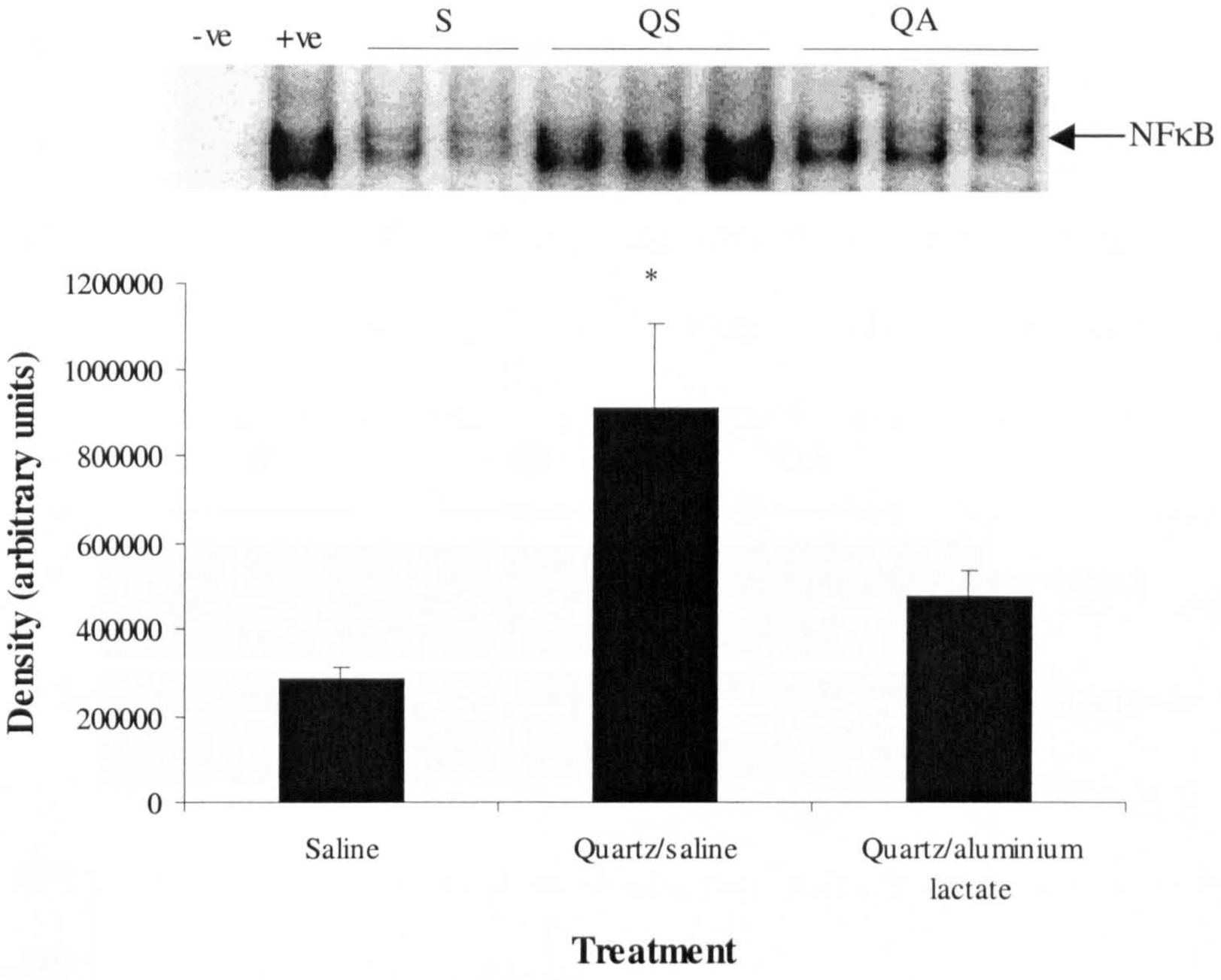

*Figure 3.5 NFκB binding to DNA using nuclear proteins extracted from rat BAL cells 6 hours post intratracheal instillation with saline (S), quartz/saline (QS) and quartz/aluminium lactate (QA). Scanned image show the EMSA results for nuclear proteins extracted from individual rats and figure shows the means and SEM. * p< 0.05, quartz/saline compared to saline.*

3.6 Expression of MIP-2 mRNA

The effect of intratracheal instillation of quartz and aluminium lactate-treated quartz on BAL cell MIP-2 mRNA expression 18 hours post instillation is shown in Figure 3.6. A low, basal level of MIP-2 mRNA expression was observed in the saline instilled control animals. MIP-2 mRNA expression was significantly increased (7-fold) with quartz exposure compared to both saline- and aluminium lactate-treated quartz. There was no

significant difference in MIP-2 mRNA expression between saline instilled control animals and aluminium lactate-treated quartz instilled animals.

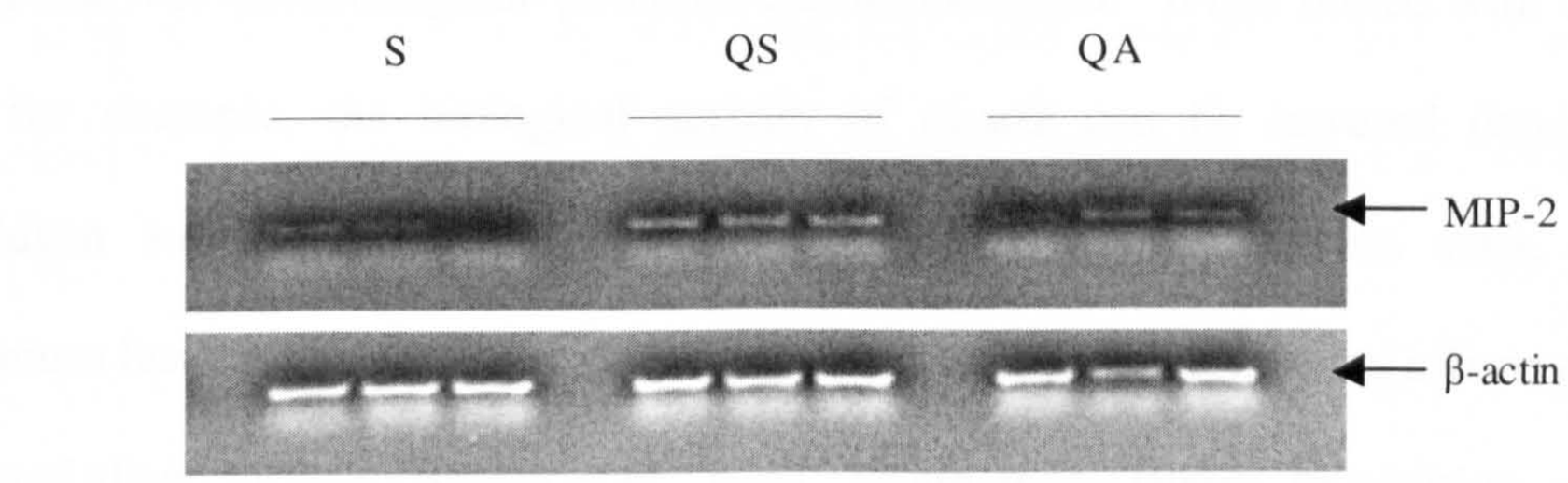

*Figure 3.6 MIP-2 mRNA expression in BAL cells 18 hours post intratracheal instillation of saline (S), quartz/saline (QS) and quartz/aluminium lactate (QA). Scanned images show the RT-PCR product of mRNA isolated from the BAL cells of individual rats and the figure shows the means and SEM. ** p< 0.01, quartz/saline compared to saline alone. †† p< 0.01, quartz/saline compared to quartz/aluminium lactate.*

3.7 Discussion

The pathological effects of quartz, manifested as fibrosis and cancer, are thought to arise, at least partly, as a direct result of the ability of quartz to cause chronic inflammation (IARC, 1997; Donaldson and Borm, 1998; Driscoll *et al.*, 1995) and the inflammogenicity of quartz itself is very well documented (Brown *et al.*, 1989; Begin *et al.*, 1986; Driscoll *et al.*, 1996; IARC, 1997). However, experimental studies have shown that this inflammogenic potential can be modified. When mixed with coalmine dust, for example, the biological activity of quartz can be lowered (reviewed in Donaldson and Borm, 1998). Incubating quartz with aluminium salts, such as aluminium lactate, has also been shown to reduce the pro-inflammatory effects of quartz in rat and sheep models (Brown *et al.*, 1989; Begin *et al.*, 1986). In addition, a number of other treatments have been reported to, in general, decrease the harmfulness of the quartz surface (reviewed in Fubini, 1998b).

Here, it was demonstrated that incubation of respirable, inflammogenic quartz particles (DQ12) with a soluble aluminium salt can inhibit the ability of the quartz particles to induce an inflammatory response *in vivo* and that this inhibition occurs at a cellular and molecular level.

In addition to preventing the influx of macrophages and neutrophils into the lungs, aluminium lactate treatment of quartz also prevented a quartz-induced increase in protein in the airspaces as indicated by BALF protein content. This may have resulted from protein exudation from plasma (microvascular leakage) or from the products of dead or injured cells released into the airspaces. Aluminium lactate-treated quartz also induced significantly less damage to airspace epithelial cells than quartz alone, as

indicated by BALF γGT activity, which is indicative of Type II and Clara cell injury. The interaction of quartz with alveolar macrophages and epithelial cells has been shown to induce increased expression of pro-inflammatory mediators such as cytokines (Rojanasakul *et al.*, 1997) and chemokines (Driscoll *et al.*, 1996) which in turn leads to inflammation. It is proposed that leukocytes attracted to a site of inflammation release oxidants and so add to the oxidative stress caused by free radicals associated with the quartz surface (Vallyathan *et al.*, 1988) which will further drive the inflammatory, fibrogenic and carcinogenic responses (Schins *et al.*, 1999; Driscoll *et al.*, 1996; Wink *et al.*, 1998).

NF-κB is an oxidative stress-responsive transcription factor (Rahman and MacNee., 1998) that is involved in the pro-inflammatory effects of many pathogenic particle types (Schins and Donaldson, 2000). Its role in discriminating between inflammogenic (native) and non-inflammogenic (aluminium lactate treated) quartz has been further demonstrated here. Activation of the oxidative stress-responsive transcription factor NF-κB has been previously reported following quartz exposure in rats (Sacks *et al.*, 1998) and in cells *in vitro* as shown by IκB depletion (Schins *et al.*, 2000). NF-κB-dependent genes are up-regulated after quartz exposure of cells (Rojanasakul *et al.*, 1997; Schins *et al.*, 2000; Driscoll *et al.*, 1996). Native quartz instillation, but not aluminium lactate–treated quartz induced an increase in the binding of nuclear protein, isolated from BAL cells 6 hours post instillation, to the NF-κB oligonucleotide concencus sequence. This finding suggests that the coating of quartz with aluminium lactate was able to inhibit quartz-induced NF-κB activation, a key step involved in the up-regulation of several proinflammatory cytokines.

The inability of aluminium lactate-treated quartz to induce MIP-2 expression as indicated by MIP-2 protein levels in BALF as well as mRNA content of BALF cells supports the contention that this was a low-hazard sample compared with quartz alone. The chemokine MIP-2, has previously been shown to play a role in the recruitment of neutrophils into the rat lung after quartz exposure (Driscoll *et al*, 1995,1996; Yuen *et al.*, 1996). The source of MIP-2 in BALF after quartz exposure in this study is unclear as the inflammatory cell profile of the lavage fluid was drastically altered by the quartz treatment, with a dramatic increase in the proportion of BALF PMN. Although it is not known if the PMN, macrophages or epithelial cells were the source of the increased MIP-2, it is clear that aluminium lactate treatment of the quartz prevented up-regulation of the events leading to increased MIP-2 expression in the lung in general. Although Driscoll *et al*, (1993) reported MIP-2 production by epithelial cells, there were negligible numbers of epithelial cells in the BALF, indicating that the source of the MIP-2 mRNA was either macrophages and/or PMNs, not the epithelial cells. The failure of aluminium lactate-treated quartz to cause inflammation could relate to changes in its surface, leading to a failure to stimulate TNF-α release from macrophages (Driscoll *et al.*, 1997), or a failure to cause direct MIP-2 production by macrophages, neutrophils or epithelial cells.

The exact mechanism of the interaction between the quartz particles and lung cells remains unknown. Using ESR, we have shown that DQ12 generates hydroxyl radicals in the presence of hydrogen peroxide, which is in keeping with previous studies (Fubini *et al.*, 1990; Vallyathan *et al*, 1991; van Maanen *et al.*, 1999). Treatment of the quartz surface with aluminium lactate reduced this hydroxyl radical formation. The mechanism by which aluminium interacts with the quartz surface is not well

understood; however, aluminium is thought to insert into the crystal lattice in place of released silicon under acid conditions (Fubini, 1998). The structure of quartz suggests an affinity of aluminium for this tetrahedral lattice, at points where defects enable this bonding to occur (Quinot *et al.*, 1979). It has been demonstrated here that treatment of the quartz particles with aluminium lactate did not affect the size of the particles, nor did it cause particle aggregation, therefore the particle surface area for biological interaction or for free radical generation was not affected. Although hydroxyl radicals may mediate the harmful effects of quartz here, a study involving workplace respirable quartz samples has shown that, although they have virtually no inflammogenic activity following instillation into the rat lung, they have more surface hydroxyl radical activity than DQ12 (Clouter *et al*, 2001). This apparent anomaly may be explained by the fact that different quartz samples have different types of surface reactivity.

Chapter 4

DIFFERENCES IN HUMAN LUNG EPITHELIAL CELL TOXICITY, PARTICLE UPTAKE AND DNA DAMAGE *IN VITRO* FOLLOWING TREATMENT WITH QUARTZ AND SURFACE MODIFIED QUARTZ.

4.1 Aims and Hypotheses.

The aim of the present study was to determine the effects of coating of respirable quartz particles on the induction of DNA damage in lung epithelial cells and to investigate whether phagocytosis may play a role in the observed effects. It is hypothesised therefore, that the genotoxic effects of the different particle treatments will be related to cytotoxicity and particle uptake in epithelial cells. Furthermore, coating of the quartz particles will reduce their genotoxicity and in the absence of cytotoxicity, particle uptake may play an important role in the induction of DNA damage by respirable quartz particles.

4.2 Haemolytic Ability of Quartz and Surface-Treated Quartz.

Haemolysis of erythrocytes due to direct membrane damage was used as a measure of surface reactivity of the treated and untreated quartz particles. Quartz particles were found to cause a dose-dependent increase in the percentage haemolysis of human erythrocytes. Treatment of the quartz particles with aluminium lactate significantly prevented haemolysis at an equivalent dose compared to untreated quartz (Figure 4.2.1 A). To further investigate the effect of surface coating of quartz particles in the haemolysis of erythrocytes, extracts from a panel of clays found in the earth's crust were used to treat quartz particles. Again quartz particles at a single dose of 5 mg/ml were found to cause an increase in the percentage haemolysis of human erythrocytes. Treatment of the quartz particles with extracts from clays 1, 2, 4, 5, 6 and 7 significantly ($p < 0.001$) prevented erythrocyte haemolysis at a single dose of 5 mg/ml compared with untreated quartz. Quartz treated with an extract from clay 3 (Hectorite) had no significant effect on erythrocyte haemolysis when compared to untreated quartz (Figure 4.2.1 B).

A.

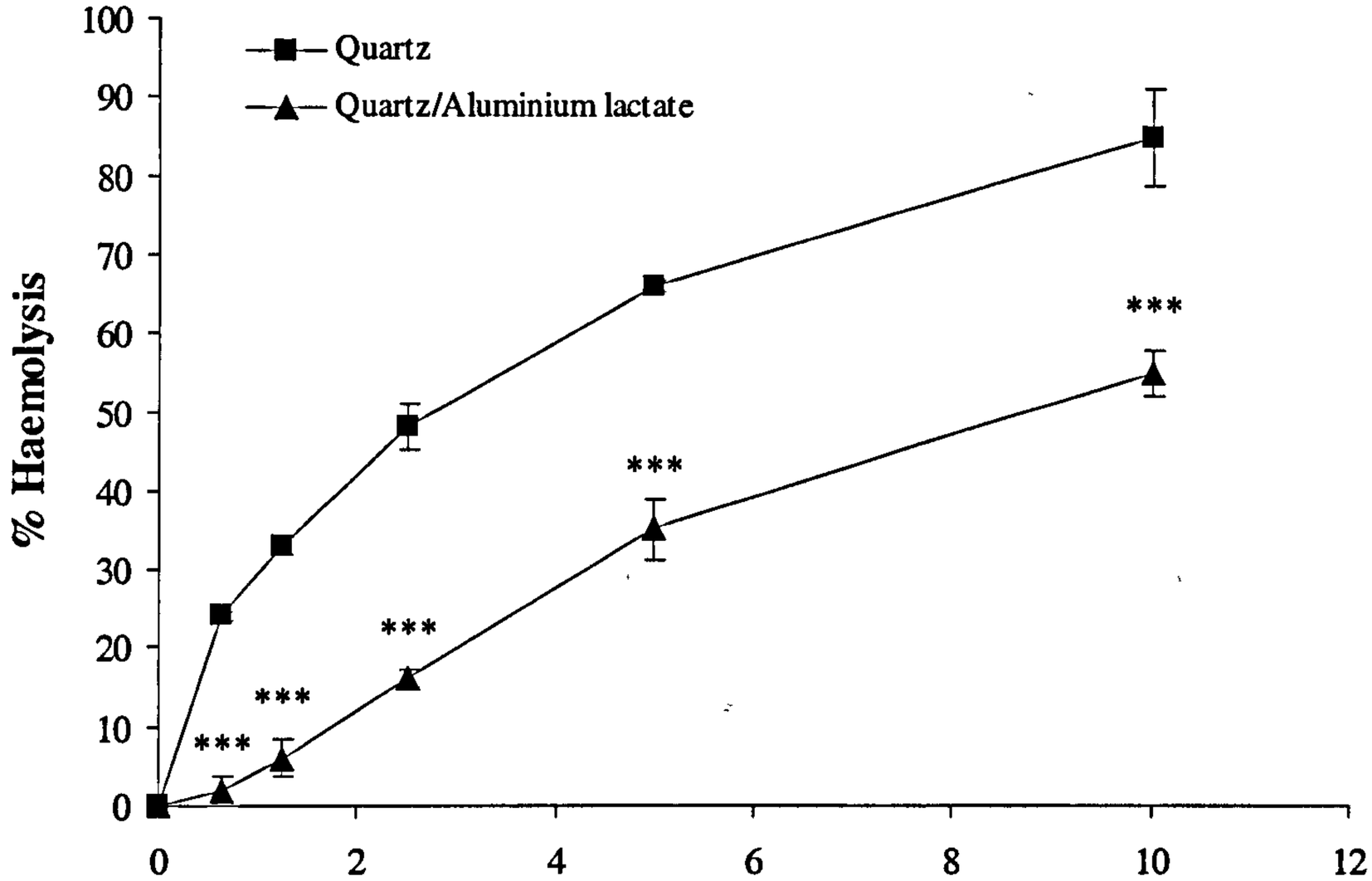

Concentration (mg/ml)

B.

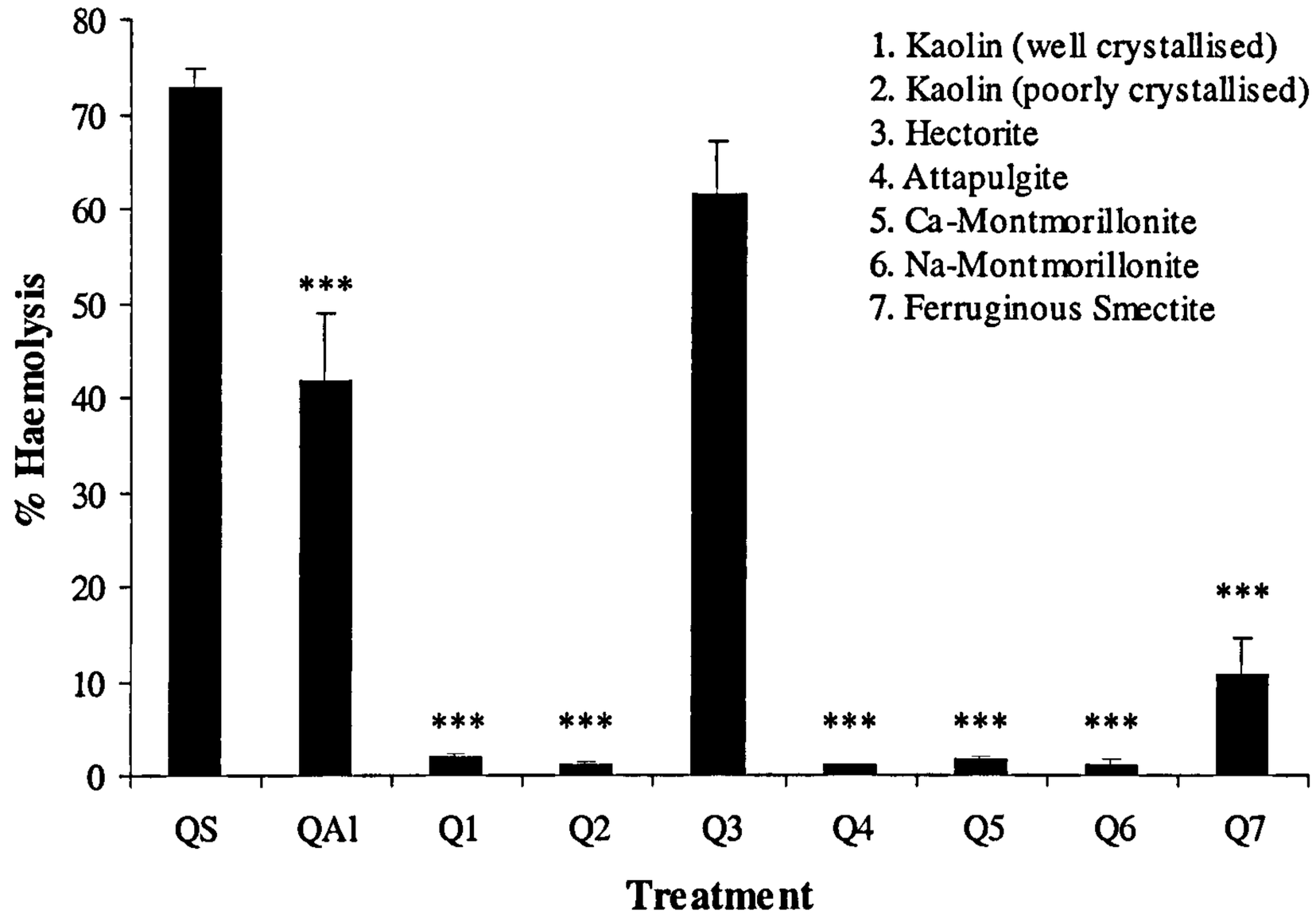

Figure 4.2.1 A. *Haemolytic activity of varying concentrations of quartz and aluminium lactate-treated quartz particles on human erythrocytes. Values are expressed as mean percentage haemolysis ± SEM of three replicates in three experiments.* *** $p < 0.001$.

B. *Haemolytic activity of quartz and treated quartz (aluminium lactate (Al) and differing clay extracts (1 – 7)) at a single dose of 5 mg/ml on human erythrocytes. Values are expressed as mean percentage haemolysis ± SEM of three replicates in three experiments.* *** $p < 0.001$.

4.3 Cytotoxicity of Quartz and Surface-Treated Quartz Particles.

The cytotoxic effect of quartz particles with or without coating, on A549 cells was determined by two independent assays, i.e. the MTT-assay and the LDH-assay. The results of the MTT-assay, as a measure of metabolic competence of the cells following

4 hours treatment with the different quartz preparations are shown in Figure 4.3.1. The toxicity of quartz, observed at a concentration of 200μg/cm^2, was significantly inhibited upon coating with aluminium lactate or PVNO. Inhibition of the toxicity of the quartz seemed to be more effective for the PVNO-coated quartz particles. The effects of quartz and coated quartz particles on cell membrane integrity, as determined by the LDH assay, are shown in Figure 4.3.2. None of the particle treatments caused a significant membranolytic effect at 4 hours, with the exception of quartz at the highest concentration, i.e. 200μg/cm^2.

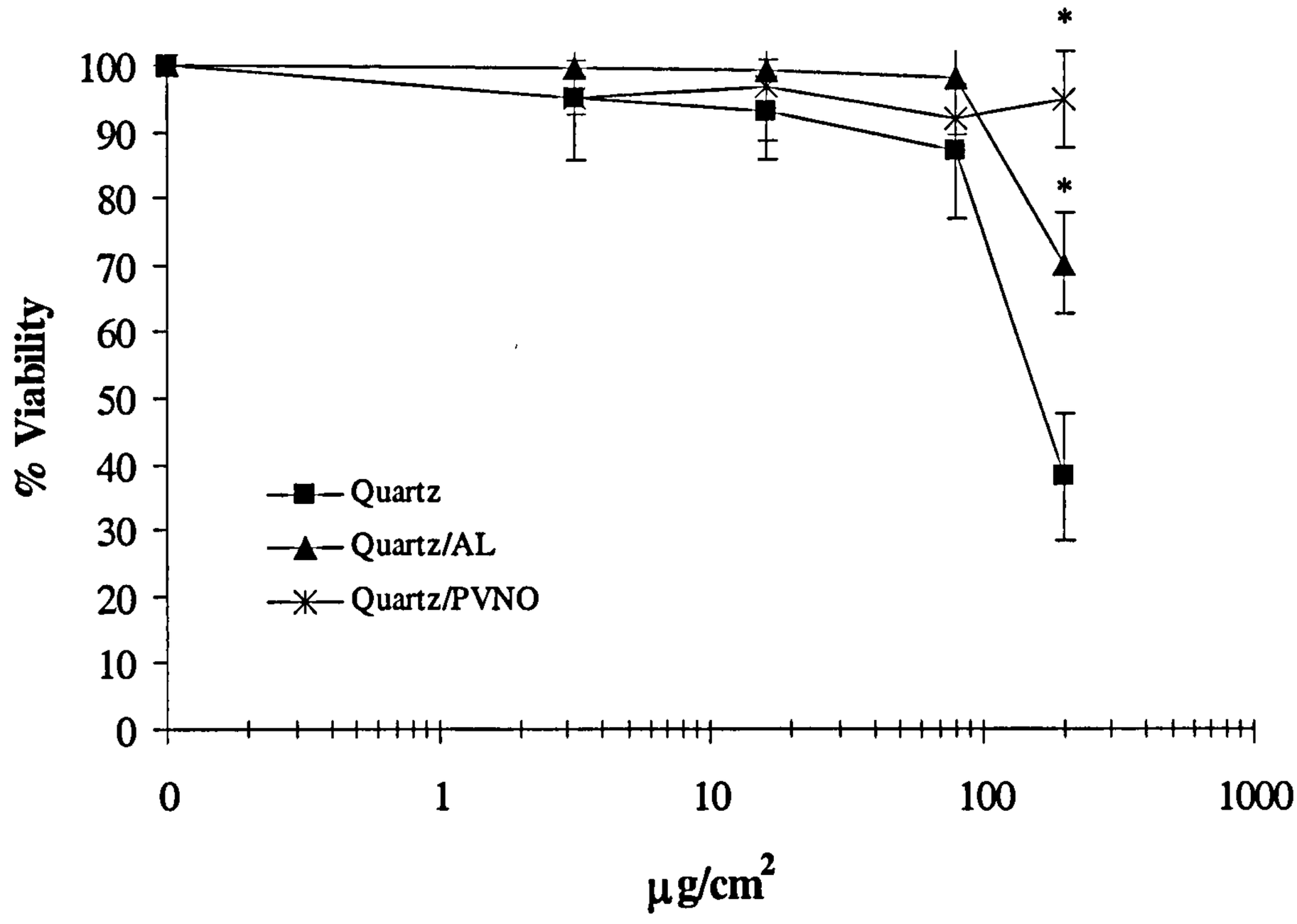

Figure 4.3.1 *Cytotoxicity (MTT-assay) of the different quartz preparations in A549 human lung epithelial cells. Cells were treated for 4 hours with quartz particles with or without surface modification with aluminium lactate or PVNO at the indicated concentrations. Cytotoxicity was measured using the MTT-assay as a measure of metabolic competence of the cells. The viability of the cells for each treatment and concentration is expressed as a percentage of control values. Data are expressed as mean and standard deviations of three independent experiments, each using 5 replicate wells per concentration. * $p<0.05$ vs Quartz.*

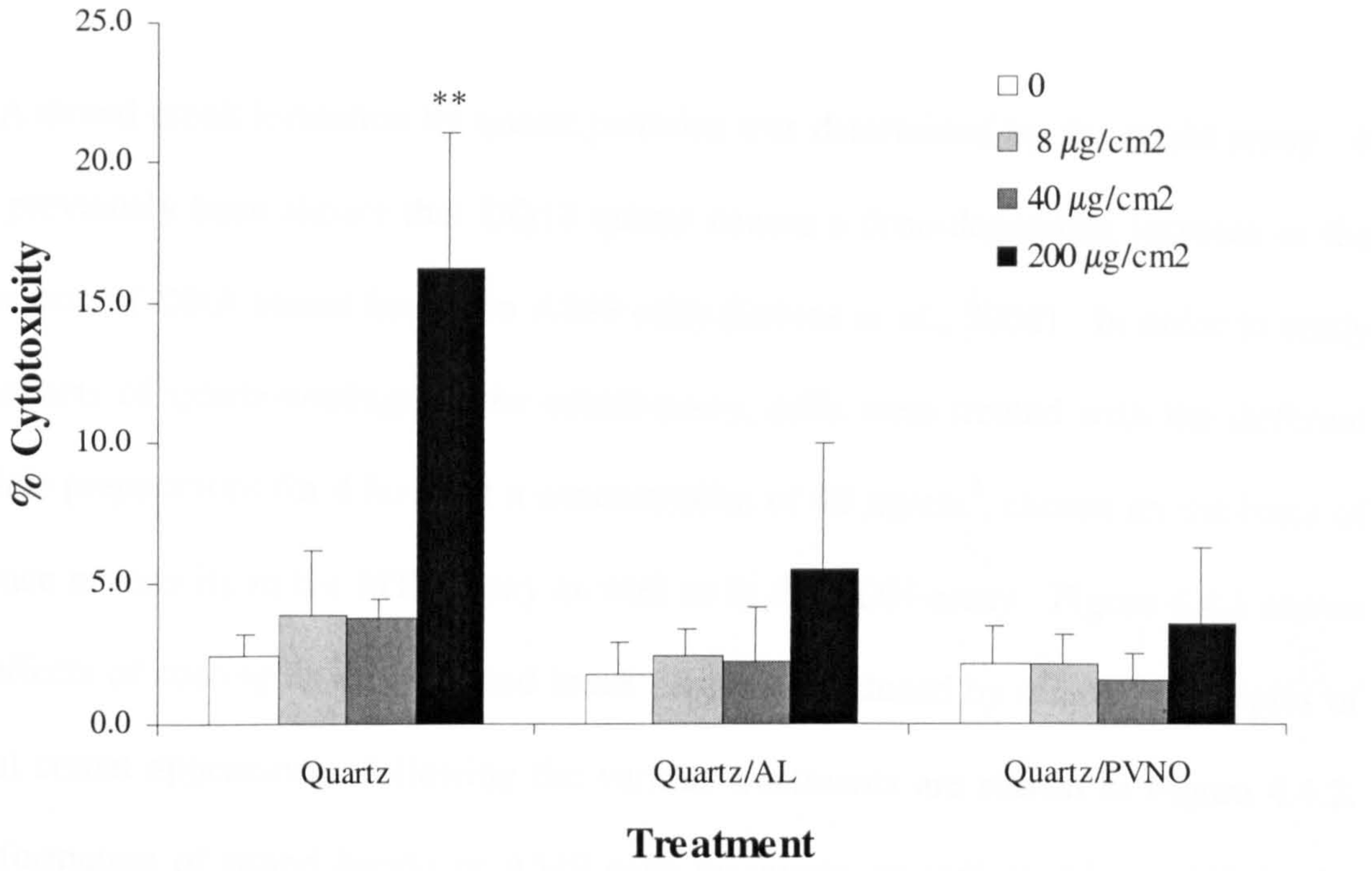

Figure 4.3.2 *Cytotoxicity (LDH-assay) of the different quartz preparations in A549 cells. Cells were treated for 4 hours with quartz particles with or without surface modification at the indicated concentrations. Cytotoxicity was determined using the LDH assay as an indicator of cell membrane damage. Data are expressed as the percentage of extracellular LDH and represent the mean and standard deviations of three independent experiments, each using duplicate wells per concentration. * $p<0.05$ and ** $p<0.01$ versus control.*

4.4 Formation of DNA Strand Breaks by Quartz and Surface-Treated Quartz.

DNA strand break formation by quartz particles was determined by the comet assay. It has previously been shown that DQ12 quartz causes a dose-dependant increase in the formation of DNA strand breaks in A549 cells (Schins *et al.*, 2002). In order to study the effects of quartz-coatings in the comet-assay, cells were treated with the different particle preparations for 4 hours at a concentration of 40 $\mu g/cm^2$, chosen on the basis of absence of toxicity in the MTT-assay as well as in the LDH-assay. Figure 4.4.1 shows the effects of coating on DNA strand break formation induced by quartz. Examples of actual comet appearances following the various treatments are shown in Figure 4.4.2. The formation of strand breaks in A549 cells by quartz, as indicated by a shift in the distribution of comet classes towards an increased level of damage, was significantly reduced for the coated quartz particles. This is demonstrated by the absence of any significant difference in comet class distribution from cells treated with coated quartz, when compared to the comet class distributions observed in untreated cells.

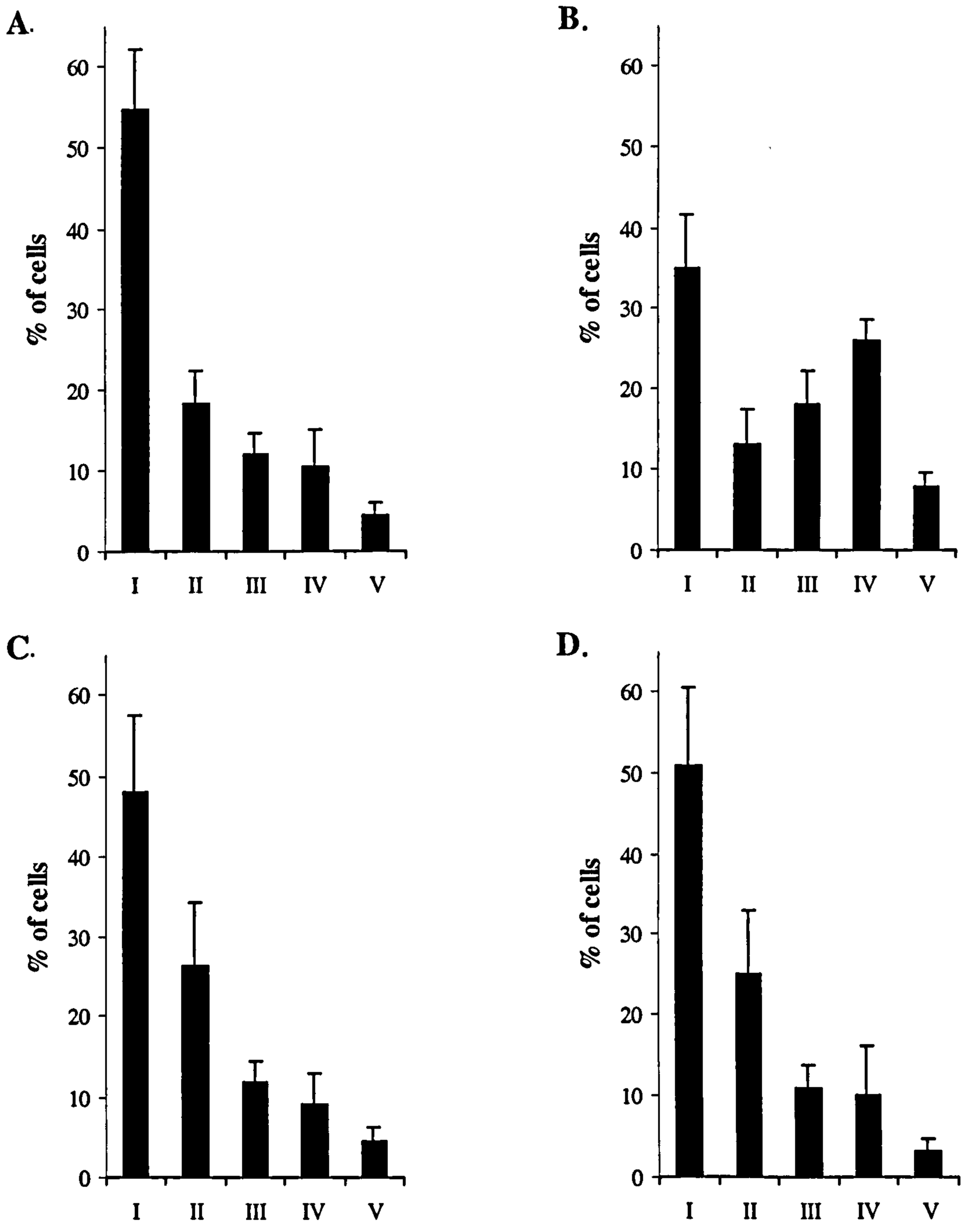

Figure 4.4.1 DNA stand break formation by quartz with and without aluminium lactate or PVNO treatment. A549 cells were treated for 4 hours with either quartz (B), aluminium lactate-treated quartz (C) or PVNO-treated quartz (D) at a concentration of 40 μg/cm^2. Data are expressed as mean and SEM of comet classes according to comet tail length (distinguished by I, II, III, IV and V) as determined in three individual experiments, using two slides per treatment (see methods for details). DNA strand breakage observed in the cells treated with quartz was significantly higher (χ^2, $p<0.01$) compared to untreated, control cells (A), as well as to DNA damage as observed in the cells treated with aluminium lactate and PVNO treated quartz.

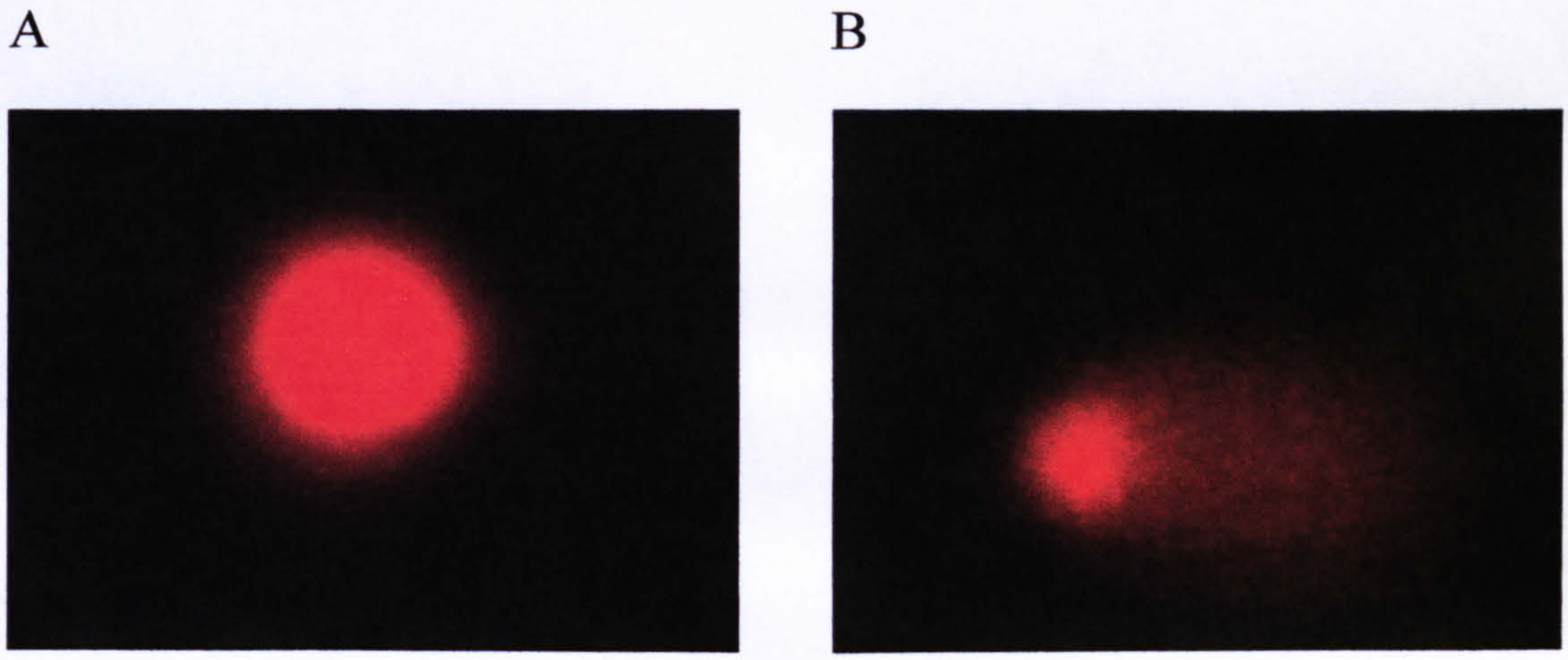

Figure 4.4.2 *Examples of comets, showing the range of appearances from a control cell (A) to a quartz treated cell (B). Pictures are shown at 1000× magnification.*

4.5 Cellular uptake of quartz particles with and without surface coatings.

The effects of the different coatings on the intracellular uptake of DQ12 quartz by the type II human lung epithelial cell line, A549 are shown in Table 4.5.1. After 2 hours of exposure, most of the epithelial cells had already ingested quartz particles, whereas quartz coated with PVNO was found in less than 15 % of the cells observed. The aluminium lactate coated particles were ingested by the cells to a larger extent in comparison to the PVNO coated particles, however markedly less when compared to the non-coated particles at 2 and 4 hours. Interestingly, at 24 hours the particle uptake appeared to be similar for the non-coated quartz and for the aluminium lactate coated quartz, whereas cellular uptake of PVNO-coated quartz remained minimal. Similar observations are made for the number of particles that were ingested (see Table 4.5.1). Figure 4.5.1 shows examples of differing particle uptake in the A549 cells following the various treatments.

Table 4.5.1 *Uptake of quartz and coated quartz particles in A549 cells*

Time	*Quartz*	*Quartz/AL*	*Quartz/PVNO*
% of cells with particles			
2 h	93.7 (91.7–94.6)	69.9 (57.6–86.4) [b]	11.8 (10.0–13.7) [b, c]
4 h	88.3 (87.7–88.9)	45.2 (17.5–81.4)	14.3 (4.4–27.2) [b]
24 h	79.7 (78.7–80.6)	84.4 (83.7–85.1)	10.1 (6.1–12.1) [b, c]
No. Particles/phagocytosing cell [a]			
2 h	7.0 (6.7–7.4)	3.6 (2.2–4.4) [b]	1.7 (1.3–2.1) [b, c]
4 h	5.2 (4.4–5.9)	3.2 (2.0–4.1) [b]	2.4 (1.5–3.5) [b]
24 h	5.3 (4.2–6.6)	5.6 (5.5–5.6)	1.9 (1.5–2.3) [b, c]

Data are expressed as mean, and between brackets, range

[a] Number of particles per phagocytosing cell, i.e. as determined for those cells that contained at least one particle.

[b] $p<0.05$ vs. Quartz, and [c] $p<0.05$ vs. Quartz/AL.

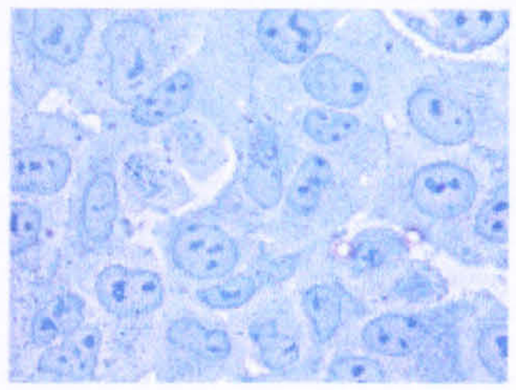

A

2 Hours **4 Hours** **24 Hours**

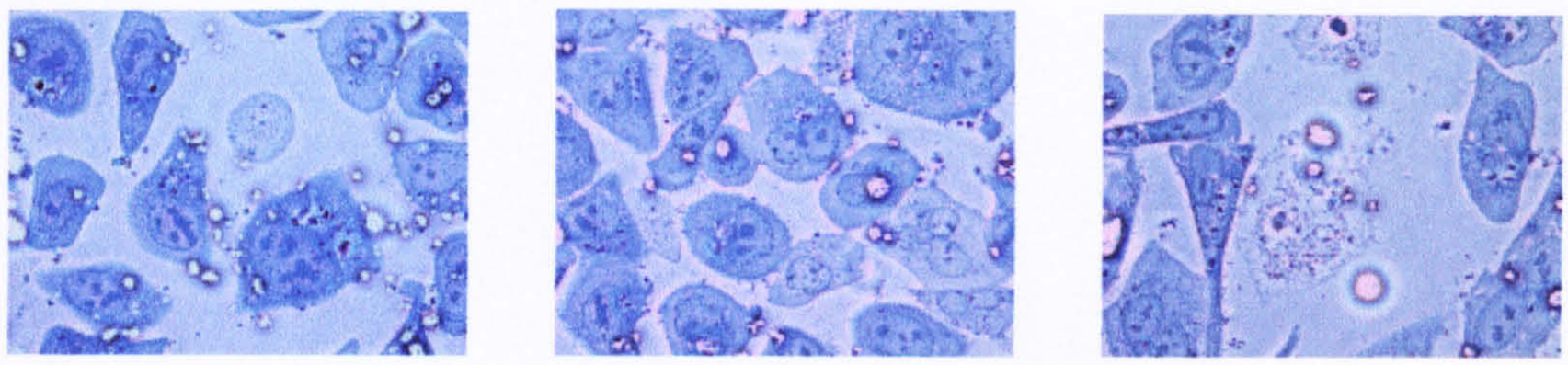

B

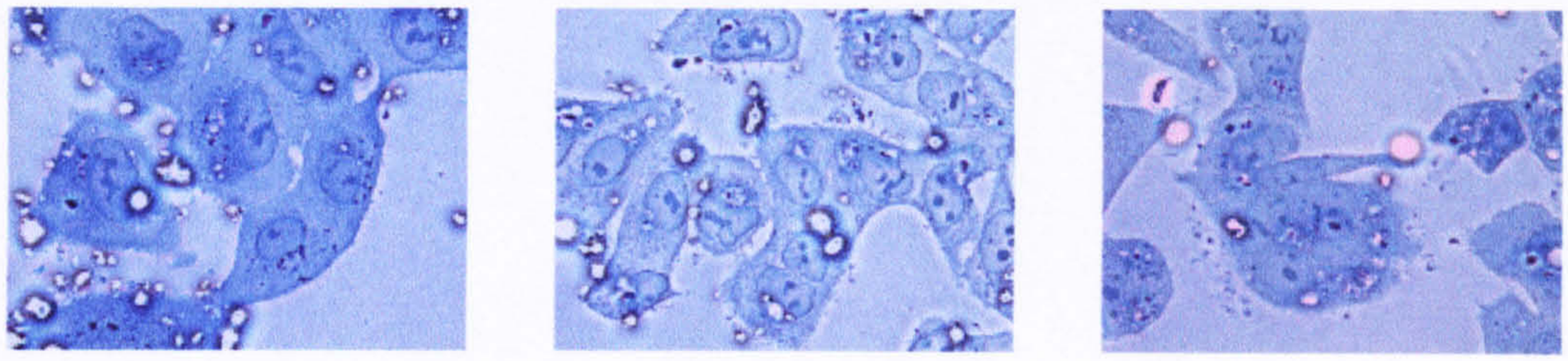

C

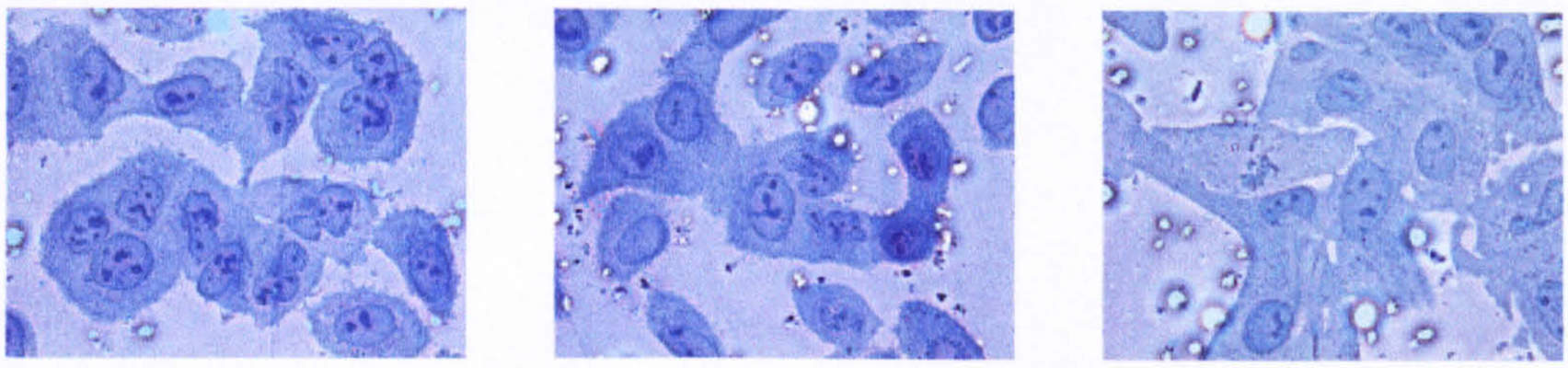

D

Figure 4.5.1 *Appearance of particle uptake in sections through A549 cells following 2, 4 and 24 hour treatments (40 μg/cm^2) with quartz (B), quartz treated with aluminium lactate (C) or quartz treated with PVNO (D) respectively. Fig. 4.4.1A shows the control cells. All pictures are shown at 1000× magnification.*

4.6 Discussion

The proposed carcinogenicity of crystalline silica (quartz) is considered to depend upon 'inherent characteristics of the material' (IARC, 1997; Donaldson and Borm, 1998; Fubini, 1998b). In terms of the known role of the surface of insoluble particles in their toxicology, this is taken to mean the inherent characteristics of the particle surface. Given the role of direct and indirect carcinogenic effects, it could be hypothesised that differences in the quartz surface reactivity might be reflected in both inflammogenic and genotoxic properties of quartz. Previous *in vitro* and *in vivo* studies with quartz using coating materials such as PVNO or aluminium lactate, have demonstrated that its surface properties play an important role in its cytotoxic, inflammogenic and/or fibrogenic effect (Begin *et al.*, 1987; Brown et al., 1989; Dufresne *et al.*, 1994; Fenoglio *et al.*, 2000). Here, it has been demonstrated that DNA strand breakage in human lung epithelial cells can be inhibited following coating of the quartz surface with aluminium lactate or PVNO. These coatings also reduced the cytotoxic capacity of the quartz and its cellular uptake by the epithelial cells. Furthermore, coating of the quartz particles with aluminium lactate as well as extracts from clays commonly found in the earth's crust, significantly inhibited the surface reactivity of the quartz as measured by its ability to cause the haemolysis of human erythrocytes.

In the past, both PVNO and aluminium lactate have been tested for their abilities to prevent or treat mineral dust-induced fibrosis, albeit with limited success (Schlipkoter *et al.*, 1970; Begin *et al.*, 1986,1987; Goldstein and Rendall, 1987). Here, both compounds were used to coat the surface of the quartz in order to evaluate the effect on DNA-damage and cytotoxicity. PVNO is considered to adsorb to quartz via H-bonding

of its NO groups with silanol groups (Gabor *et al.*, 1975; Fubini, 1998a; Fubini and Wallace, 2000). This coating phenomenon has been linked to anti-fibrogenic effect, but others have also demonstrated antioxidant properties of the PVNO (Gulumian and van Wyk, 1987), however whether this is the case with particle bound PVNO is not known. The protective effect of coating the quartz surface with PVNO provides further evidence to support the hypothesis that masking of the reactive silanol groups on the quartz surface can modify or reduce the damaging effects of the particle. The mechanism by which aluminium interacts with the quartz is less well understood and is discussed in section 3.7. Aluminium has been reported to hinder the formation of surface radicals and to block charges caused by grinding (Fubini, 1998a). The cytotoxicity data obtained using the A549 human lung epithelial cells, is in line with a variety of studies that have evaluated surface-coated quartz in relation to haemolytic activity of red cells or cytotoxicity in macrophages (Nash *et al.*, 1966; Dalal *et al.*, 1990; Fenoglio *et al.*, 2000). In addition to amelioration of the cytotoxicity due to the surface coating of the quartz particles, there is also a demonstration of a clear inhibition of the DNA-damaging properties of the quartz. Importantly, DNA damage was determined at concentrations where no cytotoxicity occurred for any of the different particle preparations. As such, the prevention of genotoxicity due to both surface coatings resulting from diminished cytotoxicity is minimal. The relevance of addressing cytotoxicity effects in genotoxicity testing has also recently been emphasised by an expert panel (Tice *et al.*, 2000). The absence of toxicity as seen with the LDH assay and the MTT assay is also important in precluding apoptosis, which has been reported in A549 cells following prolonged treatment with quartz (Lim *et al.*, 1999). However, this phenomenon is known to be highly dependent on the confluence of these cells as well as the presence or absence of serum (Garrido *et al.*, 1997; Huang *et al.*, 2000). In this case DNA damage

was determined following 4 hour treatment of the cells when near to confluency and without prior serum depletion.

In association with the observed effects of coating on DNA-damage, it was also demonstrated that both coatings dramatically affected particle uptake by the epithelial cells. These findings indicate that cellular uptake of quartz particles may play a role in its genotoxicity, although a differential effect of the two coatings was observed. The significance of phagocytosis in mineral dust-induced DNA damage has also been reported for asbestos fibres. Cytochalasin, a potent inhibitor of phagocytosis, has for instance been shown to inhibit DNA strand breakage by asbestos in rabbit pleural mesothelial cells (Liu *et al.*, 2000). On the other hand, coating of asbestos with vitronectin, which was also demonstrated to enhance fibre uptake into cells, was found to further enhance DNA strand breakage (Liu *et al.*, 2000; Wu *et al.*, 2000). In relation to these findings, it seems likely that the complete inhibition of DNA damage in the PVNO-treated quartz might be fully explained by the minimal uptake of these particles by the epithelial cells. However for the aluminium lactate-treated particles, genotoxicity was also prevented, despite considerably greater uptake at 4 hours when compared to PVNO. This indicates that the altered surface properties of the aluminium lactate-treated quartz, as was demonstrated by ESR (see section 3.3) and here using haemolytic ability, are also important within the epithelial cells. Unfortunately however, due to the relatively abundant aluminium present on the (unmodified) DQ12 quartz, it was not possible to confirm by energy dispersive X-ray analysis, whether the aluminium remained on the particle surface of the aluminium coated quartz particles following their cellular uptake.

In relation to the present data, others have shown that dipalmitoyl phosphatidylcholine, a major component of the lung surfactant, reduces micronucleus formation (a process resulting from chromosome breakage or spindle disruption) in V79 fibroblasts (Liu *et al.*, 1996), and DNA damage in rat alveolar macrophages treated with quartz, as determined by the comet assay (Liu *et al.*, 1998). These data, on the one hand emphasise that lung surfactant may play an important modulating role in particle genotoxicity *in vivo*, and on the other hand are in agreement with the present observations, i.e. that coating of the particle surface impacts substantially on the genotoxic properties of quartz particles *in vitro*. Since all particles are likely to be coated with surfactant/mucus, then this has important implications for risk assessment. The significance of radical formation and phagocytosis however was not addressed in the surfactant studies. Whether the differences in hydroxyl radical formation in the different quartz preparations shown previously (see Chapter 3), play a role in the different uptake by the A549 cells is not clear, but deserves further evaluation. In addition to the observed reductions in hydroxyl radical formation following coating, other physicochemical properties may be involved, including other surface radicals, negative surface charges, acidity or hydrophobicity of the different quartz preparations (Fubini, 1998a; Fubini and Wallace, 2000). It has also been demonstrated here that coating of the quartz surface with extracts from clays commonly found in the earth's crust (a realistic coating material which often comes into close contact with quartz during its geological history) inhibits the direct membrane damaging ability of quartz, a method used as a measure of surface reactivity and reported to correlate with the ability to cause inflammation, albeit in a small number of quartz samples (Clouter *et al.*, 2001).

These results provide important support for the proposed relationship between the radical-generating activity of the quartz surface and its genotoxicity, as well as its membrane damaging ability. The data also shed important light on the 'quartz paradox' highlighted by IARC, namely that quartz is not uniformly carcinogenic across all industries where there is quartz exposure. Relatively simple coating treatments are shown here to totally abolish the ability of quartz to exert crucial genotoxic effects that very likely play a role in quartz carcinogenesis.

Chapter 5

THE IMPORTANT ROLE OF SURFACE AREA AND SPECIFIC REACTIVITY IN THE ACUTE PULMONARY RESPONSE TO LOW AND HIGH TOXICITY PARTICLES BOTH *IN VIVO* AND *IN VITRO*.

5.1 Aims and Hypotheses.

To study the proinflammatory effects of particle surfaces in the lung, a rat instillation model of acute inflammation was developed. Whilst inhalation provides a more physiological route of delivery, it can be seen here that instillation can yield concordant results for short-term inflammatory responses and can therefore be utilised to study the effects of different particles in the lung. It has been hypothesised that (i) surface area alone drives the acute pulmonary response to 'low toxicity' poorly soluble particles (PSPs) such as titanium dioxide (TiO2), carbon black (CB) and polystyrene, suggesting that the higher the surface area instilled, the greater the inflammatory response; (ii) for quartz, a low surface area with a highly reactive surface produces inflammation and treatments which decrease its reactivity should make it act like a 'low toxicity' dust; (iii) for specific ultrafine particles with a highly reactive surface, inflammogenicity is related to both surface area and surface reactivity; and finally (iv) macrophage inflammatory protein-2 (MIP-2) levels in lavage should be related to the inflammatory cell influx.

5.2 Results *in vivo.*

All of the following instillation data are presented with the same vertical axis scale to allow direct comparison between different treatments.

5.2.1 Low Toxicity Dusts.

For 'low toxicity' dusts, the extent of inflammation as measured by neutrophil number in BAL 18 hours after instillation, was not related to the mass of particles instilled (Figure 5.2.1 A). However, when the mass dose was expressed as surface area, it determined the inflammatory response ($r^2 = 0.9907$) for a variety of very different poorly soluble particles of low toxicity (Figure 5.2.1 B). The fact that the line passes through zero, indicates that it is surface area alone that elicits inflammation for these low toxicity dusts.

A.

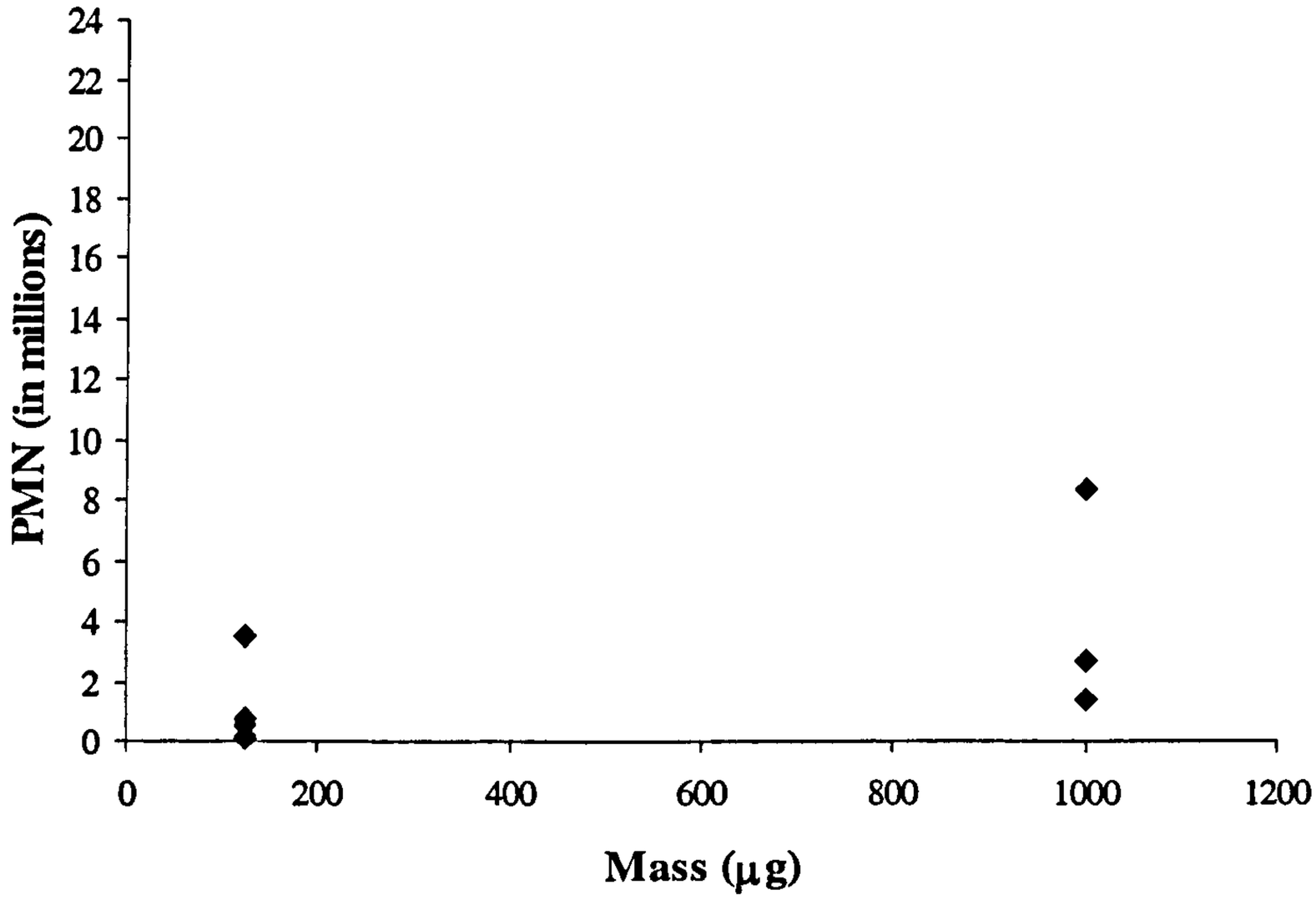

B.

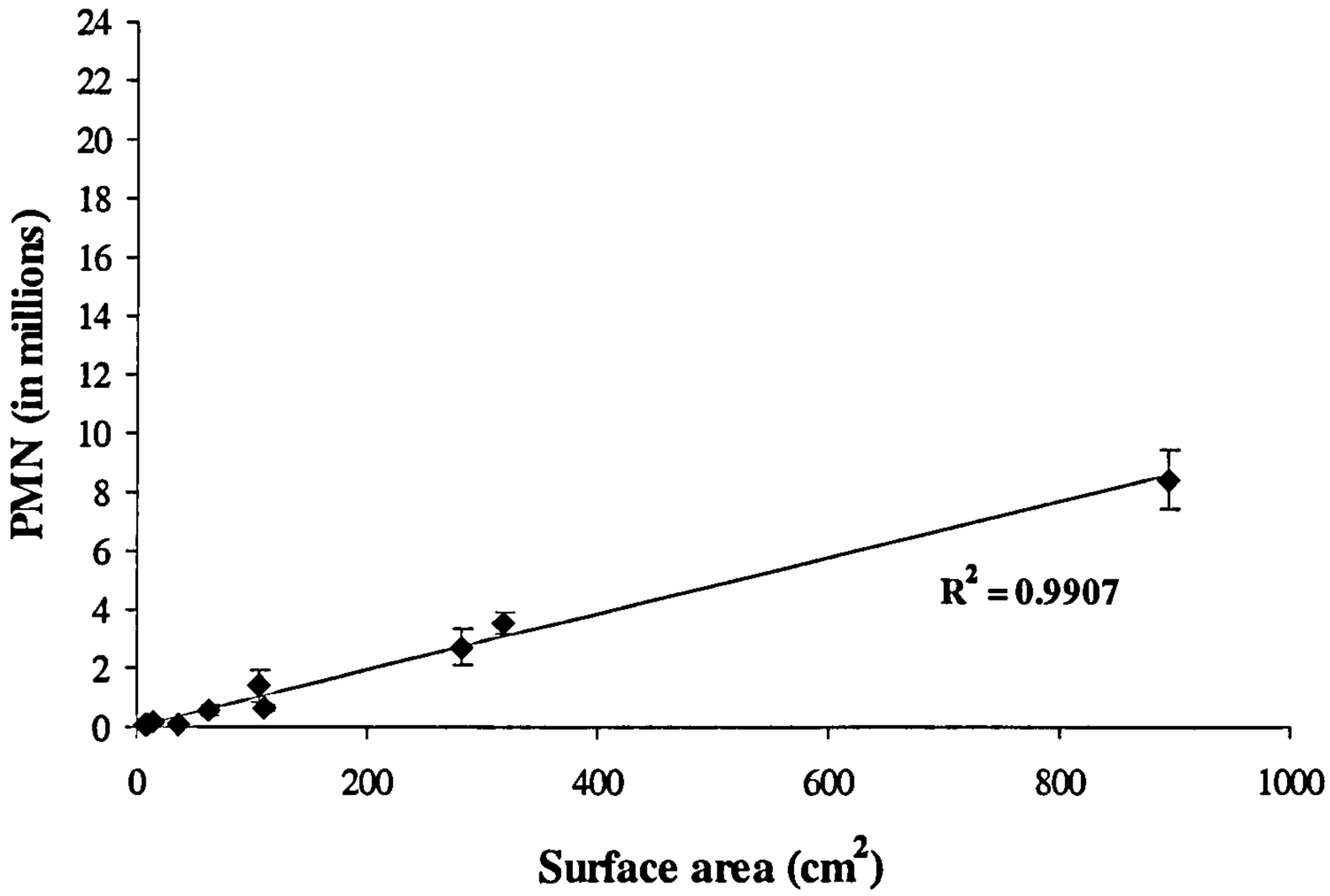

Figure 5.2.1 *Relationship between particle mass and total neutrophil number (A) and particle surface area and total neutrophil number (B) in BAL 18 hours post-instillation with a variety of low toxicity dusts including fine titanium dioxide (TiO_2), ultrafine titanium dioxide ($ufTiO_2$), fine carbon black (CB), ultrafine carbon black (ufCB) and polystyrene beads. Each point is the mean and SEM of three animals.*

5.2.2 Quartz.

In the same model, very low surface areas of quartz were sufficient to cause a relatively large scale inflammation as measured by neutrophil number in BAL (Figure 5.2.2 A). A small increase in particle surface area yielded a large increase in total PMN number, suggesting that for pure quartz particles, the surface area alone was not the only factor contributing to the inflammation observed and that the reactive quartz surface has additional ability to cause inflammation (Figure 5.2.2 B).

A

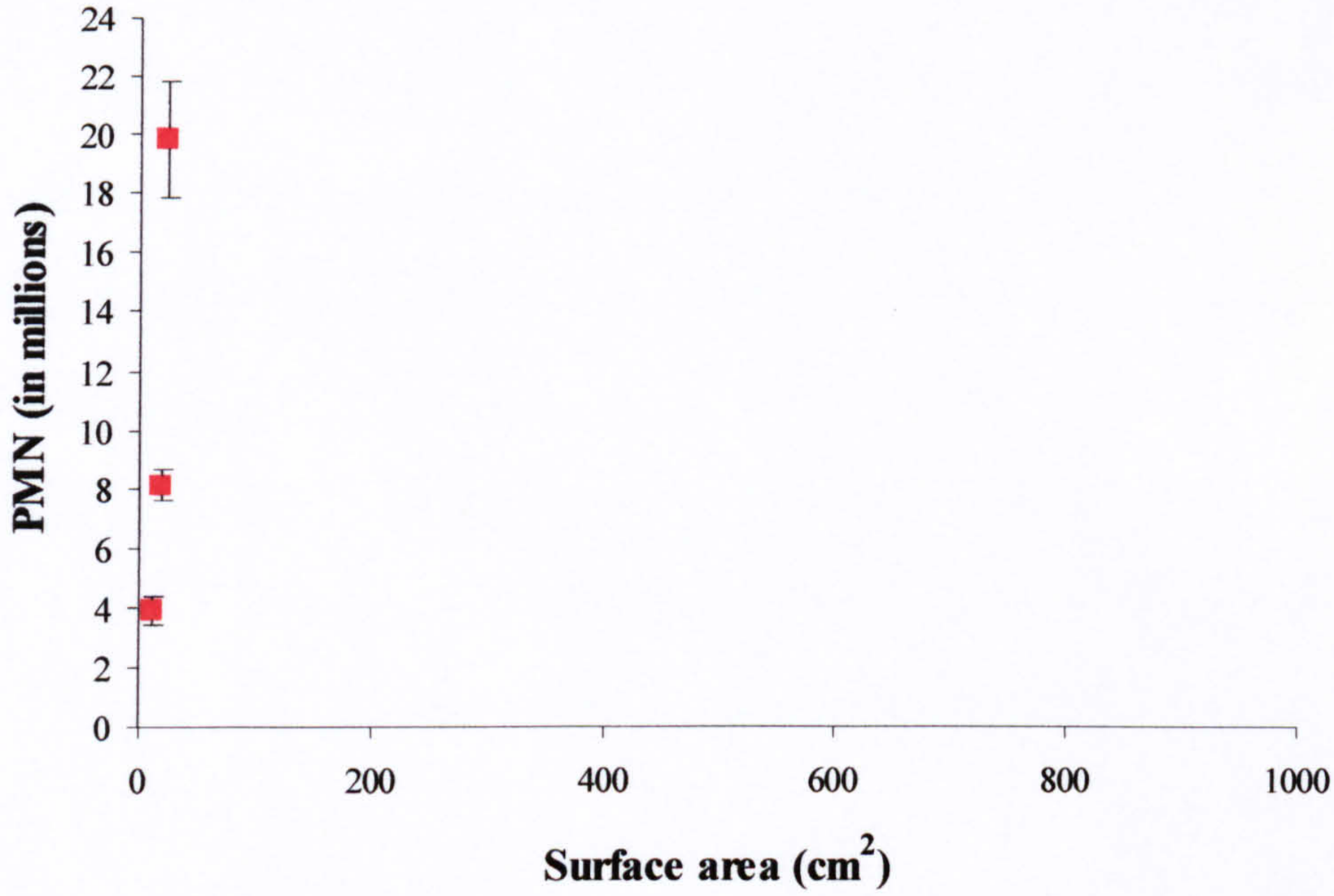

B

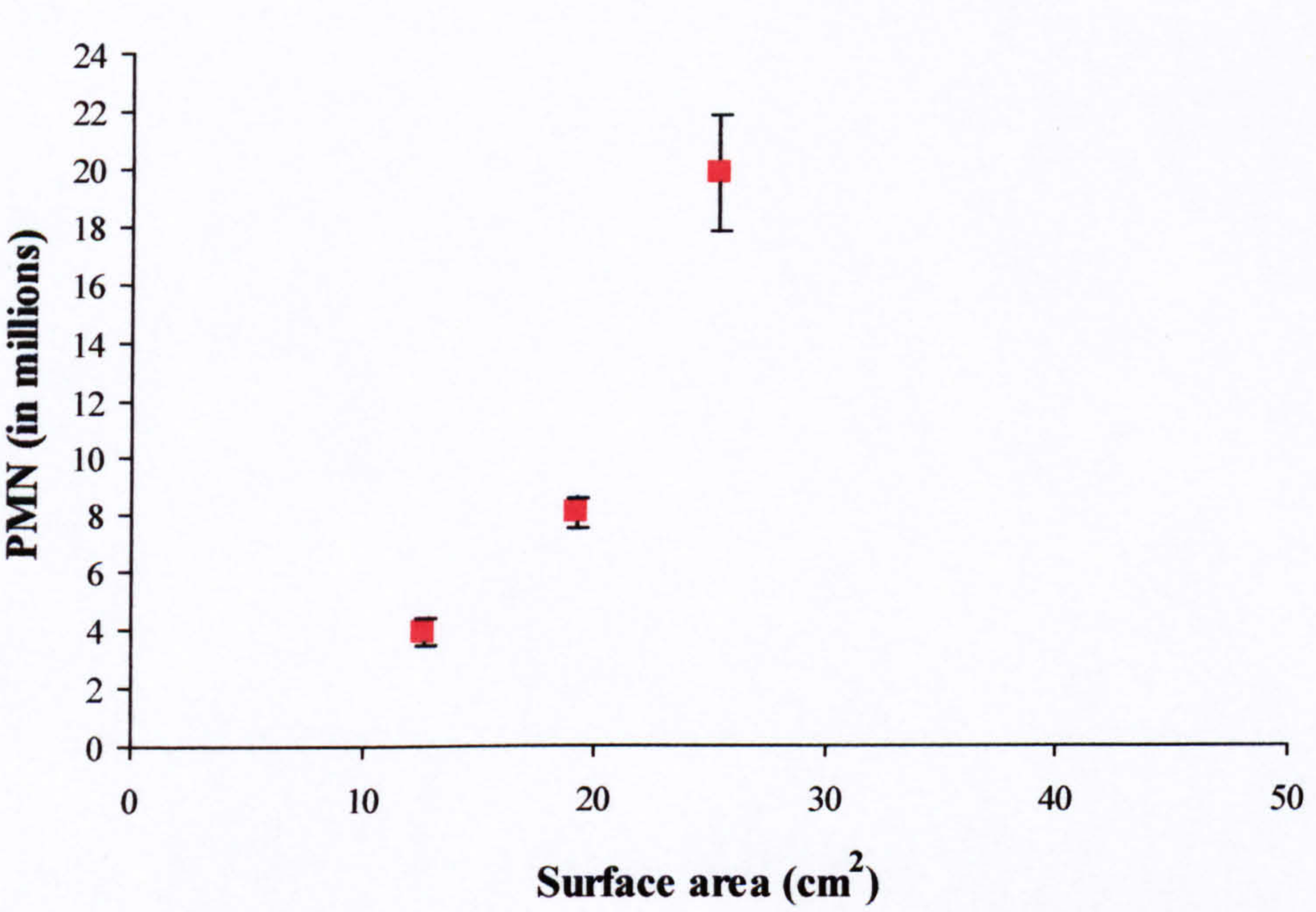

Figure 5.2.2 **A**. *Relationship between surface area of pure DQ12 quartz and total neutrophil number in BAL 18 hours post-instillation . Each point is the mean and SEM of three animals.* **B**. *Relationship between surface area of pure DQ12 quartz and total neutrophil number in BAL 18 hours post-instillation including the original x-axis scale, showing that it is not surface area alone driving the inflammation.*

5.2.3 Surface Modified Quartz.

Quartz treated with aluminium lactate to modify its surface or workplace samples of quartz showed a degree of inflammation at the larger surface areas instilled (Figure 5.2.3 A). However, to achieve these larger surface areas, a high mass of particle (up to 5 mg) had to be instilled, which in itself created a bolus mass effect often observed with instillation models. This bolus effect often results in an early surge of PMNs into the lung, which is transient. Therefore, by dividing the total PMN number by the mass instilled, it is possible to correct for this mass bolus effect. Figure 5.2.3 B demonstrates that quartz whose surface is modified by treatment with aluminium lactate, or quartz from workplaces where the surface has been affected by the industrial processes encountered, exhibited relatively low toxicity when compared to pure DQ12 quartz. In fact, aluminium lactate-treated quartz and workplace quartz are comparable to the low toxicity dusts, when the bolus mass effect is taken into consideration.

A.

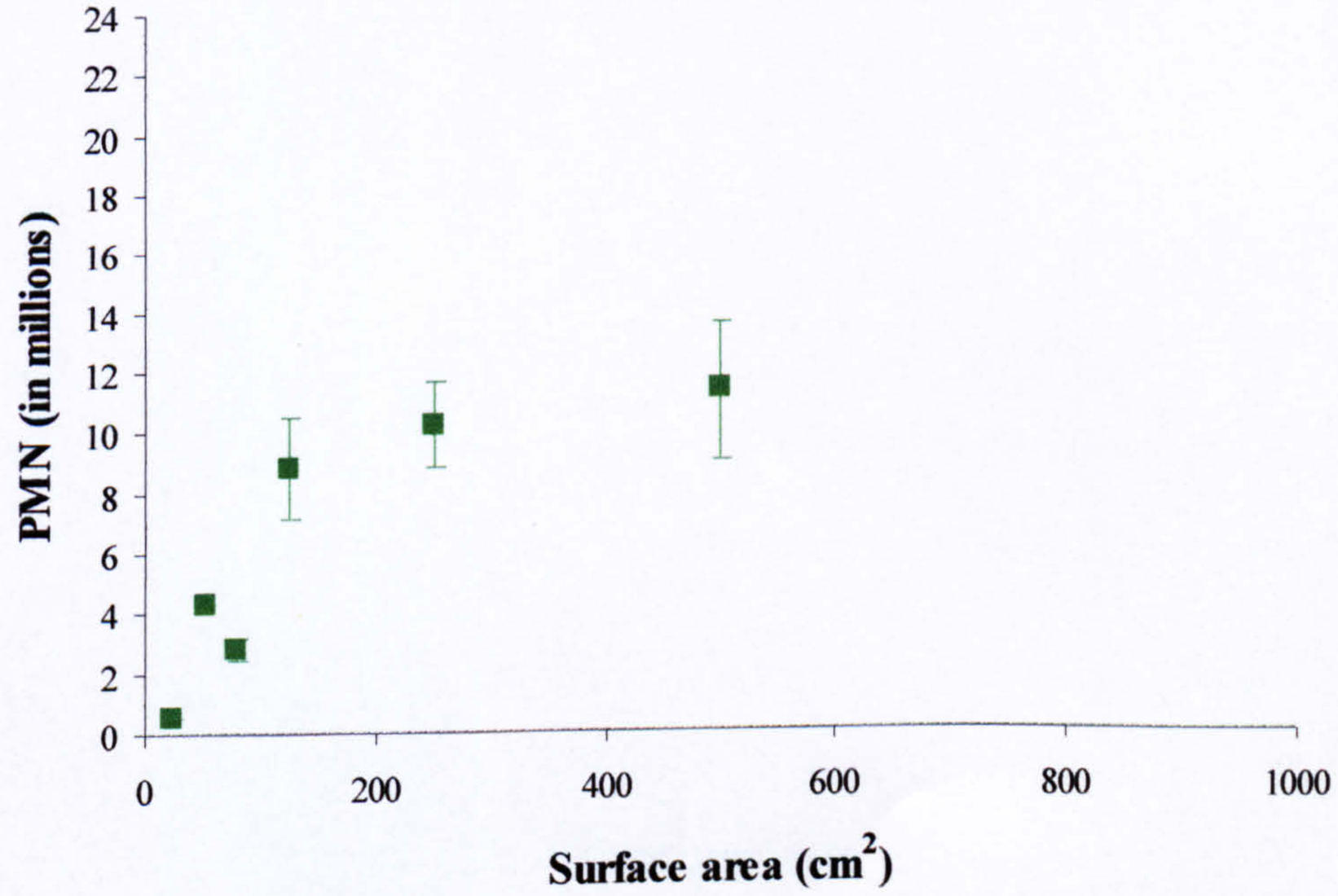

B.

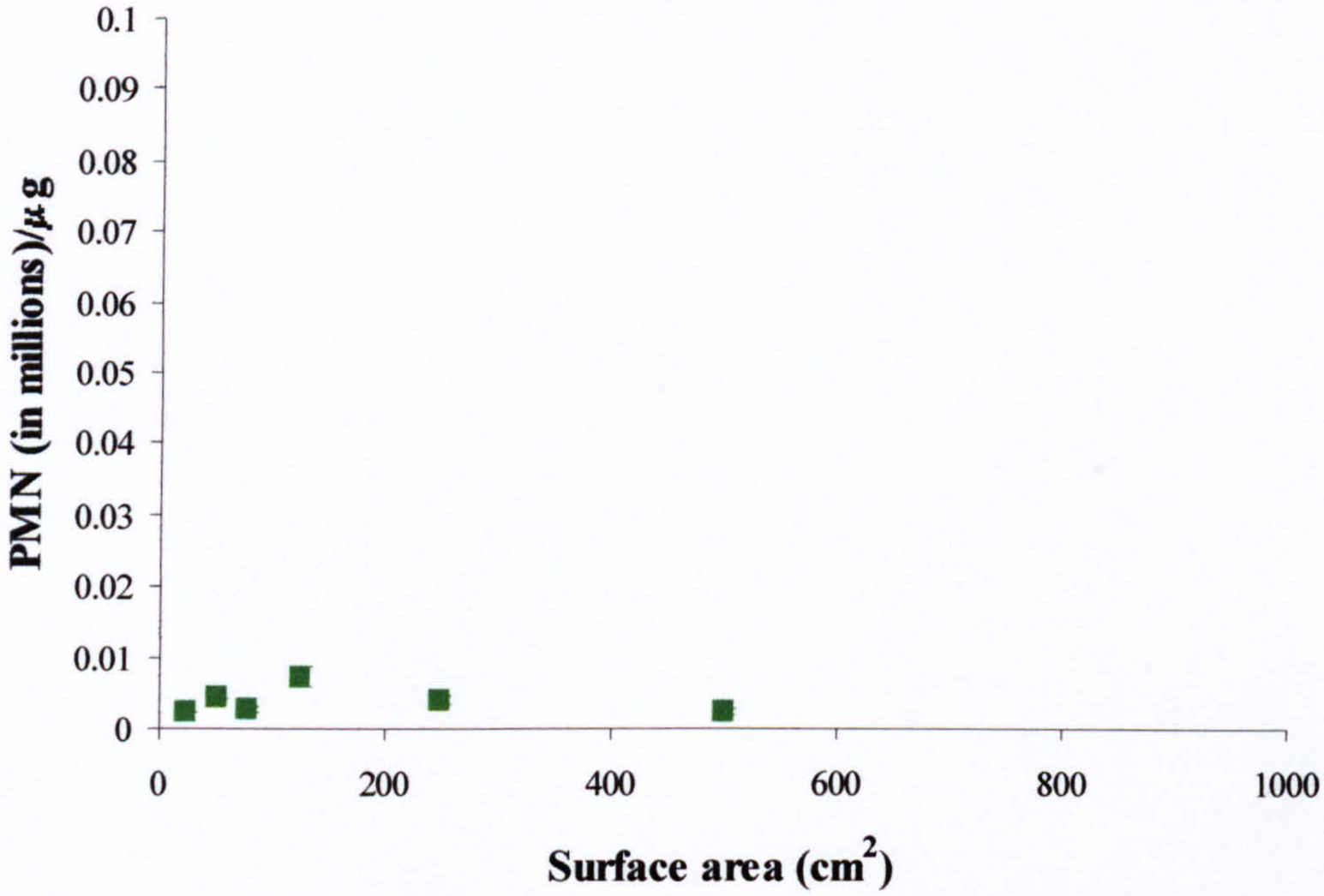

Figure 5.2.3 *Relationship between surface area of surface modified quartz and total neutrophil number(A) and surface area and total neutrophil number per microgram particle instilled (B), in BAL 18 hours post-instillation. Each point is the mean and SEM of three animals.*

5.2.4 Reactive Ultrafines.

Reactive ultrafines, such as ultrafine cobalt (ufCo) and ultrafine nickel (ufNi), induced an inflammatory response that fell midway between the highly toxic quartz and the low toxicity dusts suggesting that surface reactivity as well as surface area are important in driving the inflammation observed 18 hours post instillation (Figure 5.1.4).

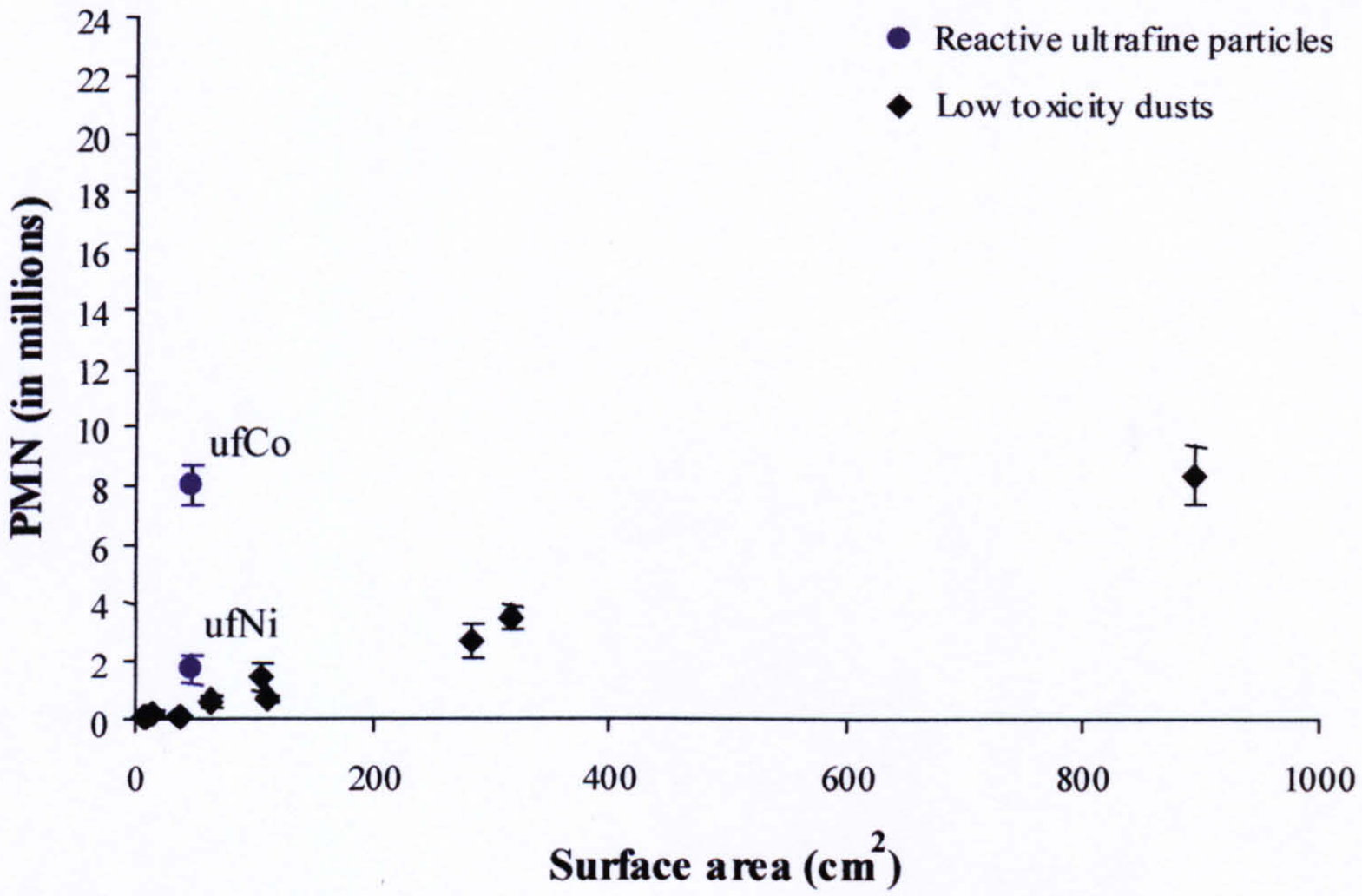

Figure 5.2.4 *Relationship between surface area and total neutrophil number in BAL 18 hours post-instillation with reactive ultrafine particles. Each point is the mean and SEM of three animals. Low toxicity dusts are included for comparison.*

5.2.5 Various Particle Relationships and the Specific Particle Response.

Figure 5.2.5A shows the relationship between the various particles and the PMN number per microgram of particles. The PMN response of the lung to unit surface area of each particle type, and allowing for the mass bolus effect gives units of PMN/μg/cm^2 and this is shown in Figure 5.2.5B. This clearly divides the particles into three categories:- 1. 'low toxicity' dusts which includes TiO_2, ufTiO_2, CB, ufCB, polystyrene beads, surface modified quartz and workplace quartz; 2. high reactivity ultrafines (ufCo and ufNi) and 3. quartz.

A.

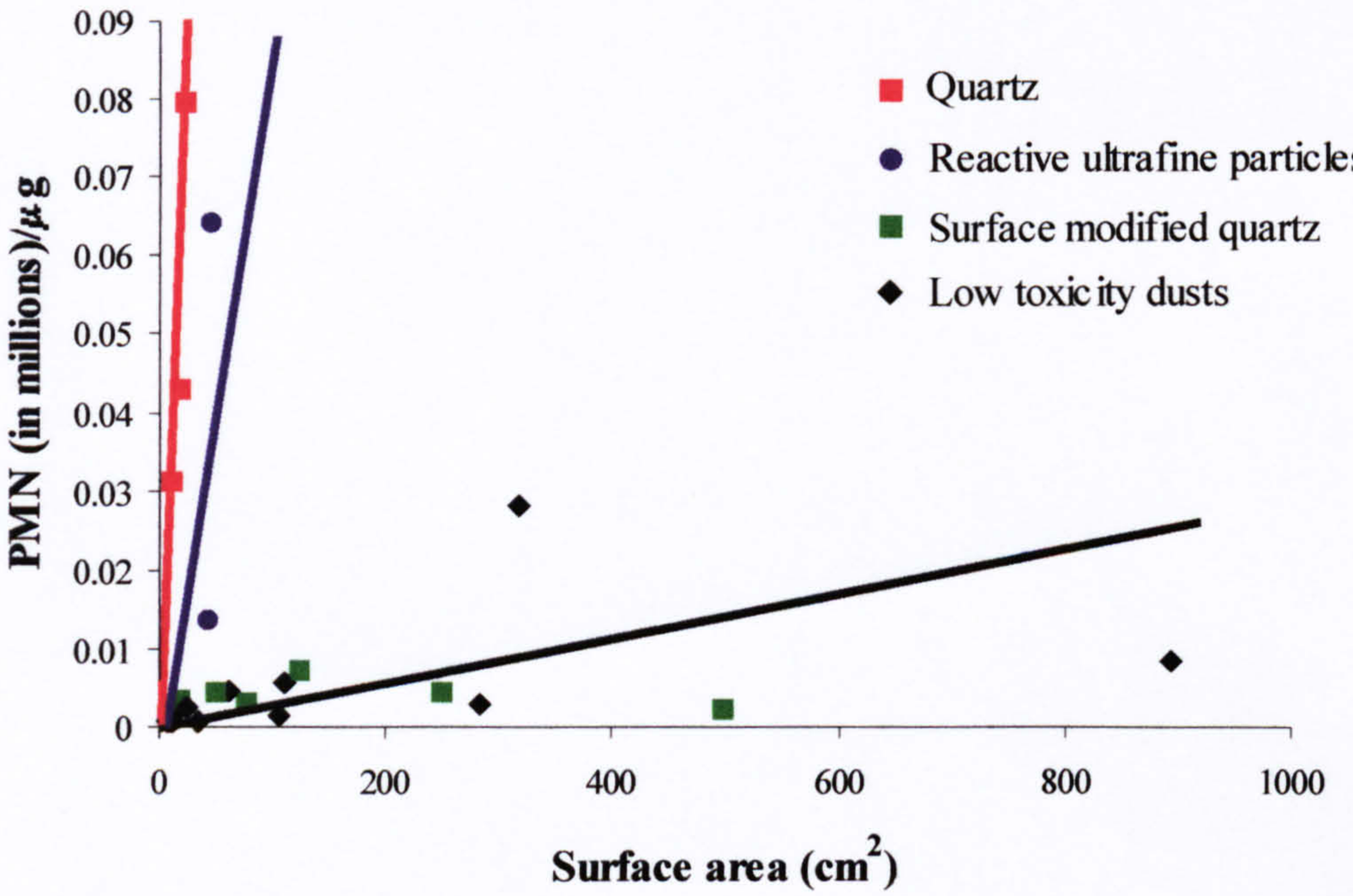

B.

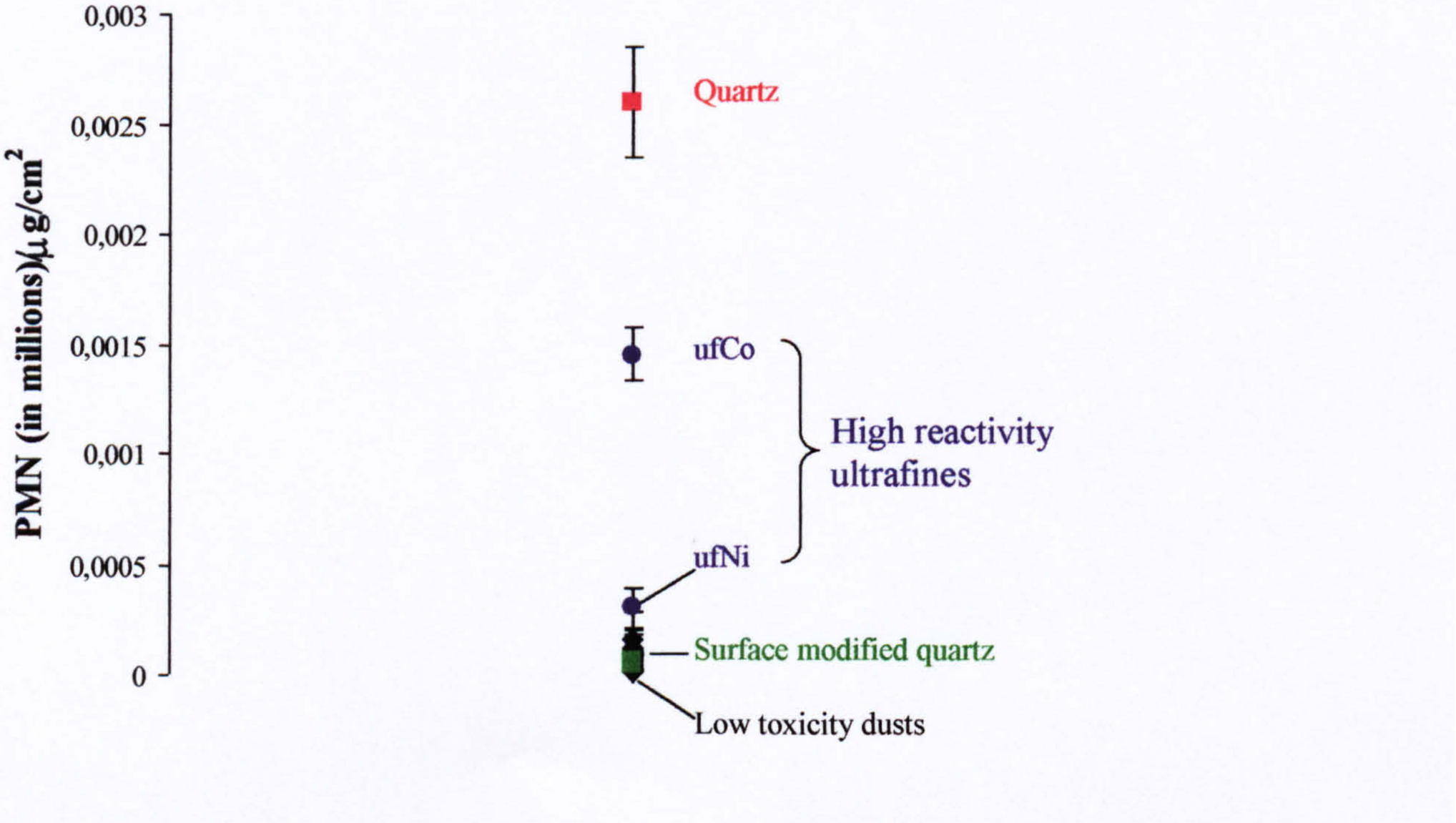

Figure 5.2.5 A. *Relationship between the various particle surface areas and the total neutrophil number/μg of particle instilled, in BAL 18 hours post-instillation. B. The Specific Response of each particle type expressed as PMN(in millions)/μg/cm*^{2}*. Each point is the mean and SEM of three animals.*

5.2.6 Macrophage Inflammatory Protein-2.

To verify whether MIP-2 protein levels in the BALF were related to the inflammatory cell influx to the lung, the relationship between MIP-2 protein levels and total PMN number was investigated. Figure 5.2.6 A shows the relationship between MIP-2 levels and total PMN number in BALF, 4 hours post instillation with the various particle types. The graph shows, that at 4 hours post-instillation, only the quartz instillation showed an increase in both PMN number and MIP-2 protein. The reactive ultrafine particles, despite having higher MIP-2 protein levels did not display an increase in total PMN number at this early time-point. Figure 5.2.6 B shows the relationship between MIP-2 protein levels and total PMN number in BALF, 18 hours post-instillation with the same particle types. At this time-point the particles follow a similar ranking as to that seen in Figure 5.2.5 B, with again quartz showing the highest PMN influx, followed by reactive ultrafine and then the surface modified quartz among the low toxicity dusts.

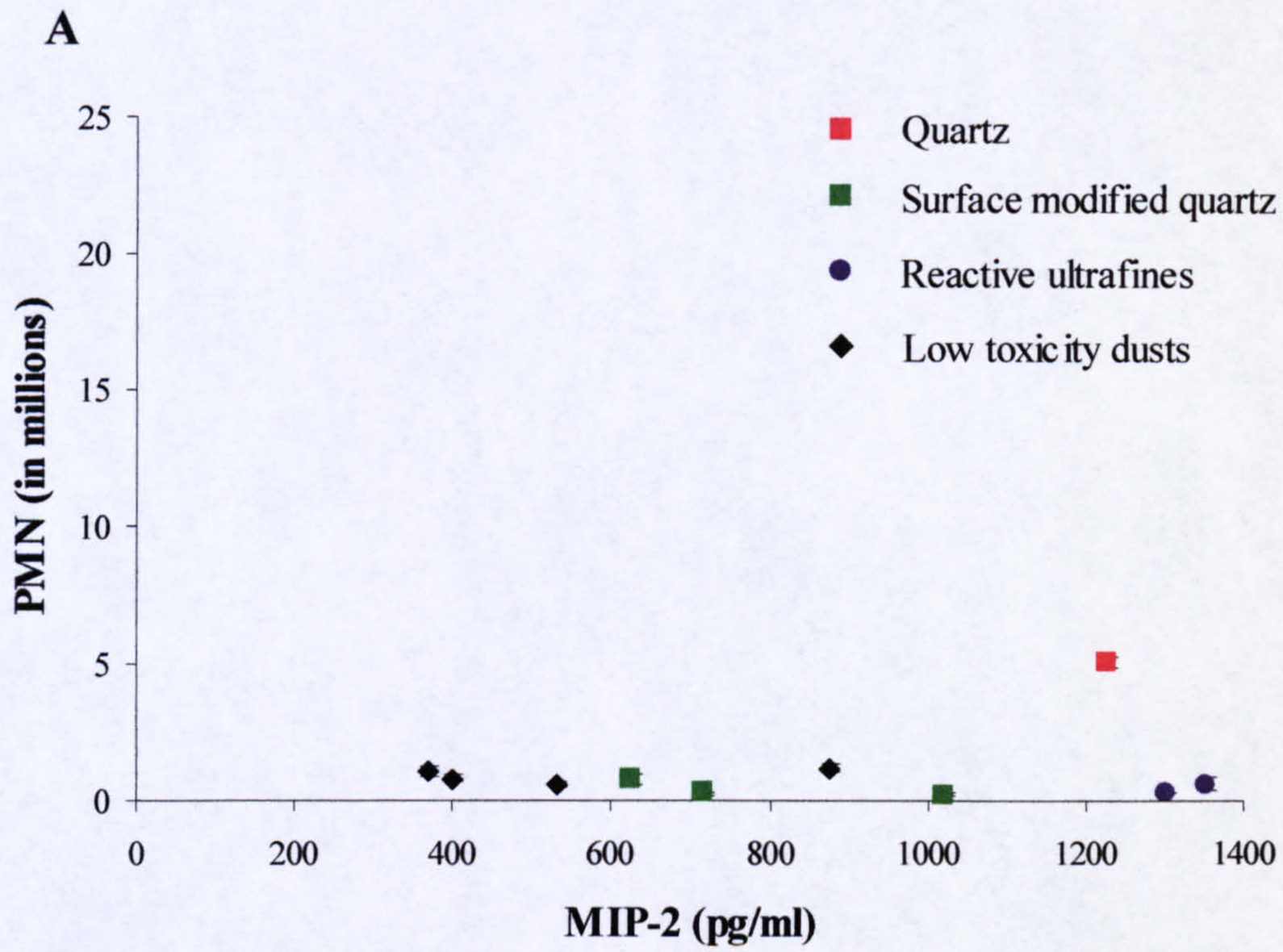

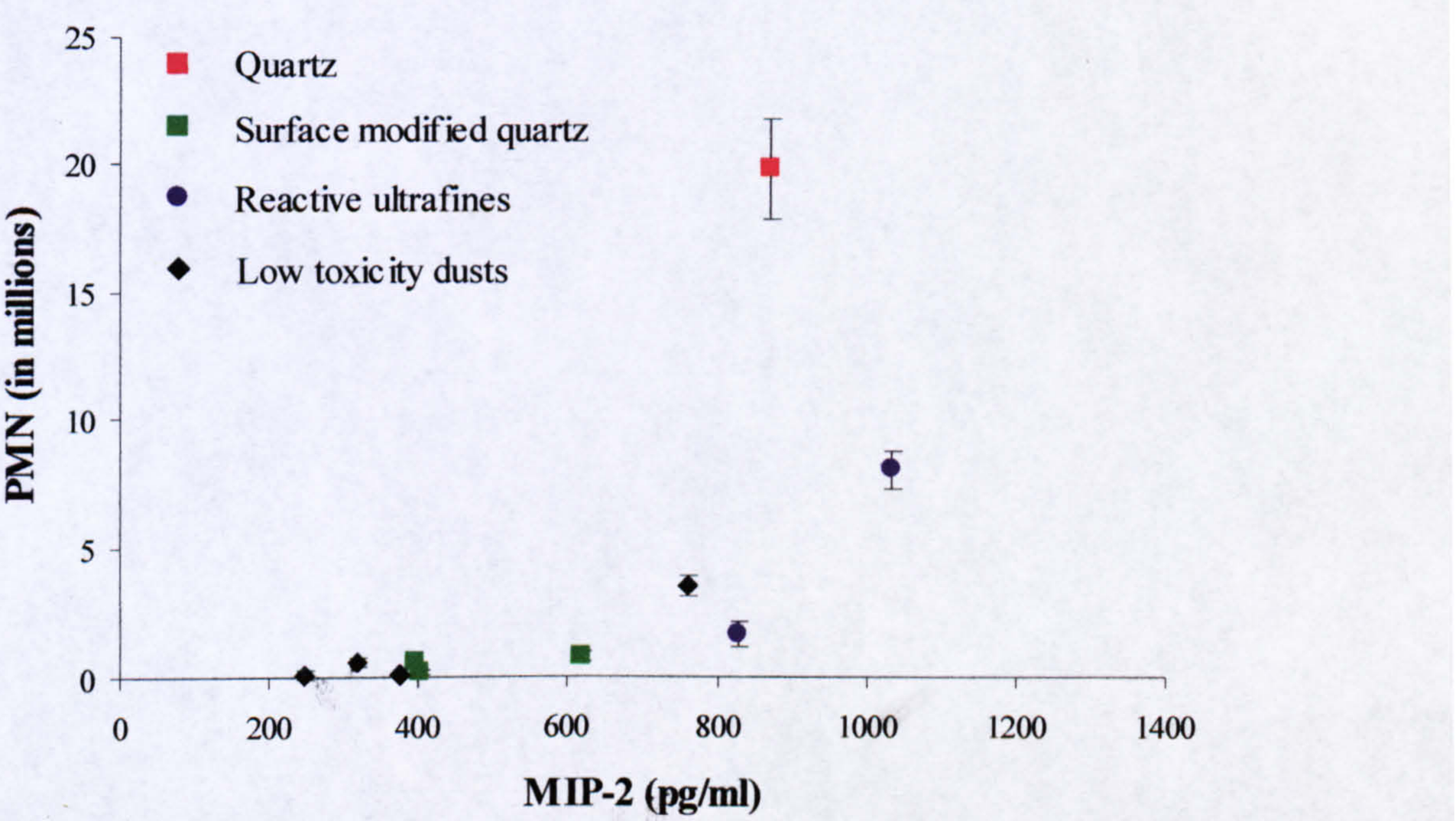

Figure 5.2.6 *Relationship between the total PMN number and levels of MIP-2 protein in lavage 4 hours (A) and 18 hours (B) post-instillation with quartz, surface modified quartz, reactive ultrafines and low toxicity dusts. Values are expressed as mean and SEM of three animals.*

5.3 Results *in vitro*

5.3.1 Cytotoxicity of Quartz, Surface Modified Quartz, Reactive Ultrafines and Low Toxicity Dusts.

The cytotoxic effects of the various particles on A549 cells were determined using the MTT and LDH assays. The results of the MTT assay following treatment for 24 hours, in serum free conditions, with the various particle types are shown in Figure 5.3.1 A. None of the particles exhibited any significant toxicity except for quartz at a concentration of 80 $\mu g/cm^2$. However, this toxicity was significantly inhibited ($p < 0.001$) upon treatment of the quartz surface with aluminium lactate. Figure 5.3.1 B shows the effects of the various particles on cell membrane integrity, as measured by the LDH assay. Again none of the particle treatments showed any significant membranolytic effect at 24 hours in serum free conditions.

A

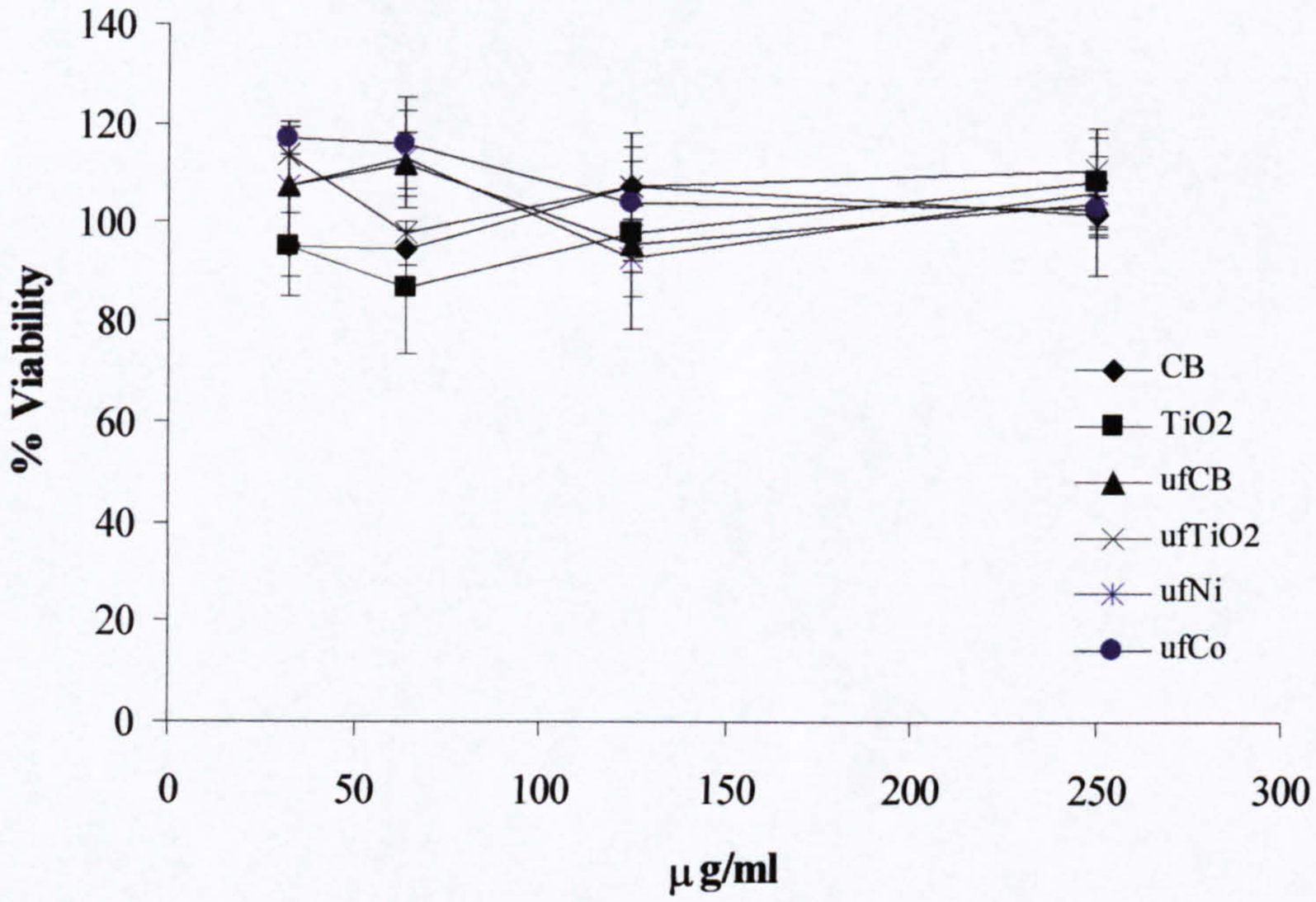
140
120
100
80
60
40
20
0
% Viability
0
50
100
150
200
250
300
μg/ml
CB
TiO2
ufCB
ufTiO2
ufNi
ufCo

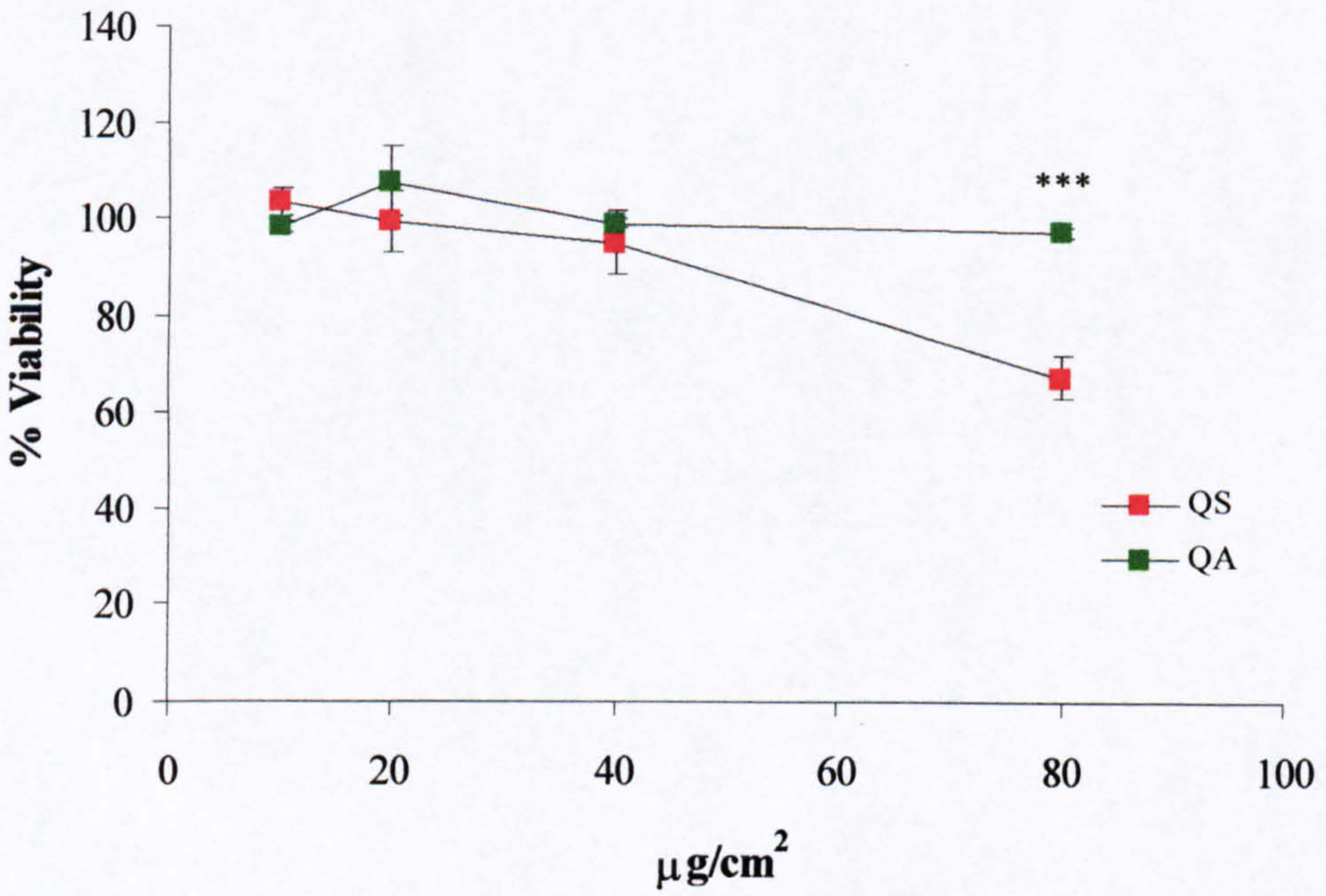
140
120
100
80
60
40
20
0
% Viability
***
0
20
40
60
80
100
μg/cm²
QS
QA

B

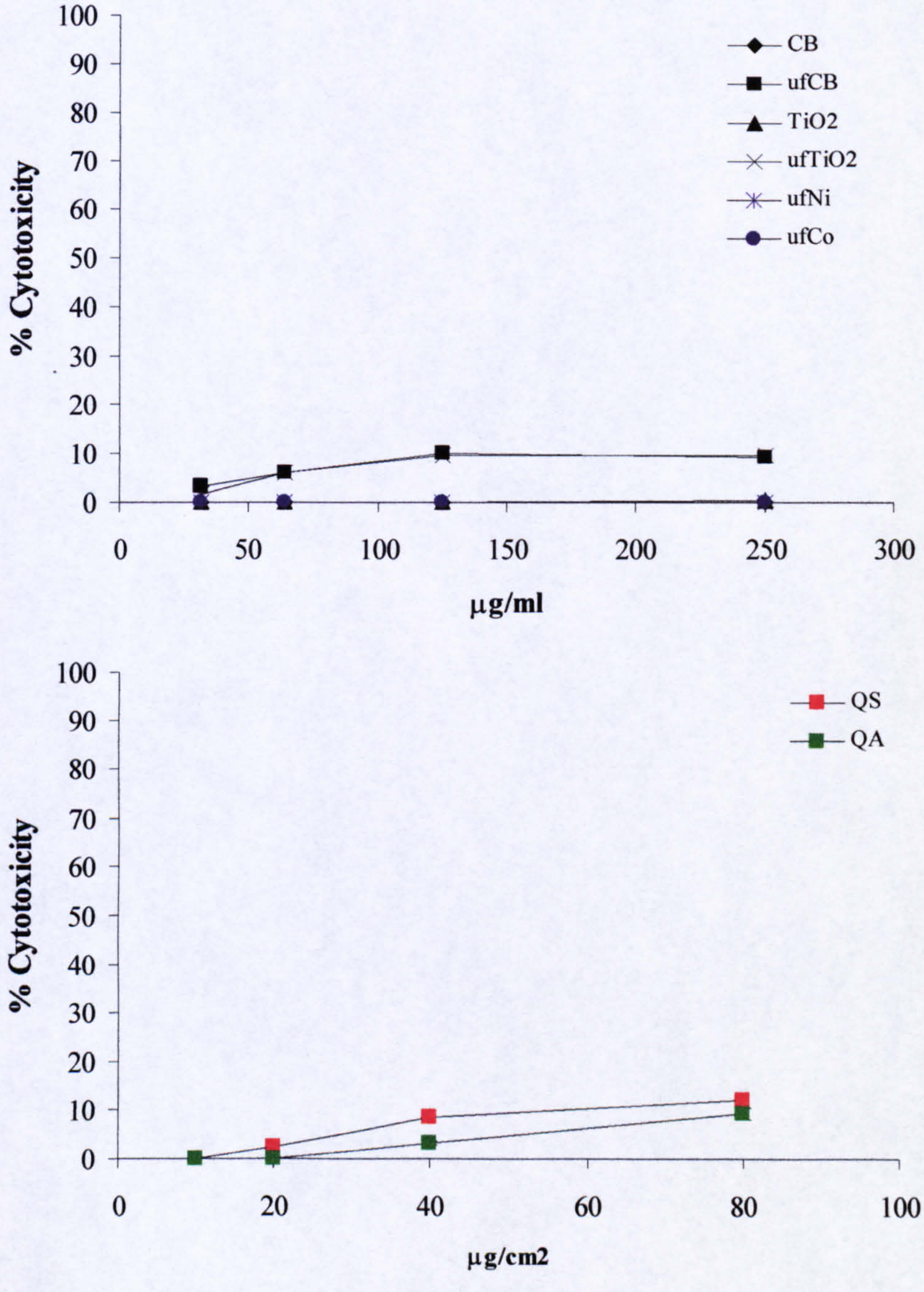

Figure 5.3.1 ***A****. Cytotoxicity (MTT assay) of the various particle treatments in A549 cells. Top graph shows the low toxicity dusts and reactive ultrafines, bottom graph shows quartz and aluminium lactate-treated quartz. Cells were treated for 24 hours in serum-free conditions, following 24 hour serum starvation. The viability of the cells for each treatment is expressed as percentage of control. Data are expressed as mean and SEM of three independent experiments. ***p<0.001 vs Quartz.* ***B****. Cytotoxicity (LDH*

assay) of the various particle treatments in A549 cells. Top graph shows the low toxicity dusts and reactive ultrafines, bottom graph shows quartz and aluminium lactate-treated quartz. Cells were treated for 24 hours in serum-free conditions, following 24 hour serum starvation. Data are expressed as the percentage of extracellular LDH and represent the mean and SEM of three independent experiments.

5.3.2 Various Particle Relationships and the Specific Particle Response.

Figure 5.3.2 A shows the relationship between the various particle treatments of A549 cells, expressed as surface area of particle per cm^2 of tissue culture flask and the total IL-8 protein present in the supernatant 18 hours post incubation. As can be seen from the graph, the results obtained *in vitro* are comparable to that which is seen when measuring total PMN number *in vivo* for each particle type. Again, a small increase in quartz particle surface area yielded a large increase in IL-8 protein whereas the IL-8 protein observed from low toxicity particle treatments seemed to be more directly related to the particle surface area alone. Surface modification of quartz with aluminium lactate again caused these particles to act like the low toxicity dusts. Unfortunately, treatment of A549 cells with the reactive ultrafine particles (ultrafine cobalt and nickel) did not cause any measurable production of IL-8 protein unlike like which was observed with total PMN number *in vivo*. The specific response of each particle type, expressed as IL-8 (pg/ml)/ cm^2(particle)/cm^2(flask) is shown in Figure 5.3.2 B. Again, this clearly ranks the particles in terms of specific reactivity and divides them into categories:- 'low toxicity' dusts (including TiO2, ufTiO_2, CB, ufCB and surface modified quartz) and quartz.

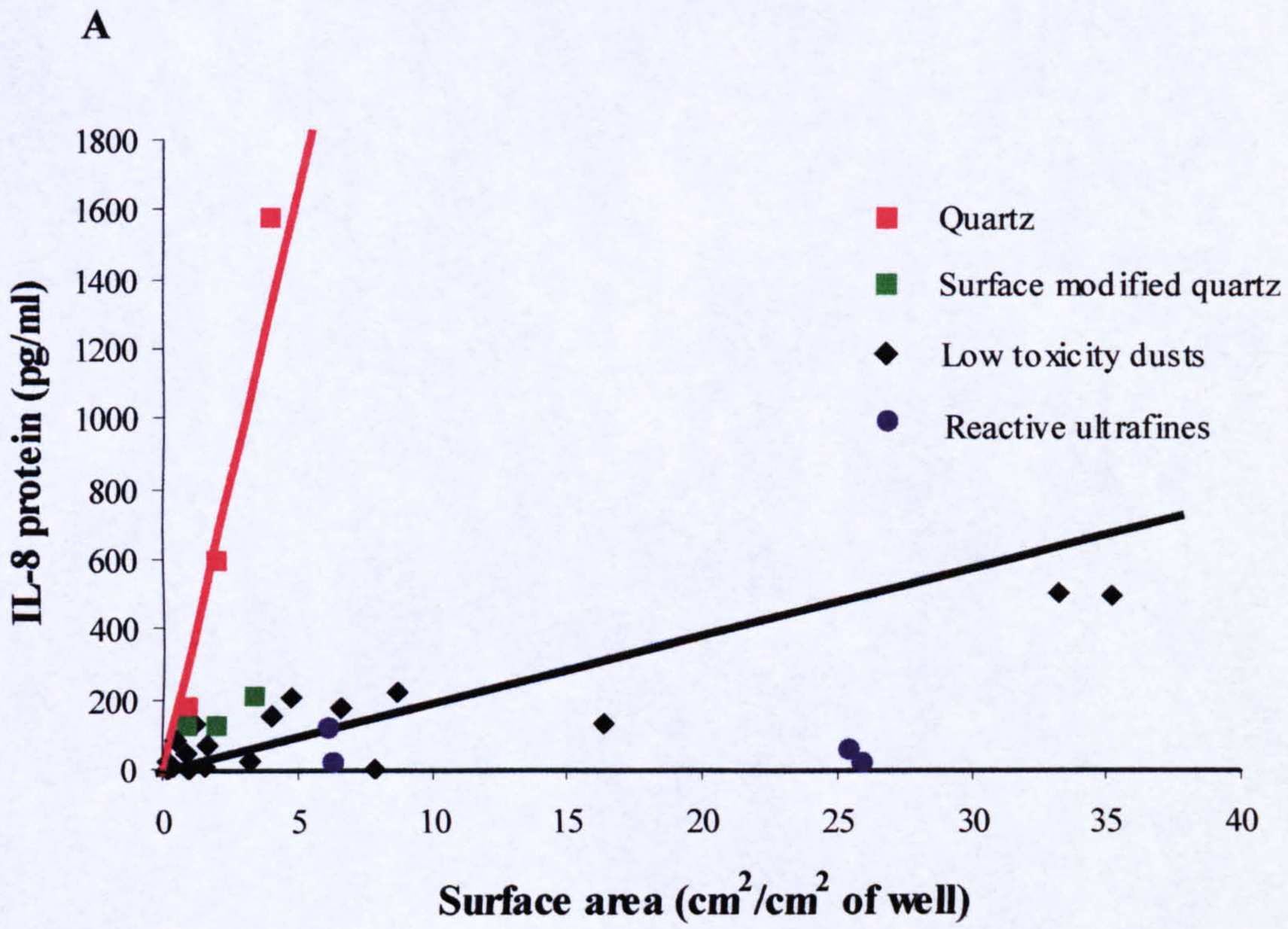

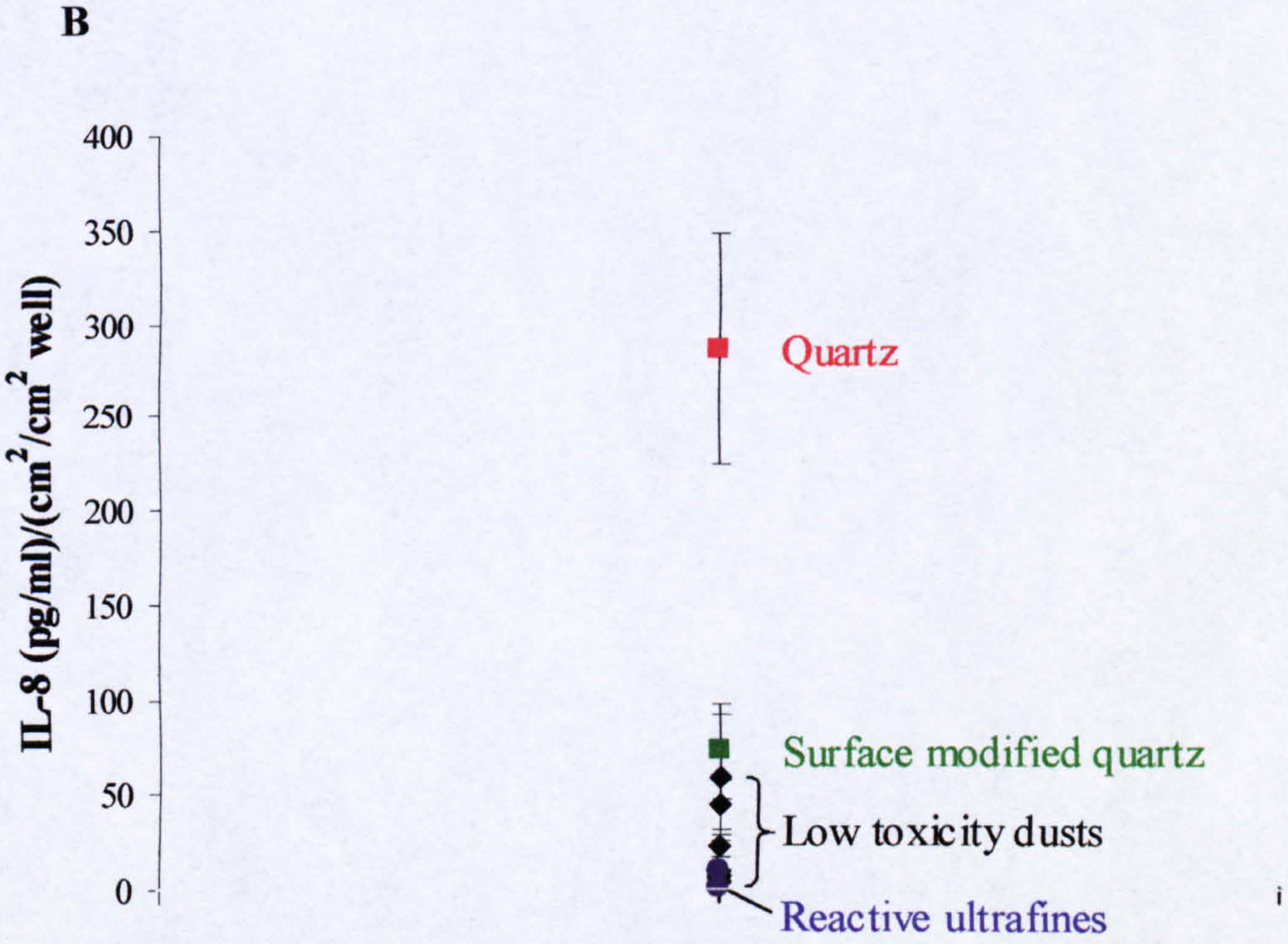

Figure 5.3.2 ***A*** *Relationship between particle surface area and the level of IL-8 protein in A549 cells 18 hours post incubation to various particle types.* ***B*** *The Specific Response of each particle type expressed as IL-8(pg/ml)/cm²/cm². Each point is the mean and SEM of three independent experiments.*

5.4 Discussion

A range of different poorly soluble particle (PSP) types can cause excessive lung inflammation that may then play a role in the resultant pathologies. For PSPs, the particle surface has always been assumed to be the 'dose' that interacts with the lung, leading to inflammation. Quartz is an example of a particle with a highly reactive surface that has been implicated in its toxicity (discussed further in Chapters 3 and 4). Recently attention has been focused on ultrafine particles and the phenomenon of lung overload. Onset of overload inflammation and impairment of particle clearance has been found to be related to the lung burden dose expressed as surface area, rather than mass or volumetric dose (Oberdorster, 1996; Tran *et al.*, 2000).

It has been demonstrated here, using an instillation model, that particle surface area is the dose metric for the acute inflammatory response seen 18 hours after instillation of a wide range of 'low toxicity' PSPs in rats. Quartz is known to have a highly reactive surface (Fubini, 1998b). Thus, it is expected that a severe inflammatory response can result from a comparatively low surface area dose. Moreover, if this surface reactivity is neutralised or blocked, then quartz is seen to behave like a 'low toxicity dust'. Interestingly, workplace samples of quartz exhibited a much lower toxicity (per unit surface area dose) than native DQ12 quartz, further indicating a variability in surface reactivity for different quartz samples, as reported by Clouter *et al.* (2001). For ultrafine particles, the toxicity of ultrafine titanium dioxide and ultrafine carbon black can be attributed to their large surface area. However, metal particles such as cobalt and nickel, in ultrafine from, had both a high surface area and a reactive surface which resulted in highly inflammogenic particles that had more ability to cause inflammation than the 'low toxicity' particles, including the ultrafines. As a result of this 'double

hazard' i.e. their surface reactivity and large surface area, these particles may be potentially more inflammogenic than active quartz, on a mass dose basis, since quartz particles are never ultrafine.

MIP-2 protein measured in BALF, 4 hours post instillation showed that only the quartz particles produced a correlation between MIP-2 and PMN number. However, MIP-2 measured in BALF 18 hours post-instillation showed a correlation between MIP-2 and PMN levels which corresponded to the differing reactivity of the various particles. This is not so surprising, as MIP-2 is a key proinflammatory chemokine for recruiting PMNs to the site of lung injury in rats (Driscoll, 1994) but interesting, in that it was only the later time-point which produced this trend. It seems likely therefore, that the MIP-2 protein levels observed 4 hours post-instillation are potentially driving the inflammatory response, as measured by total PMN number 18 hours post-instillation. As a marker for the potential of particles to cause inflammation, measurement of MIP-2 has the advantage of being measurable across both instillation and inhalation models and may have the potential as a valid *in vitro* screen for rapidly classifying particles into the categories described here, namely (i) active quartz; (ii) low toxicity particles, surface modified quartz; (iii) ultrafines with surface reactivity. Measurement of such chemoattractant proteins *in vitro* may not only be limited to MIP-2 and a rat epithelial cell line. As MIP-2 is the rat homologue to human IL-8, it may also be feasible to measure IL-8 protein in a human lung cell lines, such as the human type II epithelial cell line, A549.

To further investigate the idea of replicating the results obtained from the *in vivo* studies into an *in vitro* situation, as a possible means of a valid *in vitro* screen for rapidly

classifying particles, experiments were carried out to treat human lung epithelial cells with the various particles and measure the production of IL-8. Surprisingly, the results obtained from these experiments followed almost exactly the trend of those which were observed *in vivo* i.e. particle surface area versus PMN number as well as the specific particle response. Again, the particles became ranked in order of their overall 'reactivity', with, as expected, quartz at the top and the low toxicity dusts along with surface-modified quartz at the bottom. The only exception to this trend was that which was observed with the reactive ultrafine particles i.e. ultrafine cobalt and nickel. These reactive ultrafines failed to induce an enhanced production of IL-8 protein in A549 cells that was in keeping with the trend observed with the other particles. The fact that these particles did not induce any significant cytotoxicity, as measured by the MTT and LDH assays, suggests that the failure to increase IL-8 production cannot be explained by the particles causing increased cell death or damage. One possible explanation may be that the highly reactive surface is unstable and so over time, the surfaces have become oxidised. There was a period of time of 1-2 years between the particles being used for the *in vivo* instillations and there use during *in vitro* cells treatments. This explanation could be tested by re-instilling fresh particles obtained from the Japanese source, into the lungs of rats and observing the response.

In conclusion, the results show, in a simple instillation model of acute inflammation, the dosimetric relationship between particle surface and the inflammatory reaction. This model offers a simple model for ranking inflammogenic potency of PSPs according to their surface area and surface reactivity. Also demonstrated, is an alternative *in vitro* assay for surface reactivity, based on the *in vivo* findings. The *in vitro* assay provides a

more rapid, more ethical and less expensive method than using rats, to classify an unknown particle as quartz-like; low toxicity or grades of reactivity between these two.

Summary and Future Studies.

Silicosis has been recognised for many decades as one of the most prevalent of the occupational lung diseases. IARC reconsidered the carcinogen classification of quartz in 1997 and reclassified it as a Group 1 carcinogen on the basis of sufficient evidence for carcinogenicity in both humans and experimental animals . However, the IARC report added that carcinogenicity to humans was not detected in all industries studied and that carcinogenicity can therefore vary depending on inherent characteristics of the crystalline silica or on external factors affecting its biological activity. As a result, there has been considerable controversy regarding the IARC classification of crystalline silica within the medical community and considerable confusion among non-experts. To attempt to clarify the situation, we sought to determine whether modification of the surface of an active quartz sample could influence its ability to activate molecular pathways leading to inflammation. Furthermore, we aimed to determine the effect of surface modification on quartz-induced DNA damage (genotoxicity) and to investigate whether phagocytosis may play a role in the observed effects.

The association of chronic inflammation with the development of cancer has been recognised for a long time and there are a number of data confirming inflammation-related carcinogenesis. For example, a high rate of colon carcinomas in humans has been closely associated with chronic inflammatory bowel diseases (Collins *et al.*, 1987) and urinary bladder cancer is frequently found in patients suffering from urinary tract infection (Kantor *et al.*, 1984). Also, in the lung the presence of inflammatory diseases such as sarcoidosis, fibrosis and chronic obstructive pulmonary disease (COPD), have been associated with a higher risk of cancer development (Alavanja *et al.*, 1992; IARC,

1997; Askling *et al.*, 1999). In general, many sources of inflammation are effective in accelerating the development of cancer, including inflammatory reactions in response to particles (Wiseman and Halliwell, 1996). In the lung, a relationship between particle exposure and the induction of inflammation has been clearly established (Donaldson and Tran, 2002).

The present research has shown that intratracheal instillation of quartz into the lungs of rats results in inflammation as measured by the neutrophil influx into the lung (Chapter 3). However, the treatment of the quartz particles with a soluble aluminium salt can inhibit the ability of quartz particles to induce an inflammatory response and this inhibition occurs at a cellular and molecular level. Aluminium lactate treatment of quartz also prevented a quartz-induced increase of protein, gamma glutamyl transpeptidase and macrophage inflammatory protein-2 in to the airspaces. The oxidative stress-responsive transcription factor NF-κB is involved in the proinflammatory effects of many pathogenic particles. Instillation of native quartz, but not aluminium lactate-treated quartz, induced an increase in NF-κB activation as measured by the binding of nuclear protein isolated from BAL cells, to the NF-κB oligonucleotide consensus sequence. It seems likely that NF-κB activation occurred as a result of cell signalling events resulting in the degradation of the inhibitory protein IκB and hence the translocation of NF-κB to the nucleus. However, it is still unclear how particles interacting with the cell surface transduce a signal that leads to NF-κB activation. More work is needed in locating the protein kinases upstream from NF-κB which are switched on in response to quartz and to study what effect the treatment of quartz with aluminium salts has on these signalling events.

Using electron spin resonance, it was shown that DQ12 quartz generates hydroxyl radicals in the presence of hydrogen peroxide and it is believed that these radicals play a key role in quartz-induced inflammation. Treatment of the quartz surface with aluminium lactate significantly reduced this hydroxyl radical formation. The mechanism by which aluminium interacts with the quartz surface is poorly understood and future work to elucidate this interaction is warranted. It is also not known how effective the 'binding' of aluminium to the quartz surface is, or for how long the aluminium remains on the quartz surface once within the lung. Again more work is required to carry out chronic instillation studies (1-2 years) to determine if the activity of the quartz surface returns after residence in the lung.

Although chronic exposure to quartz has been associated with increased lung cancer rates in rats and humans, the mechanisms involved in carcinogenesis following particle exposure have only been partly elucidated. Carcinogenesis is a complicated, multi-step process and specifically in the initiation stage, genotoxic events are thought to play a crucial role. *In vitro* studies have indicated that the genotoxic properties of particles may depend on characteristics such as size, shape, surface reactivity, crystallinity and solubility. Given the role of direct (particle-induced) and indirect (inflammation-induced) carcinogenic effects, differences in the quartz surface reactivity may be reflected in both inflammogenic and genotoxic properties of quartz.

The effects of treating the quartz surface on cell membrane damage, the induction of DNA damage and the role of particle phagocytosis by lung epithelial cells were also studied. Treatment of the quartz particles with aluminium lactate and more importantly, extracts from clay minerals commonly found in the earth's crust, significantly inhibited

the surface reactivity of the quartz as measured by its ability to cause the haemolysis of human erythrocytes. This is an important finding, as clay minerals are often found in association with quartz geologically and future studies involving quartz treatments with clay mineral extracts, such as those carried out in this thesis, would lend extra weight towards understanding the variability of the quartz hazard. Here, it has also been demonstrated that treatment of the quartz surface with PVNO and aluminium lactate inhibited its ability to cause DNA strand breakage in human lung epithelial cells, an important proliferating target cell. Along with the observed DNA-damaging effects, it was also demonstrated that both coatings significantly affected particle uptake by the epithelial cells. Such findings suggest that cellular uptake of quartz particles could play a role in its genotoxicity as the particles may have a direct effect on the cellular DNA. The cellular uptake studies however did not verify the exact site of residence of the quartz particles and so further studies are required to investigate this i.e. whether or not quartz particles are located within the nucleus. The experiments involving particle uptake were carried out *in vitro* and so further work to elucidate whether the quartz particles are phagocytosed by epithelial cells *in vivo* may provide important information regarding the fate of quartz particles in the lung. The reactivity of the quartz surface plays an important role in its genotoxicity. However, whether these genotoxic effects occur as a result of direct quartz-induced (primary) genotoxicity, as inflammation-induced (secondary) genotoxicity or even as a result of both are yet to be answered. Future studies could be carried out to test if the primary genotoxicity induced by quartz has a different effect compared to secondary genotoxicity and again whether treatments which pacify the quartz surface also abolish these genotoxic effects.

Finally, the proinflammatory effects of particle surfaces in the lung were studied using a rat instillation model of acute inflammation and a comparable *in vitro* test utilising human lung epithelial cells and their production of interleukin-8 following particle treatment. A variety of poorly soluble particle types can cause excessive lung inflammation and for these different particle types, the particle surface has always been assumed to play an important role in the resultant inflammation. However, as shown earlier, quartz represents a particle with a highly reactive surface which contributes significantly to its toxicity. It has been shown here that quartz is capable of causing a severe inflammatory response as a result of a low surface area dose. Interestingly, treatments which blocked or neutralised the reactive quartz surface caused quartz to act like a low toxicity particle and furthermore samples of quartz taken from the workplace exhibited much lower toxicity than native DQ12 quartz. Within the instillation model, the toxicity of ultrafine particles such as titanium dioxide and carbon black could be attributed to their large surface area. These models offer a simple way of ranking inflammogenic potency of poorly soluble particles by way of their surface area and surface reactivity. The *in vitro* assay also provides a faster, more ethical approach to ranking unknown particles as quartz-like, low toxicity or somewhere in between. The current exposure limits for poorly soluble particles are set as a measurement of mass. From the results presented here, this may be better represented as a measurement of particle surface area, in terms of risk assessment, however further work testing more particle types is required to validate this model.

In conclusion, the work presented in this thesis has explored some of the possible mechanisms which could help explain the variability in the quartz hazard. Using model coating materials such as aluminium lactate and PVNO but also importantly extracts

from actual clay minerals commonly found in association with quartz in the earth's crust, we have demonstrated that the reactivity of the quartz surface can be masked or neutralised. Furthermore, these quartz treatments have also been shown to inhibit the inflammogenicity and genotoxicity of the quartz particles. These results should help to clarify IARC's recent classification of quartz as a Group 1 carcinogen and also explain why carcinogenictity in humans was not detected in all industrial circumstances studied. Furthermore, the other studies presented here have shown the importance of the particle surfaces in generating inflammation and highlighted quartz as having a highly reactive surface which could be converted to the same reactivity as 'low toxicity' particles by treatment with aluminium lactate or PVNO.

REFERENCES

Adamson IY. 1992. Radiation enhances silica translocation to the pulmonary interstitium and increases fibrosis in mice. *Environ.Health Perspect.* 97, 233-238.

Alavanja MC, Brownson RC, Boice JD and Hock E. 1992. Pre-existing lung disease and lung cancer among nonsmokuing women. *Am J Epidemiol* 136, 623-632.

Alberts B, Johnson A, Lewis J, Raff M, Roberts K and Walter P. 2002 *Molecular Biology of the Cell*, Garland Science, New York, USA.

Albrecht C, Adolf B, Weishaupt C, Hohr D, Zeittrager I, Friemann J and Borm PJ. 2001. Clara-cell hyperplasia after quartz and coal-dust instillation in rat lung. *Inhal.Toxicol.* 13, 191-205.

Albrecht C, Borm PJ, Adolf B, Timblin CR and Mossman BT. 2002. In vitro and in vivo activation of extracellular signal-regulated kinases by coal dusts and quartz silica. *Toxicol.Appl.Pharmacol.* 184, 37-45.

Antonini JM and Reasor MJ. 1994 . Effect of short-term exogenous pulmonary surfactant treatment on acute lung damage associated with the intratracheal instillation of silica. *J. Toxicol. Environ. Health* 43, 85–101.

Arroyo CM, Carmichael AJ, Bouscarel B, Liang JH and Weglicki WB. 1990. Endothelial cells as a source of oxygen-free radicals. An ESR study. Free *Radic.Res.Commun.* 9, 287-296.

Askling J, Grunewald, J Eklund A, Hillerdal G and Ekbom A. 1999. Increased risk for cancer following sarcoidosis. *Am J Respir Crit Care Med* 160, 1668-1672.

Babior BM. 1999. NADPH oxidase: an update. *Blood* 93, 1464-1476.

Babior BM. 2000. Phagocytes and oxidative stress. *Am.J.Med.* 109, 33-44.

Bailey WC, Brown M, Buechner HA, Weill H, Ichinose H and Ziskind M. 1974. Silico-mycobacterial disease in sandblasters. *Am.Rev.Respir.Dis.* 110, 115-125.

Balaan MR and Banks DE. 1992. Silicosis. In: Rom WN (ed) *Environmental and Occupational Medicine*, 2nd ed. Little, Brown and Company, USA, pp 345-358.

Baldridge CW and Gerard RW. 1933. The extra respiration of phagocytosis. *Am.J.Physiol.* 103: 235.

Baldwin AS. 1996. The NF-kappa B and I kappa B proteins: new discoveries and insights. *Annu.Rev.Immunol.* 14, 649-683.

Bazzoni F and Beutler B. 1996. The tumor necrosis factor ligand and receptor families. *N.Engl.J.Med.* 334, 1717-1725.

Bégin R, Massé S, Rola-Pleszcczynski M, Martel M, Desmarais Y, Geoffroy M, LeBouffant L, Daniel H and Martin J. 1986. Aluminum lactate treatment alters the lung biological activity of quartz. *Exp. Lung Res.* 10, 385-399.

Bégin R, Massé S, Sébastien P, Martel P, Bossé J, Dubois F, Geoffroy M and Labbé J. 1987. Sustained efficiacy of aluminum to reduce quartz toxicity in the lung. *Exp. Lung Res.* 13, 205-222.

Bevilacqua MP, Stengelin S, Gimbrone MA and Seed B. 1989. Endothelial leukocyte adhesion molecule 1: an inducible receptor for neutrophils related to complement regulatory proteins and lectins. *Science* 243, 1160-1165.

Blusse van Oud AA and van Furth R. 1982. The origin of pulmonary macrophages. *Immunobiology* 161, 186-192.

Borm PJ and Driscoll K. 1996. Particles, inflammation and respiratory tract carcinogenesis. *Toxicol.Lett.* 88, 109-113.

Boveris A, Oshino N and Chance B. 1972. The cellular production of hydrogen peroxide. *Biochem.J.* 128, 617-630.

Bowden DH and Adamson IY. 1980. Role of monocytes and interstitial cells in the generation of alveolar macrophages I. Kinetic studies of normal mice. *Lab Invest* 42, 511-517.

Bowden DH and Adamson IY. 1984. The role of cell injury and the continuing inflammatory response in the generation of silicotic pulmonary fibrosis. *J.Pathol.* 144, 149-161.

Brody AR, Roe MW, Evans JN and Davis GS. 1982. Deposition and translocation of inhaled silica in rats. Quantification of particle distribution, macrophage participation, and function. *Lab Invest* 47, 533-542.

Brown DM, Stone V, Findlay P, MacNee W and Donaldson K. 2000. Increased inflammation and intracellular calcium caused by ultrafine carbon black is independent of transition metals or other soluble components. *Occup.Environ.Med.* 57, 685-691.

Brown DM, Wilson MR, MacNee W, Stone V and Donaldson K. 2001. Size-dependent proinflammatory effects of ultrafine polystyrene particles: a role for surface area and oxidative stress in the enhanced activity of ultrafines. *Toxicol. Appl. Pharmacol.* 175, 191-199.

Brown DM, Wilson MR, MacNee W, Stone V and Donaldson K. 2001. Size-dependent proinflammatory effects of ultrafine polystyrene particles: a role for surface area and oxidative stress in the enhanced activity of ultrafines. *Toxicol.Appl.Pharmacol.* 175, 191-199.

Brown GM, Donaldson K and Brown DM. 1989. Bronchoalveolar leukocye response in experimental silicosis: modulation by a soluble aluminum compound. *Toxicol. Appl. Pharmacol.* 101, 95-105.

Budihardjo I, Oliver H, Lutter M, Luo X and Wang X. 1999. Biochemical pathways of caspase activation during apoptosis. *Annu.Rev.Cell Dev.Biol.* 15, 269-290.

Castranova V, Rabovsky J, Tucker JH and Miles PR. 1988. The alveolar type II epithelial cell: a multifunctional pneumocyte. *Toxicol.Appl.Pharmacol.* 93, 472-483.

Castranova V, Vallyathan V, Ramsey DM, McLaurin JL, Pack D, Leonard S, Barger MW, Ma JYC, Dalal NS and Teass A. 1997. Augmentation of pulmonary reactions to quartz inhalation by trace amounts of iron-containing particles. *Environ. Health Perspect.* 105S, 1319–1324.

Catling AD, Eblen ST, Schaeffer HJ and Weber MJ. 2001. Scaffold protein regulation of mitogen-activated protein kinase cascade. *Methods Enzymol.* 332, 368-387.

Chang L and Karin M. 2001. Mammalian MAP kinase signalling cascades. *Nature* 410, 37-40.

Chao CC, Park SH and Aust AE. 1996. Participation of nitric oxide and iron in the oxidation of DNA in asbestos-treated human lung epithelial cells. *Arch. Biochem. Biophys.* 326, 152-157.

Checkoway H, Heyer NJ, Deners PA and Breslow NE. 1993. Mortality among workers in the diatomaceous earth industry. *Br J Ind Med.* 50(7), 586-597.

Cherniack M. 1986. The Hawk's Nest Incident - America's worst industrial disaster. New Haven, CT, Yale University Press.

Churg A. 1996. The uptake of mineral particles by pulmonary epithelial cells. *Am. J. Respir. Crit. Care Med.* 154, 1124-1140.

Chytil M and Verdine GL. 1996. The Rel family of eukaryotic transcription factors. *Curr.Opin.Struct.Biol.* 6, 91-100.

Clouter A, Brown DM, Höhr D, Borm P and Donaldson K. 2001. Inflammatory effects of respirable quartz collected in workplaces versus standard DQ12 quartz: particle surface correlates. *Toxicol. Sci.* 63, 90-98.

Collins RH, Feldman M and Fordtran JS. 1987. Colon cancer, dysplasia and survieillance in patients with ulcerative collitis: A critical review. *N Eng J Med* 316, 1654-1658.

Collins AR, Ma AG and Duthie SJ. 1995. The kinetics of repair of oxidative DNA damage (strand breaks and oxidised pyrimidines) in human cells. *Mutat. Res.* 336, 69-77.

Commoner B, Townsend J, Pake GE. 1954. Free radicals in biological materials. *Nature* 174: 689-691.Corn JK. 1980. Historical aspects of industrial hygiene – silicosis. *Am Ind Hyg Assoc J.* 41: 125-132.

Costa D, Fubini B, Giamello E and Volante M. 1991. A novel type of active site at the surface of quartz and its possible impact on pathogenicity. *Can J Chem.* 69, 1427-1434.

Cowie RL. 1994. The epidemiology of tuberculosis in gold miners with silicosis. *Am.J.Respir.Crit Care Med.* 150, 1460-1462.

Craighead JE, Kleinerman J, Abraham JL, Gibbs AR, Green FHY, Harley RA, et al. 1988. Diseases associated with exposure to silica and non-fibrous silicate minerals. *Arch Pathol Lab Med.* 112: 673-720.

Cullen MR, Cherniack MG and Rosenstock L. 1990. Occupational medicine. *N. Engl. J. Med.* 322, 594-601.

Cullen RT, Vallyathan V, Hagen S and Donaldson K. 1997. Protection by Iron against the toxic effects of quartz. *Ann.Occup.Hyg.* 41, 420-425.

Culver B. 1999. In: Albert R, Spiro S, Jett J (eds). Comprehensive Respiratory Medicine. Harcourt Brace and Company Ltd, London.

Dalal NS, Shi XL and Vallyathan V. 1990. Role of free radicals in the mechanisms of hemolysis and lipid peroxidation by silica: comparative ESR and cytotoxicity studies. *J. Toxicol. Environ. Health* 29, 307-316.

Daniel LN, Mao Y and Saffiotti U. 1993. Oxidative DNA damage by crystalline silica. *Free Radic. Biol. Med.* 14, 463-472.

Daniel LN, Mao Y, Wang TC, Markey CJ, Shi X and Saffiotti, U. 1995. DNA strand breakage, thymine glycol production, and hydroxyl radical generation induced by different samples of crystalline silica in vitro. *Environ. Res.* 71, 60-73.

Ding M, Chen F, Shi X, Yucesoy B, Mossman B and Vallyathan V. 2002. Diseases caused by silica: mechanisms of injury and disease development. *Int.Immunopharmacol.* 2, 173-182.

Djeu JY, Matsushima K, Oppenheim JJ, Shiotsuki K and Blanchard DK. 1990a. Functional activation of human neutrophils by recombinant monocyte- derived neutrophil chemotactic factor/IL-8. *J.Immunol.* 144, 2205-2210.

Djeu JY, Serbousek D and Blanchard DK. 1990b. Release of tumor necrosis factor by human polymorphonuclear leukocytes. *Blood* 76, 1405-1409.

Doerschuk CM, Allard MF, Martin BA, MacKenzie A and Hogg JC. 1987. Marginated pool of neutrophils in lungs of rabbits. *J.Appl. Physiol.* 63, 1806-1815.

Don Porto Carero A, Hoet PH, Verschaeve L, Schoeters G and Nemery B. 2001. Genotoxic effects of carbon black particles, diesel exhaust particles, and urban air particulates and their extracts on a human alveolar epithelial cell line (A549) and a human monocytic cell line (THP-1). *Environ. Mol. Mutagen.* 3, 155-163.

Donaldson K, and Borm PJA. 1998. The quartz hazard: a variable entity. *Ann. Occup. Hyg.* 42, 287-294.

Donaldson K, Slight J and Bolton RE. 1988. The effect of products from bronchoalveolar-derived neutrophils on oxidant production and phagocytic activity of alveolar macrophages. *Clin.Exp.Immunol.* 74, 477-482.

Donaldson K, Stone V, Clouter A, Renwick L and MacNee W. 2001. Ultrafine particles. *Occup.Environ.Med.* 58, 211-6, 199.

Donaldson K, Tran CL and MacNee W. 2002. Deposition and effects of fine and ultrafine particles in the respiratory tract. In European Respiratory Monographs, Vol 7, Mono 21: The impact of air pollution on respiratory health. Ed GD Amato and ST Holgate.

Donaldson K and Tran CL. 2002 Inflammation caused by particles and fibres. Inhal Toxicol 14, 5-27.

Dormans JAMA and Van Bree L. 1995. Function and response of type II cells to inhaled toxicants. *Inhalat. Toxicol.* 7: 319-342.

Driscoll KE, Carter JM, Hassenbein DG and Howard B. 1997. Cytokines and particle-induced inflammatory cell recruitment. *Environ. Health Perspect.* 105 (Suppl. 5), 1159–1164.

Driscoll KE, Carter JM, Howard BW, Hassenbein DG, Pepelko W, Baggs RB and Oberdorster G. 1996. Pulmonary inflammatory, chemokine, and mutagenic responses in rats after subchronic inhalation of carbon black. *Toxicol.Appl.Pharmacol.* 136, 372-380.

Driscoll KE, Deyo LC, Carter JM, Howard BW, Hassenbein DG and Bertram TA. 1997. Effects of particle exposure and particle-elicited inflammatory cells on mutation in rat alveolar epithelial cells. *Carcinogenesis* 18, 423-430.

Driscoll KE, Deyo LC, Howard BW, Poynter J and Carter JM. 1995. Characterizing mutagenesis in the hprt gene of rat alveolar epithelial cells. *Exp. Lung Res.* 21, 941–956.

Driscoll KE, Hassenbein DG, Carter J, Poynter J, Asquith TN, Grant RA, Whitten J, Purdon MP and Takigiku R. 1993. Macrophage inflammatory proteins 1 and 2: Expression by rat alveolar macrophages, fibroblasts, and epithelial cells and in rat lung after mineral dust exposure 1. *Am. J. Respir. Cell Mol. Biol.* 8, 311–318.

Driscoll KE, Hassenbein DG, Carter JM, Kunkel SL, Quinlan TR and Mossman BT. 1995. TNF alpha and increased chemokine expression in rat lung after particle exposure. *Toxicol.Lett.* 82-83, 483-489.

Driscoll KE, Howard BW, Carter JM, Asquith T, Johnston C, Detilleux P, Kunkel SL and Isfort RJ. 1996. Alpha-quartz-induced chemokine expression by rat lung epithelial cells: Effects of in vivo and in vitro particle exposure. *Am. J. Pathol.* 149, 1627–1637.

Driscoll KE. 1996. Role of inflammation in the development of rat lung tumors in response to chronic particle exposure. *Inhal. Toxicol.* 8, 139-153.

Drost E and MacNee. 2002. Potential role of IL-8, platelet-activating factor and TNF-α in the sequestration of neutrophils in the lung: effects of neutrophil deformability, adhesionreceptor expression and chemotaxis. *Eur J Immunol.* 32, 393-403.

Dubois CM, Bissonnette E and Rola-Pleszczynski M. 1 989. Asbestos fibers and silica particles stimulate rat alveolar macrophages to release tumor necrosis factor. Autoregulatory role of leukotriene B4. *Am.Rev.Respir.Dis.* 139, 1257-1264.

Dufresne A, Sebastien P, Michaud D, Perrault G and Bégin R. 1994. Influence of aluminium treatments on pulmonary retention of quartz in sheep silicosis. *Exp. Lung Res.* 20, 157-168.

Engelbrecht FM, Yoganathan M, King EJ and Nagelschmidt G. 1958. Fibrosis and collagen in rat's lung produced by etched and unetched free silica dusts. Arch. Ind. Health. 17, 287-294.

Farber JL, Kyle ME and Coleman JB. 1990. Mechanisms of cell injury by activated oxygen species. *Lab Invest* 62, 670-679.

Fels AO and Cohn ZA. 1986. The alveolar macrophage. *J.Appl.Physiol* 60, 353-369.

Fenoglio I, Fubini B, Tiozzo R and Di Renzo F. 2000. Effect of micromorphology and surface reactivity of several unusual forms of crystalline silica on the toxicity to a monocyte-macrophage tumor cell line. *Inhal. Toxicol.* 12, 81-89.

Foster WM. 1999. Deposition and clearance of inhaled particles. In: Holgate ST, Samet JM, Koren HS and Maynard RL (eds) *Air Pollution and Health.* London, UK: Academic Press, pp 295-324.

Freeman BA and Crapo JD. 1982. Biology of disease: free radicals and tissue injury. *Lab Invest* 47, 412-426.

Friemann J, Albrecht C, Breuer P, Grover R and Weishaupt C. (1999). Time-course analysis of type II cell hyperplasia and alveolar bronchiolization in rats treated with different particulates. *Inhal.Toxicol.* 11, 837-854.

Fubini B, Giamello E, Volante M and Bolis V. 1990. Chemical functionalities at the silica surface determining its reactivity when inhaled. Formation and reactivity of surface radicals. *Toxicol. Ind. Health* 6, 571-598.

Fubini B, Mollo L and Giamello E. 1995. Free-radical generation at the solid/liquid interface in iron-containing minerals. *Free Radical Res.* 23, 593–614.

Fubini B, Wallace WE. 2000. Modulation of silica pathogenicity by surface processes. In: *Adsorption on silica surfaces* (Papirer E., Ed). Marcel Dekker, New York. pp 645-664.

Fubini B. 1998a. Health effects of silica. In *The Surface Properties of Silica* (A. P. Legrand, Ed.), pp. 415–464. Wiley, New York.

Fubini B. 1998b. Surface chemistry and quartz hazard. *Ann. Occup. Hyg.* 42, 521–530.

Fung, H, Kow YW, van Houten B and Mossman BT. 1997. Patterns of 8-hydroxydeoxyguanosine formation in DNA and indications of oxidative stress in rat and human pleural mesothelial cells after exposure to crocidolite asbestos. *Carcinogenesis* 18, 825-832.

Gabor S, Anca Z and Zugravu E. 1975. In vitro action of quartz on alveolar macrophage lipid peroxides. *Arch. Environ. Health* 30, 499-501.

Gallagher J, Heinrich U, George M, Hendee L, Phillips DH and Lewtas J. 1994. Formation of DNA adducts in rat lung following chronic inhalation of diesel emissions, carbon black and titanium dioxide particles. *Carcinogenesis* 15, 1291-1299.

Garrido C, Ottavi P, Fromentin A, Hammann A, Arrigo AP, Chauffert B and Mehlen P. 1997. HSP27 as a mediator of confluence-dependent resistance to cell death induced by anticancer drugs. *Cancer Res.* 57, 2661-2667.

Ghio AJ and Devlin RB. 2001. Inflammatory lung injury after bronchial instillation of air pollution particles. *Am.J.Respir.Crit Care Med.* 164, 704-708.

Goldstein B and Rendall RE. 1987. The prophylactic use of polyvinyl-N-oxide (PVNO) in baboons exposed to quartz dust. *Environ. Res.* 42, 469-481.

Gosset P, Lassalle P, Vanhee D, Wallaert B, Aerts C, Voisin C and Tonnel AB. 1991. Production of tumor-necrosis-factor-alpha and interleukin-6 by human alveolar macrophages exposed invitro to coal-mine dust. *Am J Resp Cell Mol Biol* 5, 431-436.

Gray H. 1918. Lungs. In: Gray's Anatomy of the Human Body, 20th Edition. Lea & Febiger, Philadelphia.

Green DR and Reed JC. 1998. Mitochondria and apoptosis. *Science* 281, 1309-1312.

Green FHY and Vallyathan V. 1995. Pathologic Responses to Inhaled Silica. In: Castranova V, Vallyathan V and Wallace WE (eds) *Silica and Silica-Induced Lung Diseases*. Florida, USA: CRC Press, pp 39-59.

Greim H, Borm P, Donaldson K, Driscoll K, Hartwig A, Kuempel E, Oberdörster G, Schins R and Speit G. 2001. Toxicity of fibers and particles. Report of a workshop held in Munich, Germany. *Inhal. Toxicol.* 13, 737-754.

Gross A, Dugas N, Spiesser S, Vouldoukis I, Damais C, Kolb JP, Dugas B and Dornand J. 1998. Nitric oxide production in human macrophagic cells phagocytizing opsonized zymosan: direct characterization by measurement of the luminol dependent chemiluminescence. *Free Radic.Res.* 28, 179-191.

Gulumian M and van Wyk A. 1987. Free radical scavenging properties of polyvinylpyridine N-oxide: a possible mechanism for its action in pneumoconiosis. *Med. Lav.* 78, 124-128.

Hardy JA and Aust AE. 1995. The effect of iron binding on the ability of crocidolite asbestos to catalyze DNA single-strand breaks. *Carcinogenesis* 16, 319-325.

Harington JS, Macnab GM, Miller K and King PC. 1971. Enhancement of haemolytic activity of asbestos by heat-labile factors in fresh serum. *Med. Lav.* 62, 171–176.

Harman D. 1956. Ageing: a theory based on free radical and radiation chemistry. *J. Gerontol* 11: 298-300.

Have-Opbroek AA, Benfield JR, van Krieken JH and Dijkman JH. 1997. The alveolar type II cell is a pluripotential stem cell in the genesis of human adenocarcinomas and squamous cell carcinomas. *Histol.Histopathol.* 12, 319-336.

Hessel PA, Sluis-Cremer GK and Hnizdo E. 1986. Case-control study of silicosis, silica exposure and lung cancer in white South African gold miners. *Am J Ind Med.* 10(1), 57-62.

Hessel PA, Sluis-Cremer GK and Hnizdo E. 1990. Silica exposure, silicosis and lung cancer: a necropsy study. *Br J Ind Med.* 47(1), 4-9.

Hessel PA, Gamble JF, Gee JB, Gibbs G, Green FH, Morgan WK and Mossman BT. 2000. Silica, silicosis, and lung cancer: a response to a recent working group report. *J.Occup.Environ.Med.* 42, 704-720.

Hesterberg TW and Barrett JC. 1984. Dependence of asbestos- and mineral dust-induced transformation of mammalian cells in culture on fiber dimension. *Cancer Res.* 44, 2170-2180.

Hevel JM, White KA and Marletta MA. 1991. Purification of the inducible murine macrophage nitric oxide synthase. Identification as a flavoprotein. *J.Biol.Chem.* 266, 22789-22791.

Hill IM, Beswick PH and Donaldson K. 1996. Enhancement of the macrophage oxidative burst by immunoglobulin coating of respirable fibers: fiber-specific differences between asbestos and man-made fibers. *Exp.Lung Res.* 22, 133-148.

Hnizdo E and Sluis-Cremer GK. 1993. Risk of silicosis in a cohort of white South African gold miners. *Am.J.Ind.Med.* 24, 447-457.

Hoidal JR, Schmeling D and Peterson PK. 1981. Phagocytosis, bacterial killing, and metabolism by purified human lung phagocytes. *J.Infect.Dis.* 144, 61-71.

Huang Y, Hutter D, Liu Y, Wang X, Sheikh MS, Chan AM and Holbrook NJ. 2000. Transforming growth factor-beta 1 suppresses serum deprivation-induced death of A549 cells through differential effects on c-Jun and JNK activities. *J. Biol. Chem.* 275, 18234-18242.

Huffman LJ, Judy DJ and Castranova V. 1998. Regulation of nitric oxide production by rat alveolar macrophages in response to silica exposure. *J.Toxicol.Environ.Health* 53, 29-46.

International Agency for Research on Cancer (IARC) (1997) Monograph on the Evaluation of the Carcinogenic Risk of Chemicals to Humans, Vol. 68: *silica, some silicates, coal dust and para-aramid fibrils.* Geneva, IARC Press.

Iyer GYN, Islam MF, Quastel JH. 1961. Biochemical aspects of phagocytosis. *Nature* 192: 535-541.

Iyer R and Holian A. 1997. Involvement of the ICE family of proteases in silica-induced apoptosis in human alveolar macrophages. *Am.J.Physiol* 273, L760-L767.

Iyer R, Hamilton RF, Li L and Holian A. 1996. Silica-induced apoptosis mediated via scavenger receptor in human alveolar macrophages. *Toxicol Appl Pharmacol* 141, 84-92.

Janssen YM, Soultanakis R, Steece K, Heerdt E, Singh RJ, Joseph J and Kalyanaraman B. 1998. Depletion of nitric oxide causes cell cycle alterations, apoptosis and oxidative stress in pulmonary cells. *Am J Physiol.* 275, L1100-L1109.

Johnson NF, Smith DM, Sebring R and Holland LM. 1987. Silica-induced alveolar cell tumors in rats. *Am.J.Ind.Med.* 11, 93-107.

Johnston C J, Driscoll KE, Finkelstein JN, Baggs R, O'Reilly MA, Carter J, Gelein R and Oberdörster G. 2000. Pulmonary chemokine and mutagenic responses in rats after subchronic inhalation of amorphous and crystalline silica. *Toxicol. Sci.* 56, 504-413.

Jones AD, McMillan CH, Johnston AM, Mcintosh C, Cowie H, Bolton RE, Borzucki G and Vincent JH. 1988. Pulmonary clearance of UICC amosite fibres inhaled by rats during chronic exposure at low concentration. *Br.J.Ind.Med.* 45, 300-304.

Kantor AF, Hartge P, Hoover RN, Narayana AS, Sullivan JW and Fraumenti JF Jr. 1984. Urinary tract infection and risk of bladder cancer. *Am J Epidemiol* 119, 510-515.

Karin M and Hunter T. 1995. Transcriptional control by protein phosphorylation: signal transmission from the cell surface to the nucleus. *Curr.Biol.* 5, 747-757.

Karin M and Delhase M. 2000a. The I kappa B kinase (IKK) and NF-kappa B: key elements of proinflammatory signalling. *Semin.Immunol.* 12, 85-98.

Karin M and Ben Neriah Y. 2000b. Phosphorylation meets ubiquitination: the control of NF-kappa B activity. *Annu.Rev.Immunol.* 18, 621-663.

Kelley J. 1990. Cytokines of the lung. *Am Rev Respir Dis.* 141(3), 765-788.

Kensler TW and Trush MA. 1984. Role of oxygen radicals in tumor promotion. *Environ. Mutagen.* 6, 593-616.

Kim HN, Morimoto Y, Tsuda T, Ootsuyama Y, Hirohashi M, Hirano T, Tanaka I, Lim, Y, Yun IG and Kasai H. 2001. Changes in DNA 8-hydroxyguanine levels, 8-hydroxyguanine repair activity, and hOGG1 and hMTH1 mRNA expression in human lung alveolar epithelial cells induced by crocidolite asbestos. *Carcinogenesis* 22, 265-269.

Kinnula VL, Chang L, Everitt JI and Crapo JD. 1992. Oxidants and antioxidants in alveolar epithelial type II cells: in situ, freshly isolated, and cultured cells. *Am.J.Physiol* 262, L69-L77.

Kinnula VL, Crapo JD and Raivio KO. 1995. Generation and disposal of reactive oxygen metabolites in the lung. *Lab Invest* 73, 3-19.

Klebanoff SJ, Vadas MA, Harlan JM, Sparks LH, Gamble JR, Agosti JM and Waltersdorph AM. 1986. Stimulation of neutrophils by tumor necrosis factor. *J.Immunol.* 136, 4220-4225.

Klebanoff SJ. 1967. A peroxidase-mediated antimicrobial system in leukocytes. *J Clin Invest* 46: 1478.

Klebanoff SJ. 1999. Myeloperoxidase. *Proc.Assoc.Am.Physicians* 111, 383-389.

Knaapen AM, Albrecht C, Becker A, Hohr D, Winzer A, Haenen GR, Borm PJ, and Schins RP. 2002. DNA damage in lung epithelial cells isolated from rats exposed to quartz: role of surface reactivity and neutrophilic inflammation. *Carcinogenesis* 23, 1111-1120.

Knaapen AM, Schins RPF, Steinfartz Y, Höhr D, Dunemann L and Borm PJA. 2000. Ambient particulate matter induces oxidative DNA damage in lung epithelial cells. *Inhal. Toxicol.* 12, 125-132.

Kobzik L. 1995. Lung macrophage uptake of unopsonized environmental particulates. Role of scavenger-type receptors. *J.Immunol.* 155, 367-376.

Kovacikova Z and Tatrai E. 1996. Significance of alveolar macrophages, pneumocyte type II and Clara cells in lung toxicology. *Biologia, Bratislava.* 51: 425-429.

Kraal G, van der Laan LJ, Elomaa O and tryggvason K. 2000. The macrophage receptor MARCO. *Microbes Infect.* 2(3), 313-316.

Kuempel ED, Tran CL, Bailer AJ, Porter DW, Hubbs AF and Castranova V. 2001. Biological and statistical approaches to predicting human lung cancer risk from silica. *J.Environ.Pathol.Toxicol.Oncol.* 20 Suppl 1, 15-32.

Kuida K. 2000. Caspase-9. *Int.J.Biochem.Cell Biol.* 32, 121-124.Lapp NL. 1981. Lung disease secondary to inhalation of nonfibrous minerals. *Clin.Chest Med.* 2, 219-233.

Kusiak RA, Springer J, Ritchie AC and Miller J. 1991. Carcinoma of the lung in Ontario gold miners: possible aetiological factors. *Br J Ind Med.* 48(12), 808-817.

Kyriakis JM and Avruch J. 2001. Mammalian mitogen-activated protein kinase signal transduction pathways activated by stress and inflammation. *Physiol Rev.* 81(2), 807-869.

Lapp NL. 1981. Lung disease secondary to inhalation of nonfibrous minerals. *Clin Chest Med.* 2(2), 219-233.

Lee KP, Trochimowicz HJ and Reinhardt CF. 1985. Transmigration of titanium dioxide (TiO2) particles in rats after inhalation exposure. *Exp.Mol.Pathol.* 42, 331-343.

Leigh J, Wang H, Bonin A, Peters M and Ruan X. 1997. Silica-induced apoptosis in alveolar and granulomatous cells in vivo. *Environ.Health Perspect.* 105 Suppl 5, 1241-1245.

Leslie CC, McCormick-Shannon K, Cook JL and Mason RJ. 1985. Macrophages stimulate DNA synthesis in rat alveolar type II cells. *Am.Rev.Respir.Dis.* 132, 1246-1252.

Li K, Brown D, Smith S, MacNee W and Donaldson K. 1999. Short-term inflammatory responses following intratracheal instillation of fine and ultrafine carbon black in rats. *Inhal. Toxicol.* 11, 709–731.

Lim Y, Kim JH, Kim KA, Chang HS, Park YM, Ahn BY and Phee YG. 1999. Silica-induced apoptosis in vitro and in vivo. *Toxicol. Lett.* 108, 335-339.

Liu W, Ernst JD and Broaddus VC. 2000. Phagocytosis of crocidolite asbestos induces oxidative stress, DNA damage, and apoptosis in mesothelial cells. *Am. J. Respir. Cell. Mol. Biol.* 23, 371-378.

Liu X, Keane MJ, Harrison JC, Cilento EV, Ong T and Wallace WE. 1998. Phospholipid surfactant adsorption by respirable quartz and in vitro expression of cytotoxicity and DNA damage. *Toxicol. Lett.* 96-97, 77-84.

Liu X, Keane MJ, Zhong B, Ong T and Wallace WE. 1996. Micronucleus formation in V79 cells treated with respirable silica dispersed in medium and in simulated pulmonary surfactant. *Mutat. Res.* 361, 89-94.

Lohmann-Matthes ML, Steinmuller C and Franke-Ullmann G. 1994. Pulmonary macrophages. *Eur.Respir.J.* 7, 1678-1689.

Luster AD. 1998. Chemokines--chemotactic cytokines that mediate inflammation. *N.Engl.J.Med.* 338, 436-445.

Majno G and Joris I. 1995. Apoptosis, Oncosis and Necrosis: An overview of cell death. *Am. J. Path.* 146, 3-15.

Mandel G and Mandel N. 1995. The Structure of Crystalline SiO_2. In: Castranova V, Vallyathan V and Wallace WE (eds) *Silica and Silica-Induced Lung Diseases*. Florida, USA: CRC Press, pp 63-78.

Marnett LJ. 2000 Oxyradicals and DNA damage. *Carcinogenesis* 21, 361-370.

McClellan R. 2000. Particle interactions with the respiratory tract. In: Gehr P, Heyder J. (eds) *Particle-lung interactions*, Vol. 143, Marcel Dekker, Inc., New York, NY. pp 3 - 63.

McCord JM, Fridovich I. 1969. Superoxide dismutase. An enzymatic function for erythrocuprein. *J Biol Chem* 244: 6049-6055.

McDonald AD, McDonald JC, Raudo RJ, Hughes JM and Weill H. 2001. Cohort mortality study of North American industrial sand workers. I. Mortality from lung cancer, silicosis and other causes. *Ann Occup Hyg.* 45(3), 193-199.

Meier B, Radeke HH, Selle S, Raspe HH, Sies H, Resch K and Habermehl GG. 1990. Human fibroblasts release reactive oxygen species in response to treatment with synovial fluids from patients suffering from arthritis. *Free Radic.Res.Commun.* 8, 149-160.

Metchnikoff E. 1905. Immunity to infectious diseases. Cambridge University Press, London.

Metinko AP, Kunkel SL, Standiford TJ and Strieter RM. 1992. Anoxia-hyperoxia induces monocyte-derived interleukin-8. *J.Clin.Invest* 90, 791-798.

Middleton EL. 1929. The present position of silicosis in industry in Britain. *Br. Med. J.*, 2, 485.

Millard FJC, Pepper JR. 1990. Pleural Disease. In: Brewis RAL, Gibson GJ, Geddes DM. (eds) Respiratory Medicine, Balliere Tindal WB Saunders, London.

Miller BG and Jacobsen M. 1985. Dust exposure, pneumoconiosis and mortality of coalminers. *Br J Ind Med.* 42(11), 723-733.

Miller BG, Hagen S, Love RG, Soutar CA, Cowie HA, Kidd MW and Robertson A. 1998. Risks of silicosis in coalworkers exposed to unusual concentrations of respirable quartz. *Occup.Environ.Med.* 55, 52-58.

Minamoto T, Mai M and Ronai Z. 1999. Environmental factors as regulators and effectors of multistep carcinogenesis. *Carcinogenesis* 20, 519–527.

Morgan WKC and Seaton A. 1995. *Occupational Lung Diseases.* Saunders, Philadelphia.

Morrow PE. 1988. Possible mechanisms to explain dust overloading of the lungs. *Fundam.Appl.Toxicol.* 10, 369-384.

Mosmann T. 1983. Rapid colorimetric assay for cellular growth and survivial: application to proliferation and cytotoxicity assays. *J. Immunol. Meth.* 65, 517-527.

Mossman BT, Alder KB and Craighead JE. 1978. Interaction of carbon particles with tracheal epithelium in organ culture. *Environ Res.* 16(1-3), 110-122.

Mossman BT and Churg A. 1998. Mechanisms in the pathogenesis of asbestosis and silicosis. *Am.J.Respir.Crit Care Med.* 157, 1666-1680.

Mossman BT and Marsh JP. 1989. Evidence supporting a role for active oxygen species in asbestos- induced toxicity and lung disease. *Environ.Health Perspect.* 81, 91-94.

Mossman BT, Adler KB and Craighead JE. 1978. Interaction of carbon particles with tracheal epithelium in organ culture. *Environ.Res.* 16, 110-122.

Mossman BT. 2000. Signal transduction by oxidants: look who's talking. Free *Radic.Biol.Med.* 28, 1315-1316.

Moyer VD, Cistulli CA, Vaslet CA and Kane AB. 1994. Oxygen radicals and asbestos carcinogenesis. *Environ.Health Perspect.* 102 Suppl 10, 131-136.

Muhle H, Mermelstein R, Dasenbrock C, Takenaka S, Mohr U, Kilpper R, MacKenzie J and Morrow P. 1989a. Lung response to test toner upon 2-year inhalation exposure in rats. *Exp.Pathol.* 37, 239-242.

Muhle H, Takenaka S, Mohr U, Dasenbrock C and Mermelstein R. 1989b. Lung-tumor induction upon long-term low-level inhalation of crystalline silica. *Am.J.Ind.Med.* 15, 343-346.

Muir DC, Julian JA, Shannon HS, Verma DK, Sebestyen A and Bernholz CD. 1989. Silica exposure and silicosis among Ontario hardrock miners: III. Analysis and risk estimates. *Am.J.Ind.Med. 16*, 29-43.

Mukaida N, Matsumoto T, Yokoi K, Harada A and Matsushima K. 1998. Inhibition of neutrophil-mediated acute inflammation injury by an antibody against interleukin-8 (IL-8). *Inflamm.Res.* 47 Suppl 3, S151-S157.

Mullen PG, Windsor ACJ, Walsh CJ, Fowler AA and Sugerman HJ. 1995. Tumour necrosis factor-α and interleukin-6 selectively regulate neutrophil function *in vitro*. *J Surg Res.* 58, 124-130.

Nagalakshmi R, Nath J, Ong T and Whong WZ. 1995. Silica-induced micronuclei and chromosomal aberrations in Chinese hamster lung (V79) and human lung (Hel 299) cells. *Mutat. Res.* 335, 27-33.

Nash T, Allison AC and Harington JS. 1966. Physico-Chemical properties of silica in relation to its toxicity. *Nature* 210, 259-261.

Nathan CF. 1987. Neutrophil activation on biological surfaces. Massive secretion of hydrogen peroxide in response to products of macrophages and lymphocytes. *J.Clin.Invest* 80, 1550-1560.

Nehls P, Seiler F, Rehn B, Greferath R and Bruch J. 1997. Formation and persistence of 8-oxoguanine in rat lung cells as an important determinant for tumor formation following particle exposure. *Environ. Health Perspect.* 105, 1291-1296.

Ng TP and Chan SL. 1992. Lung function in relation to silicosis and silica exposure in granite workers. *Eur.Respir.J.* 5, 986-991.

Nikula KJ, Avila KJ, Griffith WC and Mauderly JL. 1997. Sites of particle retention and lung tissue responses to chronically inhaled diesel exhaust and coal dust in rats and cynomolgus monkeys. *Environ.Health Perspect.* 105 Suppl 5, 1231-1234.

Nolan RP, Langer AM, Harington JS, Oster G and Selikoff IJ. 1981. Quartz hemolysis as related to its surface functionalities. *Environ. Res.* 26, 503–520.

Oberdorster G. 1995. Lung particle overload: implications for occupational exposure to particles. *Regul Toxicol Pharmacol.* 21(1), 123-135.

Oberdorster G. 1996. Significance of particle parameters in the evaluation of exposure-dose-response relationships of inhaled particles. *Particulate Science And Technology* 14.

Oberdorster G. 1997. Pulmonary carcinogenicity of inhaled particles and the maxium tolerated dose. *Environ Health Perspect.* 105, 1347-1355.

Oberdorster G. 2001. Pulmonary effects of inhaled ultrafine particles. *Int.Arch.Occup.Environ.Health* 74, 1-8.

Offen D, Ziv I, Sternin H, Melamed E and Hochman A. 1996. Prevention of dopamine-induced cell death by thiol antioxidants: possible implications for treatment of Parkinson's disease. *Exp.Neurol.* 141, 32-39.

Offen D, Ziv I, Barzilai A, Gorodin S, Glater E, Hochman A and Melamed E. 1997. Dopamine-melanin induces apoptosis in PC12 cells; possible implications for the etiology of Parkinson's disease. *Neurochem.Int.* 31, 207-216.

Olbruck H, Seemayer NH, Voss B and Wilhelm M. 1998. Supernatants from quartz dust treated human macrophages stimulate cell proliferation of different human lung cells as well as collagen- synthesis of human diploid lung fibroblasts in vitro. *Toxicol.Lett.* 96-97, 85-95.

Olive PL, Banath JP and Durand RE. 1990. Heterogeneity in radiation-induced DNA damage and repair in tumor and normal cells measured using the "comet" assay. *Radiat. Res.* 122, 86-94.

Palecanda A and Kobzik L. 2001. Receptors for unopsonized particles: the role of alveolar macrophage scavenger receptors. *Curr.Mol.Med.* 1, 589-595.

Palecanda A, Paulauskis J, Al Mutairi E, Imrich A, Qin G, Suzuki H, Kodama T, Tryggvason K, Koziel H and Kobzik L. 1999. Role of the scavenger receptor MARCO in alveolar macrophage binding of unopsonized environmental particles. *J.Exp.Med.* 189, 1497-1506.

Piguet PF, Collart MA, Grau GE, Sappino AP and Vassalli P. 1990. Requirement of tumor-necrosis-factor for development of silica- induced pulmonary fibrosis. *Nature.* 344, 245-247.

Porter AG and Janicke RU. 1999. Emerging roles of caspase-3 in apoptosis. *Cell Death.Differ.* 6, 99-104.

Quinot E, Cavelier C and Merceron MO. 1979. Surface chemistry and cytotoxic properties of silica. *Biomedicine* 30, 155–160.

Rahman I and MacNee W. 1996. Oxidant/antioxidant imbalance in smokers and chronic obstructive pulmonary disease. *Thorax* 51, 348-350.

Rahman I and MacNee W. 1998. Role of transcription factors in inflammatory lung diseases. *Thorax* 53, 601-612.

Rahman I and MacNee W. 2000. Oxidative stress and regulation of glutathione in lung inflammation. *Eur.Respir.J.* 16, 534-554.

Renwick LC, donaldson K and Clouter A. 2001. Impairment of alveolar macrophage phagocytosis by ultrafine particles. *Toxicol Appl Pharmacol.* 172, 119-127.

Reynolds HY, Atkinson JP, Newball HH and Frank MM. 1975. Receptors for immunoglobulin and complement on human alveolar macrophages. *J.Immunol.* 114, 1813-1819.

Reynolds HY. 1987. Bronchoalveolar lavage. *Am.Rev.Respir.Dis.* 135, 250-263.Rom WN. 1992. *Environmental and Occupational Medicine*, 2nd ed. Little, Brown and Company, USA.

Rice FL, Park R, Stayner L, Smith R, Gilbert S and Checkoway H. 2001. Crystalline silica exposure and lung cancer mortality in diatomaceous earth industry workers: a quantitative risk assessment. *Occup Environ Med.* 58(1), 38-45.

Rich EA, Panuska JR, Wallis RS, Wolf CB, Leonard ML and Ellner JJ. 1989. Dyscoordinate expression of tumor necrosis factor-alpha by human blood monocytes and alveolar macrophages. *Am.Rev.Respir.Dis.* 139, 1010-1016.

Robock K. 1973. Standard quartz DQ12 greater than 5 μm for experimental pneumoconiosis research projects in the Federal Republic of Germany. *Ann. Occup. Hyg.* 16, 63–66.

Rojanasakul Y, Weissman DN, Shi XL, Castranova V, Ma JH and Liang WW. 1997. Antisense inhibition of silica-induced tumor necrosis factor in alveolar macrophages. *J. Biol. Chem.* 272, 3910–3914.

Sacks M, Gordon J, Bylander J, Porter D, Shi XL, Castranova V, Kaczmarczyk W, Van Dyke K and Reasor MJ. 1998. Silica-induced pulmonary inflammation in rats: activation of NF-kappa B and its suppression by dexamethasone. *Biochem.Biophys.Res.Commun.* 253, 181-184.

Saffiotti U, Lambert DN, Mao Y, Williams AO, Kaighn ME, Ahmed H, Knapton AD. 1993. Biological studies on the carcinogenic mechanisms of quartz. In: Guthrie GD, Mossman BT (eds). *Reviews in minerology: health effects of mineral dusts.* Washington DC: Minerology Society of America, 28: 523-544.

Saffiotti U. 1998. Respiratory tract carcinogenesis by mineral fibres and dusts: models and mechanisms. *Monaldi Arch.Chest Dis.* 53, 160-167.

Schins RPF and Borm PJA. 1999. Mechanisms and mediators in coal dust induced toxicity: a review. *Ann. Occup. Hyg.* 43, 7-33.

Schins RPF and Donaldson K. 2000. Nuclear factor kappa B activation by particles and fibres. *Inhal. Toxicol.* 12(Suppl. 3), 317–326.

Schins RPF, Knaapen AM, Cakmak GD, Shi T, Weishaupt C and Borm PJA. 2002. Oxidant-induced DNA damage by quartz in alveolar epithelial cells. *Mutat. Res* 517: 77-86.

Schins RPF. 2000. Mechanisms of genotoxicity of particles and fibres. *Inhal. Toxicol.* 14, 57-78.

Schlipkoter HW, Hilscher W, Pott F and Beck EG. 1970. Investigations on the aetiology of coal workers' pneumoconiosis with the use of PVN-oxide. *Inhaled Part.* 1, 379-390.

Schultz H, Brand P and Heyder J. 2000. Particle deposition in the respiratory tract. In: Gehr P, Heyder J. (eds) Particle-lung interactions, Vol. 143, Marcel Dekker, Inc., New York, NY. pp 229 – 290.

Seaton A, Legge JS, Henderson J and Kerr KM. 1991. Accelerated silicosis in Scottish stonemasons. *Lancet* 337, 341-344.

Seaton A. 2000. In: Seaton A, Seaton D, Leitch G. (eds) Crofton and Douglas's Respiratory Diseases, 5th Edition, Vol. 1, Blackwell Sciences Ltd.

Seaton A. 1995. Silicosis. In: *Occupational Lung Diseases.* Saunders, Philadelphia.

Seiler F, Rehn B, Rehn S and Bruch J. 2001. Quartz exposure of the rat lung leads to a linear dose response in inflammation but not in oxidative DNA damage and mutagenicity. *Am. J. Respir. Cell Mol. Biol.* 24, 492-498.

Selby C, Drost E, Lannan S, Wraith PK and MacNee W. 1991. Neutrophil retention in the lungs of patients with chronic obstructive pulmonary disease. *Am Rev Respir Dis.* 143, 1359-1364.

Shen HM, Zhang Z, Zhang QF and Ong CN. 2001. Reactive oxygen species and caspase activation mediate silica-induced apoptosis in alveolar macrophages. *Am.J.Physiol Lung Cell Mol.Physiol* 280 , L10-L17.

Shi X, Mao Y, Daniel LN, Saffiotti U, Dalal NS and Vallyathan V. 1994. Silica radical-induced DNA damage and lipid peroxidation. *Environ.Health Perspect.* 102 Suppl 10, 149-154.

Shukla A, Timblin CR, Hubbard AK, Bravman J and Mossman BT. 2001. Silica-induced activation of c-Jun-NH2-terminal amino kinases, protracted expression of the activator protein-1 proto-oncogene, fra-1, and S-phase alterations are mediated via oxidative stress. *Cancer Res.* 61, 1791-1795.

Sibille Y and Marchandise FX. 1993. Pulmonary immune cellsin health and disease: polymorphonuclear neutrophils. *Am Respir J.* 6, 1529-1543.

Sibille Y and Reynolds HY. 1990. Macrophages and polymorphonuclear neutrophils in lung defence and injury. *Am Rev Respir Dis.* 141, 471-501.

Singh NP, McCoy MT, Tice RR and Schneider EL. 1988. A simple technique for quantitation of low levels of DNA damage in individual cells. *Exp. Cell Res.* 175, 184-191.

Spencer JP, Jenner A, Chimel K, Aruoma OI, Cross CE, Wu R and Halliwell B. 1995. DNA strand breakage and base modification induced by hydrogen peroxide treatment of human respiratory tract epithelial cells. *FEBS Lett.* 374, 233-236.

Staal FJ, Roederer M, Herzenberg LA and Herzenberg LA. 1990. Intracellular thiols regulate activation of nuclear factor kappa B and transcription of human immunodeficiency virus. *Proc. Natl. Acad. Sci. USA* 87, 9943–9947.

Stalder K and Stöber W. 1965. Hemolytic activity of suspensions of different silica modifications and inert dusts. *Nature* 207, 874-875.

Stearns RC, Paulauskis JD, Godleski JJ. 2001. Endocytosis of ultrafine particles by A549 cells. *Am. J. Respir. Cell Mol. Biol.* 24, 108-115.

Steerenberg PA, Zonnenberg JA, Dormans JA, Joon PN, Wouters IM, van Bree L, Scheepers PT and Van Loveren H. 1998. Diesel exhaust particles induced release of interleukin 6 and 8 by (primed) human bronchial epithelial cells (BEAS 2B) in vitro. *Exp.Lung Res.* 24, 85-100.

Stringer B and Kobzik L. 1998. Environmental particulate-mediated cytokine production in lung epithelial cells (A549): role of preexisting inflammation and oxidant stress. *J.Toxicol.Environ.Health* A 55, 31-44.

Suzuki Y, Churg J and Ono T. 1972. Phagocytic activity of the alveolar epithelial cells in pulmonary asbestosis. *Am.J.Pathol.* 69, 373-388.

Takeuchi T and Morimoto K. 1994. Crocidolite asbestos increased 8-hydroxydeoxyguanosine levels in cellular DNA of a human promyelocytic leukemia cell line, HL60. *Carcinogenesis* 15, 635-639.

Thannickal VJ and Fanburg BL. 2000. Reactive oxygen species in cell signaling. *Am.J.Physiol Lung Cell Mol.Physiol* 279, L1005-L1028.

Thornberry NA. 1998. Caspases: key mediators of apoptosis. *Chem.Biol.* 5, R97-103.

Tice RR, Agurell E, Anderson D, Burlinson B, Hartmann A, Kobayashi H, Miyamae Y, Rojas E, Ryu JC and Sasaki YF. 2000. Single cell gel/comet assay: guidelines for in vitro and in vivo genetic toxicology testing. *Environ. Mol. Mutagen.* 35, 206-221.

Tolbert NE and Essner E. 1981. Microbodies: peroxisomes and glyoxysomes. *J.Cell Biol.* 91, 271s-283s.

Toyokuni S, Tanaka T, Hattori Y, Nishiyama Y, Yoshida A, Uchida K, Hiai H, Ochi H and Osawa T. 1997. Quantitative immunohistochemical determination of 8-hydroxy-2'-deoxyguanosine by a monoclonal antibody N45.1: Its application to ferric nitrolotriacetate-induced renal carcinogenesis model. *Lab. Invest.* 76, 365-374.

Tran CL, Buchanan D, Cullen RT, Searl A, Jones AD and Donaldson K. 2000. Inhalation of poorly soluble particles. II. Influence Of particle surface area on inflammation and clearance. *Inhal.Toxicol.* 12, 1113-1126.

Trush MA and Kensler TW. 1991. An overview of the relationship between oxidative stress and chemical carcinogenesis. *Free Radic. Biol. Med.* 10, 201-210.

Vallyathan V, Kang JH, Van Dyke K, Dalal NS and Castranova V. 1991. Response of alveolar macrophages to in vitro exposure to freshly fractured versus aged silica dust: the ability of Prosil 28, an organosilane material, to coat silica and reduce its biological reactivity. *J. Toxicol. Environ. Health* 33, 303-15.

Vallyathan V, Shi X, Dalal NS, Irr W and Castranova V. 1988. Generation of free radicals from freshly fractured silica dust: potential role in acute silica-induced lung injury. *Am. Rev. Respir. Dis.* 138, 1213-1219.

van der Vliet, O'Neill CA, Cross CE, Koostra JM, Volz WG, Halliwell B and Louie S. 1999. Determination of low-molecular-mass antioxidant concentrations in human respiratory tract lining fluids. *Am.J.Physiol* 276, L289-L296.

van Klaveren RJ, Roelant C, Boogaerts M, Demedts M and Nemery B. 1997. Involvement of an NAD(P)H oxidase-like enzyme in superoxide anion and hydrogen peroxide generation by rat type II cells. *Thorax* 52, 465-471.

van Maanen JM, Borm PJ, Knaapen A, van Herwijnen M, Schilderman PA, Smith KR, Aust AE, Tomatis M and Fubini B. 1999. In vitro effects of coal fly ashes: hydroxyl radical generation, iron release, and DNA damage and toxicity in rat lung epithelial cells. *Inhal.Toxicol.* 11, 1123-1141.

Wallace WE, Vallyathan V, Keane MJ and Robinson V. 1985. In vitro biologic toxicity of native and surface-modified silica and kaolin. *J. Toxicol. Environ. Health* 16, 415–424.

Warheit DB, Overby LH, George G and Brody AR. 1988. Pulmonary macrophages are attracted to inhaled particles through complement activation. *Exp.Lung Res.* 14, 51-66.

Warren JS, Kunkel SL, Cunningham TW, Johnson KJ and Ward PA. 1988. Macrophage-derived cytokines amplify immune complex-triggered O2-. responses by rat alveolar macrophages. *Am.J.Pathol.* 130, 489-495.

Weinberg JB, Misukonis MA, Shami PJ, Mason SN, Sauls DL, Dittman WA, Wood ER, Smith GK, McDonald B, Bachus KE. 1995. Human mononuclear phagocyte inducible nitric oxide synthase (iNOS): analysis of iNOS mRNA, iNOS protein, biopterin, and nitric oxide production by blood monocytes and peritoneal macrophages. *Blood* 86, 1184-1195.

Weiss SJ. 1989. Tissue destruction by neutrophils. *New Eng J Med.* 320, 365-376.

West JB. 2000. Respiratory Physiology: the essentials. 6th Edition. Lippencott Williams and Wilkins, Philadelphia.

Williams AO and Saffiotti U. 1995. Transforming growth factor beta1, ras and p53 in silica-induced fibrogenesis and carcinogenesis. *Scand.J.Work Environ.Health* 21 Suppl 2, 30-34.

Wilson ME. 1985. Effects of bacterial endotoxins on neutrophil function. *Rev Infect Dis.* 7, 404-418.

Wilson MR, Lightbody JH, Donaldson K, Sales J and Stone V. 2002. Interactions between ultrafine particles and transition metals in vivo and in vitro. *Toxicol.Appl.Pharmacol.* 184, 172-179.

Wink DA, Vodovotz Y, Laval J, Laval F, Dewhirst MW and Mitchell JB. 1998. The multifaceted roles of nitric oxide in cancer. *Carcinogenesis* 19, 711–721.

Wiseman H and Halliwell B. 1996. Damage to DNA by reactive oxygen and nitrogen species: role in inflammatory disease and progression to cancer. *Biochem.J.* 313 (Pt 1), 17-29.

Wu, J, Liu W, Koenig K, Idell S and Broaddus VC. 2000. Vitronectin adsorption to chrysotile asbestos increases fiber phagocytosis and toxicity for mesothelial cells. *Am. J. Physiol. Lung Cell Mol. Physiol.* 279, L916-923.

Wycoff RWG. 1963. *Crystal Structures*, 2nd ed. Vol.1, Interscience Publishers, New York, 312-322.

Wyllie AH, Bellamy CO, Bubb VJ, Clarke AR, Corbet S., Curtis L, Harrison DJ, Hooper ML, Toft N, Webb S and Bird CC. 1999. Apoptosis and carcinogenesis. *Br.J.Cancer* 80 Suppl 1, 34-37.

Xu A, Wu LJ, Santella RM and Hei TK. 1999. Role of oxyradicals in mutagenicity and DNA damage induced by crocidolite asbestos in mammalian cells. *Cancer Res.* 59, 5922-5926.

Yamano Y, Kagawa J, Hanaoka T, Takahashi T, Kasai H, Tsugane S and Watanabe S. 1995. Oxidative DNA damage induced by silica in vivo. *Environ. Res.* 69, 102-107.

Yoshikawa T, Minamiyama Y, Naito Y and Kondo M. 1994. Antioxidant properties of bromocriptine, a dopamine agonist. *J.Neurochem.* 62, 1034-1038.

Young MR, Li JJ, Rincon M, Flavell RA, Sathyanarayana BK, Hunziker R and Colburn N. 1999. Transgenic mice demonstrate AP-1 (activator protein-1) transactivation is required for tumor promotion. *Proc.Natl.Acad.Sci.U.S.A* 96, 9827-9832.

Yuen IS, Hartsky MA, Snajdr SI and Warheit DB. 1996. Time course of chemotactic factor generation and neutrophil recruitment in the lungs of dust-exposed rats. *Am. J. Respir.Cell Mol. Biol.* 15, 268–274.

Zhang Y, Lee TC, Guillemin B, Yu MC, and Rom WN. 1993. Enhanced IL-1 beta and tumor necrosis factor-alpha release and messenger RNA expression in macrophages from idiopathic pulmonary fibrosis or after asbestos exposure 11. *J.Immunol.* 150, 4188-4196.

Zhong BZ, Whong WZ and Ong TM. 1997. Detection of mineral-dust-induced DNA damage in two mammalian cell lines using the alkaline single cell gel/comet assay. *Mutat. Res.* 393, 181-187.